



ELSEVIER

Contents lists available at ScienceDirect

Physics Letters B

journal homepage: www.elsevier.com/locate/physletb

Search for pair-production of vector-like quarks in pp collision events at $\sqrt{s} = 13$ TeV with at least one leptonically decaying Z boson and a third-generation quark with the ATLAS detector

The ATLAS Collaboration*

ARTICLE INFO

Article history:

Received 28 October 2022

Received in revised form 7 June 2023

Accepted 9 June 2023

Available online 15 June 2023

Editor: M. Doser

Dataset link: <https://www.hepdata.net/>

ABSTRACT

A search for the pair-production of vector-like quarks optimized for decays into a Z boson and a third-generation Standard Model quark is presented, using the full Run 2 dataset corresponding to 139fb^{-1} of pp collisions at $\sqrt{s} = 13$ TeV, collected in 2015–2018 with the ATLAS detector at the Large Hadron Collider. The targeted final state is characterized by the presence of a Z boson with high transverse momentum, reconstructed from a pair of same-flavour leptons with opposite-sign charges, as well as by the presence of b -tagged jets and high-transverse-momentum large-radius jets reconstructed from calibrated smaller-radius jets. Events with exactly two or at least three leptons are used, which are further categorized by the presence of boosted W , Z , and Higgs bosons and top quarks. The categorization is performed using a neural-network-based boosted object tagger to enhance the sensitivity to signal relative to the background. No significant excess above the background expectation is observed and exclusion limits at 95% confidence level are set on the masses of the vector-like partners T and B of the top and bottom quarks, respectively. The limits depend on the branching ratio configurations and, in the case of 100% branching ratio for $T \rightarrow Zt$ and 100% branching ratio for $B \rightarrow Zb$, this search sets the most stringent limits to date, allowing $m_T > 1.60$ TeV and $m_B > 1.42$ TeV, respectively.

© 2023 The Author(s). Published by Elsevier B.V. This is an open access article under the CC BY license (<http://creativecommons.org/licenses/by/4.0/>). Funded by SCOAP³.

Contents

1. Introduction	1
2. ATLAS detector	2
3. Data and simulated event samples	2
4. Object reconstruction	3
5. Event selection and categorization	4
6. Systematic uncertainties	5
7. Results	7
8. Conclusions	11
Declaration of competing interest	12
Data availability	12
Acknowledgements	12
References	12
The ATLAS Collaboration	14

1. Introduction

The Standard Model (SM) has had astonishing success in describing the interactions of elementary particles, culminating in the

discovery [1,2] of the Higgs boson by the ATLAS and CMS collaborations. Nevertheless, there remain some shortcomings, such as the quadratically divergent corrections predicted to contribute to the square of the Higgs boson mass [3]. In many theories beyond the SM, including Composite Higgs [4,5] and Little Higgs [6,7] models, a recurrent theme that addresses these issues is the existence

* E-mail address: atlas.publications@cern.ch.

of vector-like quarks (VLQs): coloured spin-1/2 fermions that have left- and right-handed components transforming identically under the SM gauge group. In such models, VLQs are often assumed to couple preferentially to a third-generation quark [8–11], potentially regulating the divergent corrections to the Higgs boson mass. The VLQs therefore decay into SM quarks and a W/Z (V) or Higgs (H) boson, with branching ratios (BR) that depend on the VLQ masses and their configuration in weak-isospin multiplets. In renormalizable extensions of the SM that include VLQs, the canonical representation of VLQs constitutes one of seven multiplets: two singlets, three doublets, and two triplets. Vector-like partners, T and B , of the top and bottom quarks can exist with electric charges $(2/3)e$ and $-(1/3)e$, respectively, and can be arranged in singlets, doublets, and triplets. VLQs with exotic charges can also exist, namely X and Y with electric charges $(5/3)e$ and $-(4/3)e$, respectively, which can be arranged in doublets and triplets with the T and B . Assuming an almost degenerate VLQ mass hierarchy [11], the singlet and triplet representations are phenomenologically similar in terms of chiral structure and BR composition. As a consequence, the singlet and doublet representations are those that are primarily assumed in searches at the Large Hadron Collider (LHC). While models with extreme values of 100% BR for decay into a third-generation quark and either a W/Z boson or a Higgs boson are often used as benchmarks, intermediate BR configurations are expected in the more physically motivated singlet and doublet models. In the former, the BR for $T \rightarrow Zt$ or $B \rightarrow Zb$ reaches $\approx 25\%$ at high VLQ masses [11]. For the (T, B) and (X, Y) doublets the BR for $T \rightarrow Zt$ reaches $\approx 50\%$ [11], as does the BR for $B \rightarrow Zb$ for the (B, Y) doublet.

VLQs were searched for at ATLAS and CMS focusing mainly on the pair-production mode [12–25]. Constraints on VLQ production were also derived recently [26] from a range of differential cross-section measurements at the LHC, complementing the direct searches. VLQ pair production, proceeding primarily via the strong interaction with a cross-section that depends only on the VLQ mass, is expected to be the dominant mode for masses up to approximately 1 TeV. The most stringent limits at 95% confidence level (CL) on T and B masses depend on the assumed BR configuration; for 100% BR for $T \rightarrow Zt$, $T \rightarrow Ht$, $T \rightarrow Wb$, and $B \rightarrow Wt$, masses up to 1.48 TeV, 1.50 TeV, 1.50 TeV, and 1.56 TeV are excluded, respectively [25]. For 100% BR for $B \rightarrow Zb$ and $B \rightarrow Hb$, B masses up to 1.39 TeV and 1.57 TeV are excluded, respectively [20]. A singlet T is excluded for masses below 1.48 TeV and a singlet B is excluded for masses below 1.47 TeV, while in the (T, B) doublet case, T and B masses below 1.49 TeV and 1.37 TeV are excluded, respectively [12,25,26]. Single VLQ production has also been searched for [13,15,27–33], but the interpretation [34] of the search results depends on an additional coupling constant for the coupling to electroweak bosons.

This Letter presents a search for pair production of T and B in events with at least two electrons or muons where at least two same-flavour leptons with opposite-sign charges originate from the decay of a Z boson. Various BR configurations for the decay of the VLQ into a V or H boson and a third-generation quark are considered, including the singlet and doublet models, assuming that only one type of VLQ is present, and it is also assumed that the VLQ signal kinematics are similar for different configurations. It is further assumed that the production of VLQ pairs is dominated by the strong interaction and that the contribution from electroweak processes is negligible. A diagram illustrating the targeted event topologies is shown in Fig. 1. The search is performed across several different event categories included in a maximum-likelihood fit, improving on a previous ATLAS search [13] in the same final state. In addition to benefiting from the larger dataset, the search is also improved by the use of a deep neural network (DNN) to

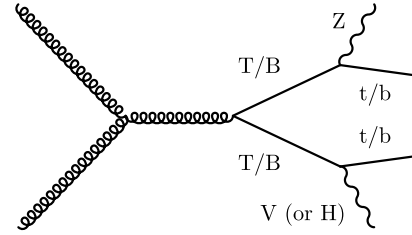


Fig. 1. Feynman diagram showing the pair production of T or B quarks in which at least one of the VLQs decays into a Z boson in association with a SM t - or b -quark, respectively. In this analysis, events in which the Z boson decays into a pair of electrons or a pair of muons are targeted. At least one b -tagged jet is required to be present after pair production of either type of VLQ, and additional leptons can be produced in the decays of V (W/Z), or H bosons on the second leg of the VLQ pair production.

classify the jets in each event as originating from either a Z or W boson, H boson, or top quark.

2. ATLAS detector

ATLAS [35] is a multipurpose particle detector at the Large Hadron Collider (LHC) with a forward–backward symmetric cylindrical geometry and a near 4π coverage in solid angle.¹ It consists of an inner tracking detector (ID) [36,37] surrounded by a thin superconducting solenoid providing a 2 T axial magnetic field, electromagnetic and hadron calorimeters, and a muon spectrometer (MS). The ID covers the pseudorapidity range $|\eta| < 2.5$ and consists of silicon pixel, silicon microstrip, and transition radiation tracking detectors. Lead/liquid-argon (LAr) sampling calorimeters provide electromagnetic (EM) energy measurements with high granularity. A steel/scintillator-tile hadronic calorimeter covers the central pseudorapidity range ($|\eta| < 1.7$). The endcap and forward regions are instrumented with LAr calorimeters for both EM and hadronic energy measurements up to $|\eta| = 4.9$. The MS surrounds the calorimeters and uses three large air-core toroidal superconducting magnets with eight coils each. The field integral of the toroids ranges between 2.0 and 6.0 Tm across most of the detector. The MS includes a system of precision chambers for tracking and fast detectors for triggering [38]. A two-level trigger system is used to select events. The first-level trigger is implemented in hardware and uses a subset of the detector information to accept events at a rate below 100 kHz. This is followed by a software-based trigger that reduces the accepted event rate to 1 kHz on average depending on the data-taking conditions. An extensive software suite [39] is used in the reconstruction and analysis of real and simulated data, in detector operations, and in the trigger and data acquisition systems of the experiment.

3. Data and simulated event samples

The analysed dataset comprises pp collisions at a centre-of-mass energy $\sqrt{s} = 13$ TeV recorded by ATLAS between 2015 and 2018 with all detector subsystems operational and with the LHC operating in stable beam conditions with 25 ns bunch spacing. The combined Run 2 dataset corresponds to an integrated luminosity of 139 fb^{-1} with an average of about 34 simultaneous interactions per bunch crossing (pile-up).

¹ ATLAS uses a right-handed coordinate system with its origin at the nominal interaction point (IP) in the centre of the detector and the z -axis along the beam pipe. The x -axis points from the IP to the centre of the LHC ring, and the y -axis points upwards. Cylindrical coordinates (r, ϕ) are used in the transverse plane, ϕ being the azimuthal angle around the z -axis. The pseudorapidity is defined in terms of the polar angle θ as $\eta = -\ln \tan(\theta/2)$. Angular distance is measured in units of $\Delta R \equiv \sqrt{(\Delta\eta)^2 + (\Delta\phi)^2}$.

All the nominal Monte Carlo (MC) simulation samples used in the analysis were produced with the ATLAS full-simulation framework [40] based on GEANT4 [41]. In all samples, pile-up was modelled by combining simulated inelastic pp events with the physics event. The nominal sample for Z boson production in association with jets (Z +jets) was generated with SHERPA 2.2.1 [42–45] and the nominal diboson (VV) sample was generated with SHERPA 2.2.2, with the NNPDF3.0 [46] next-to-next-to-leading-order (NNLO) parton distribution function (PDF) set. The Z +jets sample includes events generated with up to two partons at next-to-leading order (NLO) and up to four partons at leading order (LO) and is normalized to the NNLO cross-section [47]. The VV sample is normalized to the SHERPA NLO cross-section and includes $q\bar{q}$ -initiated events with up to one parton at NLO and up to three partons at LO and gg -initiated processes generated using LO matrix elements for up to one additional jet. For both samples, COMIX [44] and OPENLOOPS [48] were used and the matrix element (ME) was merged with the SHERPA parton shower [45] according to the MEPS@NLO prescription [49]. To estimate modelling uncertainties, an additional Z +jets sample was produced with MADGRAPH5_AMC@NLO 2.2.3 [50], using the NNPDF3.0NLO PDF set and interfaced to PYTHIA 8.210 [51] with the A14 set of tuned parameters (tune) [52] and the NNPDF2.3LO PDF for showering. These samples were generated including LO matrix elements for up to four jets [53].

The nominal SM $t\bar{t}$ background sample uses the POWHEG method [54,55] implemented in POWHEGBOX v2 [56,57] with the NNPDF3.0NLO PDF set. POWHEGBOX was interfaced with PYTHIA 8.230 with the A14 tune for showering. The sample is normalized to the NNLO cross-section in QCD including resummation of next-to-next-to-leading logarithmic (NNLL) soft gluon terms calculated with TOP++ [58–64]. For the evaluation of modelling uncertainties, samples were produced with the same ME generator as the nominal sample, but HERWIG7 was used with the H7-UE-MMHT tune [65] for the showering. Additional samples [66] were generated with MADGRAPH5_AMC@NLO 2.3.3 and the NNPDF3.0NLO PDF set, using the same showering configuration as the nominal sample.

The nominal sample including $t\bar{t}$ production in association with a vector boson ($t\bar{t} + X$) was generated with MADGRAPH5_AMC@NLO 2.3.3 interfaced with PYTHIA 8.210 for showering, using the NNPDF2.3LO PDF set and the A14 tune. The sample includes $t\bar{t} + Z$ and $t\bar{t} + W$ events normalized to the NLO cross-sections calculated with MADGRAPH5_AMC@NLO. To evaluate modelling uncertainties, samples were produced using SHERPA 2.2.1. Alternative samples were also produced with the nominal sample's ME generator, and in these samples either the A14 tune was varied or HERWIG7 was used with the H7-UE-MMHT tune for the showering. The nominal $t\bar{t} + X$ sample also includes $t\bar{t}t\bar{t}$ and $t\bar{t}WW$ events generated at LO and normalized to cross-sections calculated [50,67] with NLO QCD and EW corrections.

The single-top processes were simulated with POWHEGBOX [68, 69] using the NNPDF3.0NLO PDF set and interfaced to PYTHIA 8.234 with the A14 tune. The samples are normalized to their respective NLO QCD cross-sections [70,71] for the t-channel and s-channel, and with additional NNLL soft gluon terms for Wt production [72–74]. The diagram-removal scheme [75] was used in the generation of Wt events to address overlaps with the $t\bar{t}$ sample.

Signal samples for the pair production of T and B quarks were generated with PROTOS [76] interfaced with PYTHIA 8.186 using the NNPDF2.3LO PDF set and the A14 tune. The samples were generated under the assumption that the coupling is small therefore the width of the VLQ is driven by the experimental resolution. The generated VLQ masses have widths typically smaller than 2% of the mass. Masses from 600 GeV to 2 TeV were simulated in the singlet model, but with the BR for each of the three decays to a vector or Higgs boson fixed to 1/3 for all samples. A BR reweight-

ing procedure is performed event-by-event in order to achieve any BR configuration for a given VLQ mass, including the configurations expected for the doublet models. Dedicated signal samples in the doublet models for the 700 GeV and 1.2 TeV mass points were also produced to validate the reweighting procedure and to verify that the singlet and doublet signal kinematics are indistinguishable in the analysis as is assumed. The signal sample cross-sections were calculated with TOP++ at NNLO+NNLL in QCD using the MSTW2008NNLO [77–79] PDF set.

4. Object reconstruction

Events are required to have at least one vertex candidate with at least two tracks with transverse momentum $p_T > 0.5$ GeV. The primary vertex (PV) is defined to be the candidate with the largest Σp_T^2 , where the sum is performed over all associated tracks.

Electrons are reconstructed [80] from clusters in the EM calorimeter matched with ID tracks and must fulfil the *tight likelihood* identification criteria. Electrons are calibrated and are required to have $p_T > 28$ GeV and to be reconstructed within $|\eta| < 2.47$, excluding the barrel–endcap transition regions ($1.37 < |\eta| < 1.52$). In order to maintain a high acceptance for the expected signal events, no isolation requirements are applied to electron candidates beyond those implicit in the trigger requirements. Furthermore, electron candidates must be associated with the PV by requiring that the longitudinal impact parameter with respect to the PV satisfies $|z_0 \cdot \sin\theta| < 0.5$ mm and that the transverse impact parameter with respect to the beamline (d_0) has a significance $|d_0|/\sigma(d_0) < 5$.

Muons are reconstructed [81] from combined tracks in the MS and the ID and must fulfil *medium* identification criteria. Muons are calibrated [82] and are required to have $p_T > 28$ GeV and to be reconstructed within $|\eta| < 2.5$. Muon candidates must also satisfy the track-based isolation requirements defined by the *FixedCut-TightTrackOnly* working point. This working point uses the scalar sum of the p_T of all tracks that are within a cone of size $\Delta R = \min\{0.3, 10 \text{ GeV}/p_T(\mu)\}$ around the muon candidate, where $p_T(\mu)$ is the candidate muon p_T . The track associated with the muon candidate under consideration is excluded from the sum. The muon is selected if this sum is less than 15% of $p_T(\mu)$. Finally, muon candidates are required to have $|z_0 \cdot \sin\theta| < 0.5$ mm and a d_0 significance smaller than 3.

Jets are reconstructed using the anti- k_t algorithm [83,84] with a radius parameter of 0.4 from topological clusters of energy deposits in the calorimeter [85,86]. Jets are calibrated to an energy scale obtained from a combination of simulation-based corrections and measurements in data [87] and are required to fulfil $p_T > 25$ GeV for $|\eta| < 2.5$ and $p_T > 35$ GeV for $2.5 < |\eta| < 4.5$. To reduce jet contributions from pile-up, a ‘jet vertex tagger’ algorithm using a two-dimensional likelihood discriminant [88] is applied to jets with $|\eta| < 2.4$ and $p_T < 60$ GeV. The MV2c10 algorithm [89] is used to identify jets in the central region ($|\eta| < 2.5$) containing a b -hadron decay (b -tagging) with a working point corresponding to a b -tagging efficiency in simulated $t\bar{t}$ events of 77%, a c -jet rejection factor of ~ 6 , and a light-jet rejection factor of ~ 130 .

The missing transverse momentum [90], with magnitude E_T^{miss} , is defined as the negative vectorial sum of the transverse momenta of all the calibrated reconstructed lepton and jet candidates in the event and includes a ‘soft term’ with contributions from tracks emanating from the PV but not associated with any of the reconstructed objects.

A procedure to remove potential overlaps between reconstructed leptons and jets is performed sequentially as follows. First, any muon that leaves energy deposits in the calorimeters and shares a track in the ID with an electron is removed. After

such muons have been removed, any electron sharing an ID track with one of the remaining muons is removed. Next, any jet within $\Delta R = 0.2$ of an electron is removed, followed by the removal of electrons within $\Delta R = 0.4$ of any remaining jet. Subsequently, any jet with at most two tracks with $p_T > 0.5$ GeV within $\Delta R = 0.2$ of a muon is removed, unless it has been b -tagged. At the end of the procedure, any muon within $\Delta R = \min\{0.4, 0.04 + 10 \text{ GeV}/p_T(\mu)\}$ of any remaining jet is removed.

Finally, large-radius ‘reclustered’ (RC) jets [91] are reconstructed by applying the anti- k_t algorithm with a radius parameter of 1.0, using the set of selected and already calibrated smaller-radius jets defined above. To reduce dependence on pile-up, the RC jets are trimmed [92] by removing all constituent jets with p_T below 5% of the RC jet p_T . These RC jets are used only for event categorization, and therefore no additional checks for potential overlaps with the previously defined objects are performed.

5. Event selection and categorization

An initial preselection of events is performed as follows. Events are required to satisfy at least one of the single-lepton triggers operating during Run 2 [38,93,94]. These triggers had varying p_T thresholds for electrons and muons for different data-taking periods, as well as isolation requirements that were typically more relaxed with increasing p_T threshold. For data collected in 2015, the thresholds are 24, 60, and 120 GeV for electrons and 20 and 50 GeV for muons. For the remainder of the dataset, the thresholds are slightly increased to 26, 60, and 140 GeV for electrons and to 26 and 50 GeV for muons. Events are additionally required to have at least two opposite-sign-charge, same-flavour (OS-SF) leptons and to have at least two jets in the central region. The pair of OS-SF leptons with an invariant mass $m(\ell\ell)$ closest to $m_Z = 91.2$ GeV is referred to as ‘the Z boson candidate’ and only events with $|m(\ell\ell) - m_Z| < 10$ GeV are kept.

Preselected events are divided into two orthogonal and individually optimized channels: one requiring exactly two leptons (dilepton, labelled as ‘ 2ℓ ’) and a second requiring at least three leptons (trilepton, labelled as ‘ 3ℓ ’). The channels are combined statistically to obtain the final result, taking advantage of the relatively high signal acceptance achieved by the 2ℓ channel and the higher signal purity offered by the 3ℓ channel.

Fig. 2 shows distributions of example kinematic variables for the expected background and for benchmark signal processes obtained from MC simulation. In addition to the lepton multiplicity, the analysis exploits the high multiplicities of jets, large-radius jets, and b -tagged jets expected for pair-produced VLQ signal. Requirements on the momentum of the Z boson candidate, $p_T(\ell\ell)$, and the scalar sums of the transverse momenta of objects reconstructed in the events, H_T , are applied to suppress the background. Furthermore, the analysis uses RC jets as an input to a ‘multi-class boosted object tagger’ (MCBOT) in order to identify (tag) the origin of each RC jet as being either a hadronically decaying V boson, H boson, or top quark.

MCBOT is based on a multi-class DNN using the Keras [95] and TensorFlow [96] software libraries. The DNN is trained using RC jets from simulated $Z' \rightarrow t\bar{t}$ events, $W' \rightarrow WZ$ events, and events with a Kaluza–Klein graviton in the bulk Randall–Sundrum model [97] decaying into a pair of H bosons which each decay into $b\bar{b}$ with a BR fixed to 100%. These dedicated events are generated so that RC jets with a mass of at least 40 GeV are uniformly distributed in an RC jet p_T range between 150 GeV and 3 TeV. The three signal labels (V , H , top) are assigned by matching the RC jet to the corresponding hadronically decaying boson or top quark within a ΔR of 0.75 at generator level. Simulated multijet events are used to obtain the RC jets with a *background* label. The RC jets in these four classes are reweighted such that their distribu-

tions are uniform in RC jet p_T and η . The 18 input variables of the DNN are the RC jet p_T and mass, the number of the RC jet constituent smaller-radius jets, the four-momentum vectors of the three highest- p_T constituent jets, and the b -tagging decisions for those three jets. The DNN consists of four fully connected hidden layers with *Rectified Linear Unit* [98] activation functions and a four-dimensional output layer in which nodes are activated using the *softmax* [99] function. The first hidden layer uses 32 nodes, reduced to 27, 14, and 12 nodes for the second, third, and fourth hidden layer, respectively. The ADAM [100] optimizer is used to minimize the categorical cross-entropy as a loss function in order to find the optimal weights. The set of hyper-parameters as optimized for a related ATLAS analysis [14] is used. The projections of the four-dimensional output of the DNN are used to define a working point for each of the signals in order to define a V -tag, a H -tag, and a top-tag. Fig. 3 shows an example set of these projections for RC jets with p_T between 150 GeV and 1 TeV. In cases where the same RC jet satisfies the requirements for more than one tag, the tag with the highest neural-network output value is retained. Therefore, at most one signal label can be assigned to any RC jet. For the selected working point, and for $T\bar{T}$ signal with $m_T = 1400$ GeV in the singlet configuration, efficiencies of 55%, 41%, and 54% are measured for V , H , and top signals, respectively.

In the 2ℓ channel, events are required to satisfy $p_T(\ell\ell) > 300$ GeV in order to select leptonic Z boson candidates originating from the decay of a heavy VLQ. In addition, given the large amount of jet activity expected in signal events and to take advantage of a potentially invisible decay of the Z boson in the decay chain of the second VLQ in the pair, requirements are placed on the scalar sum of the jet transverse momenta, $H_T(\text{jet})$, and E_T^{miss} . Two exclusive signal regions (SR) are defined by requiring $H_T(\text{jet}) + E_T^{\text{miss}} > 1380$ GeV and either exactly one b -tagged jet ($1b$ SR) or at least two b -tagged jets ($2b$ SR). The chosen kinematic requirements are motivated by the selection criteria of the earlier ATLAS analysis [13] and are optimized using a procedure that maximizes the expected sensitivity for a few benchmark signal models. The most relevant event selection criteria are shown in Table 1, which additionally shows the definitions of the signal regions and background control regions. The events in each SR are divided into exclusive categories based on combinations of the numbers of signal-tagged RC jets of various types identified by MCBOT. A signal significance optimization procedure is used to group the possible tagging combinations so as to reduce the set of categories to seven, as shown in Table 2. These include ‘Double tag’ categories with different combinations of at least two RC jets with tags of any signal type, as well as a final ‘Overflow’ category that includes events with more than two tags but also leftover two-tag combinations that are not included in the former categories. In order to recover some of the events in which RC jets might be misidentified, combinations with more than one V or H boson are included even though one of the two VLQs is required to decay to a leptonically decaying Z boson in the targeted event topology.

In the 3ℓ channel, the Z candidate transverse momentum requirement is relaxed to $p_T(\ell\ell) > 200$ GeV to increase signal efficiency given the significant background suppression due to the three-lepton requirement. To take advantage of the additional lepton activity, events must also satisfy $H_T(\text{jet} + \text{lep}) > 300$ GeV, where $H_T(\text{jet} + \text{lep})$ is the scalar sum of the jet and lepton transverse momenta. Events in the 3ℓ SR are also required to have at least one b -tagged jet and are divided into five exclusive categories based on the number of MCBOT tags, similarly to the 2ℓ channel, as shown in Table 2.

The signal efficiency, defined as the ratio of the number of events selected by the signal regions to the number of events generated in the signal samples, for the benchmark of a 1.2 TeV singlet

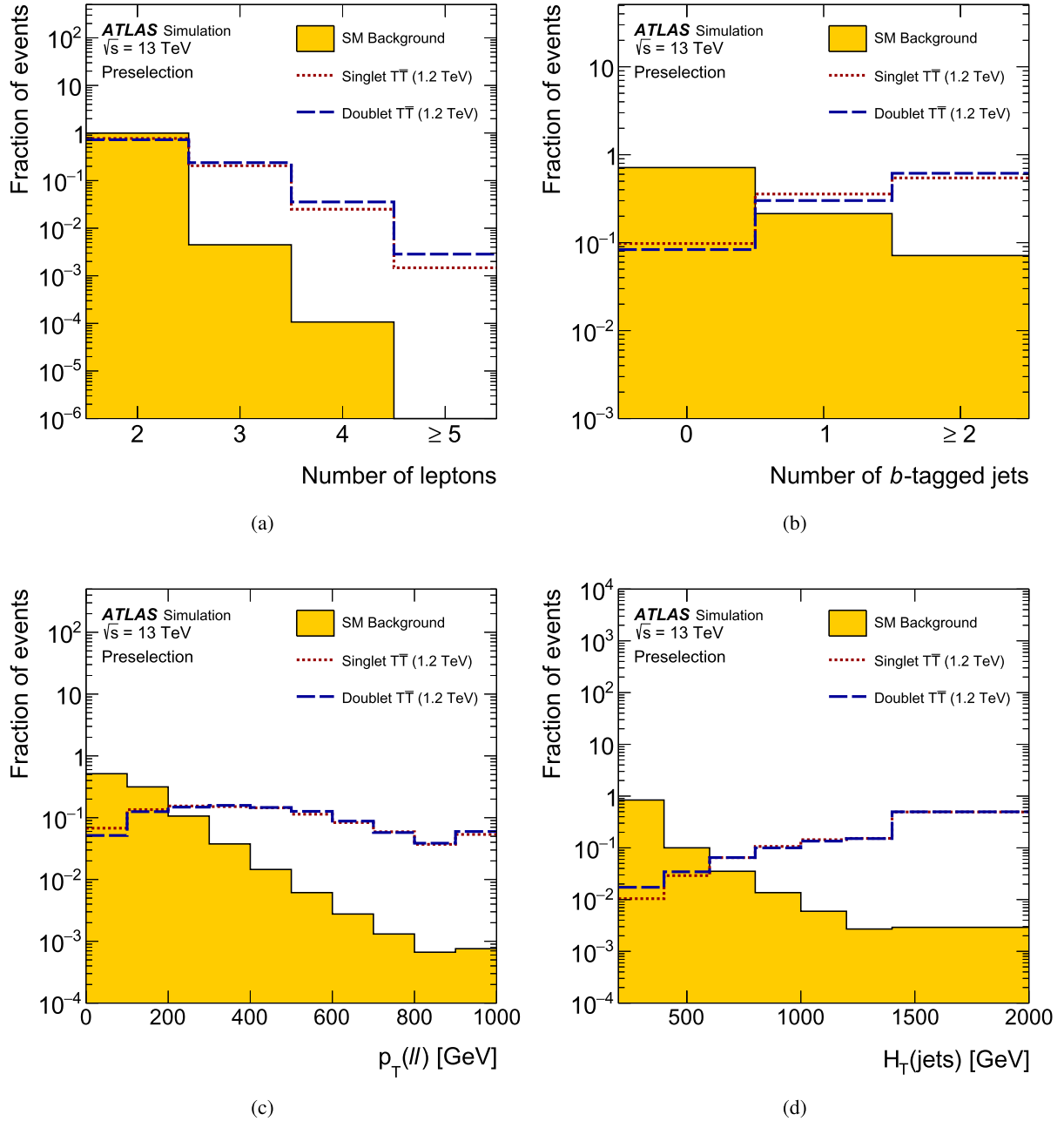


Fig. 2. Distributions, normalized to unit area, obtained from MC simulation for the sum of all the background processes (solid area) and for benchmark signal processes (dashed lines): (a) lepton multiplicity, (b) b -tagged jet multiplicity, (c) transverse momentum of the Z boson candidate, $p_T(\ell\ell)$, and (d) scalar sum of the jet transverse momenta, $H_T(\text{jet})$. The signal processes concern the pair production of vector-like T or B quarks with a mass of 1.2 TeV in either the singlet or doublet configurations. The last bin contains the overflow.

T , is 0.3% and 0.5% in the $1b$ and $2b$ 2ℓ signal regions, respectively, and 0.5% in the 3ℓ signal regions.

The SM background contribution is estimated using MC simulation and is adjusted in the final simultaneous maximum-likelihood fit to the data with the help of signal-depleted control regions (CR), designed to be similar in phase-space to the SR. Leading backgrounds include Z +jets, which is the dominant background for 2ℓ , as well as VV and $t\bar{t} + X$, which are dominant for 3ℓ . Smaller backgrounds include those from $t\bar{t}$, single top quark and four top quark.

The inputs to the fit are binned distributions of final discriminants optimized for each of the two channels. In the 2ℓ channel, in all the $1b$ SR categories, the invariant mass of the leptonically decaying Z candidate and the leading b -tagged jet, $m(Zb_1)$,

is used as a final discriminant, while for the $2b$ SR categories the subleading b -tagged jet is used instead and the discriminating variable is $m(Zb_2)$. Two 2ℓ CR corresponding to each SR are defined by requiring $920 \text{ GeV} < H_T(\text{jet}) + E_T^{\text{miss}} < 1380 \text{ GeV}$. These CR are not further categorized using MCBOT and participate in the fit using the distribution of $H_T(\text{jet}) + E_T^{\text{miss}}$. In the 3ℓ channel a single VV CR is defined by requiring exactly zero b -jets. The final discriminant for all 3ℓ SR categories and for the VV CR is $H_T(\text{jet} + \text{lep})$.

6. Systematic uncertainties

Several experimental and theoretical systematic uncertainties that can affect the normalization or the shape of the fitted distributions are considered. For each considered source of uncertainty,

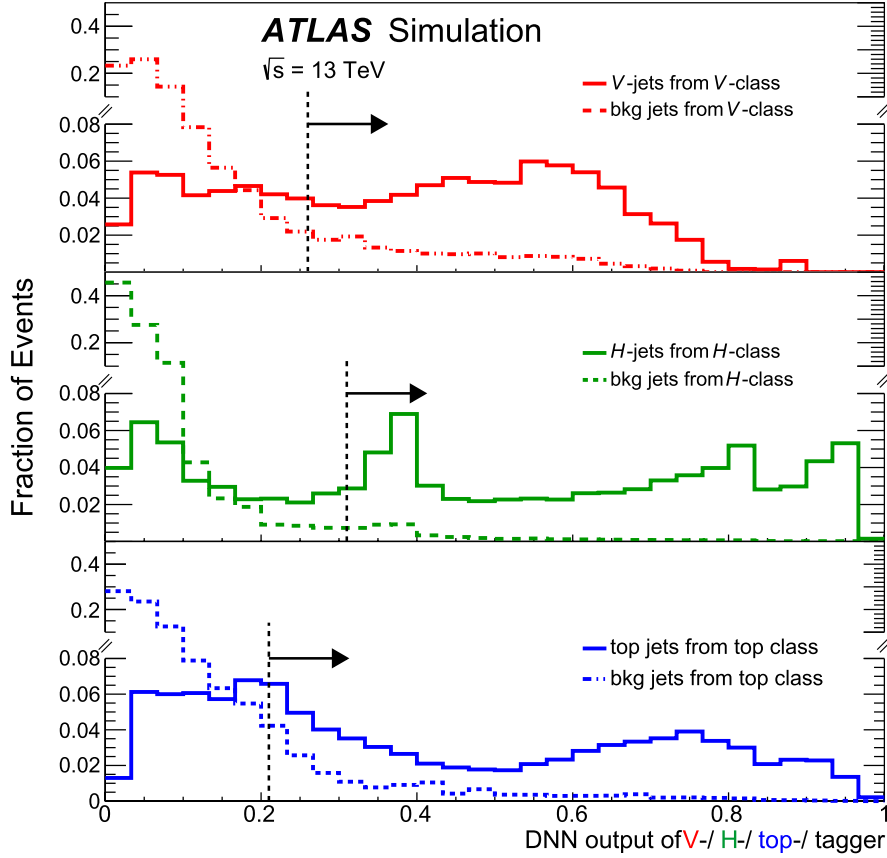


Fig. 3. The distributions of the DNN output of MCBOT for the V boson, H boson, and top quark classes for RC jets with p_T between 150 GeV and 1 TeV. For each tagger (V , H , or top) the response to the corresponding signal jets (solid lines) is compared with the response to the background jets (dashed lines). The responses to signal jets other than the corresponding signal for each tagger are not shown for simplicity. Signal jets are defined by geometrically matching the RC jets to the corresponding generator-level particles. Background jets are obtained from multijet events. The colours red, green, and blue indicate the DNN output values for the V -, H -, or top-tagger, respectively. The RC jet p_T is reweighted together with the RC jet η to be uniform over the full range. All distributions are normalized to unit area. The y -axis is split for better readability.

Table 1

Definitions of analysis regions and the most relevant event selection criteria. The final discriminating variables used in the fit are also indicated for each region: $m(Zb_1)$ and $m(Zb_2)$ refer to the mass of the system of the Z boson candidate and either the leading b -jet or subleading b -jet, respectively. $H_T(\text{jet})$ is defined as the scalar sum of the transverse momenta of all selected jets, while $H_T(\text{jet} + \text{lep})$ is defined as the scalar sum of the transverse momenta of all selected jets and leptons.

Preselection	≥ 2 central jets at least two SF leptons with $p_T > 28$ GeV at least one pair of OS-SF leptons $ m(\ell\ell) - m_Z < 10$ GeV					
Channel definitions	2ℓ $= 2\ell$ $p_T(\ell\ell) > 300$ GeV $H_T(\text{jet}) + E_T^{\text{miss}} > 920$ GeV			3ℓ $\geq 3\ell$ $p_T(\ell\ell) > 200$ GeV $H_T(\text{jet} + \text{lep}) > 300$ GeV		
Region definitions	$1b$ SR $H_T(\text{jet}) + E_T^{\text{miss}} > 1380$ GeV $= 1$ b -jet	$2b$ SR ≥ 2 b -jet	$1b$ CR $H_T(\text{jet}) + E_T^{\text{miss}} < 1380$ GeV $= 1$ b -jet	$2b$ CR ≥ 2 b -jet	SR ≥ 1 b -jet	VV CR $= 0$ b -jet
MCBOT categories	7	7	-	-	5	-
Fitted variable	$m(Zb_1)$	$m(Zb_2)$	$H_T(\text{jet}) + E_T^{\text{miss}}$		$H_T(\text{jet} + \text{lep})$	

variations representing the -1σ and $+1\sigma$ confidence interval are derived. The analysis selection, including the MCBOT categorization, is applied on each variation to estimate their effect on the final discriminants. Several of these modelling uncertainties are constrained after the fit due to the significantly larger number of events in the control regions compared to the signal regions. However, these constraints do not impact the final limit. Furthermore, the analysis is dominated by statistical uncertainties; the expected lower limits on the VLQ masses decrease by no more than 4%

when all the systematic uncertainties are included in the analysis.

Experimental uncertainties include effects on the electron energy scale and energy resolution [80], the muon momentum scale and resolution [81], as well as uncertainties in the data-to-MC correction factors for the electron and muon trigger, reconstruction, identification, and isolation efficiencies [80,81]. Jet energy scale and resolution uncertainties are also included, as obtained from studies in data and simulation [87]. A 10% uncertainty [101] is assigned to the small-radius jet mass, which is not calibrated but is

Table 2

Definitions of the categorization of events in the 2ℓ and 3ℓ channels based on the number of MCBOT tags. Unless otherwise noted, the columns indicate the exact number of required tagged RC jets for each type. Categories labelled as ‘Double tag’ include combinations with exactly two tags of any type. Categories labelled as ‘Overflow (OF)’ include all the tagging combinations that are not explicitly included in the other categories.

Category	2 ℓ channel						3 ℓ channel		
	1b SR			2b SR			–		
	V-tags	H-tags	top-tags	V-tags	H-tags	top-tags	V-tags	H-tags	top-tags
No tag	0	0	0	0	0	0	0	0	0
V tag	1	0	0	1	0	0	≥ 1	0	0
H tag	0	1	0	0	1	0	0	≥ 1	0
Top tag	0	0	1	0	0	1	0	0	≥ 1
	2	0	0	2	0	0	–	–	–
Double tag 1	0	2	0	0	2	0	–	–	–
	1	0	1	1	1	0	–	–	–
	–	–	–	0	0	2	–	–	–
Double tag 2	0	1	1	0	1	1	–	–	–
	0	0	2	–	–	–	–	–	–
	1	1	0	1	0	1	0	≥ 1	≥ 1
Overflow (OF)	or > 2 tags			or > 2 tags			≥ 1	0	≥ 1
	–	–	–	–	–	–	≥ 1	≥ 1	0
	–	–	–	–	–	–	≥ 1	≥ 1	≥ 1

used in the RC jet mass calculation. Flavour-tagging uncertainties include uncertainties in the b -jet tagging, c -jet tagging, and light-jet mis-tagging efficiencies, and uncertainties due to extrapolations to regions not covered by the data used for the efficiency measurements [89,102,103]. Subdominant uncertainties include uncertainties related to the soft term in the E_T^{miss} calculation [90] and to the E_T^{miss} energy scale and resolution, uncertainties in the reweighting of the MC event samples to match the pile-up conditions in data, and a 1.7% [104] uncertainty in the integrated luminosity of the combined 2015–2018 dataset.

Theoretical uncertainties include cross-section and other modelling uncertainties for all background samples. The cross-section uncertainties considered are of order 5% to 6% for the Z +jets, $t\bar{t}$, and VV samples [105,106] and of order 10% [105] $t\bar{t} + Z$ samples. A conservative 50% uncertainty is used for the $t\bar{t} + W$ sample. Uncertainties due to the choice of generator or showering algorithm are estimated using additional samples from alternative generators. The uncertainties due to the choice of factorization and renormalization scales, the modelling of ISR and FSR, and the choice of PDF set are estimated by varying the nominal sample via additional generator weights, if available, or by using alternative samples. An additional shape uncertainty is applied to the modelling of the heavy-flavour fraction (HF) of jets in the Z +jets and VV samples. This uncertainty is estimated by separating, using generator-level information, the events with jets originating from b or c quarks from events with jets originating from light quarks and rescaling the HF contribution by 50%. In the 2ℓ channel, the HF uncertainty is uncorrelated between the categories requiring exactly one or at least two b -tagged jets. In the 3ℓ channel, the HF uncertainty is applied in a correlated way across the SR categories and the VV CR, since both regions have the same b -tagging requirements. Uncertainties in the VLQ pair-production cross-section similarly include the independent variation of the factorization and renormalization scales and variations in the PDF and strong coupling constant, following the PDF4LHC [107] prescription with the MSTW 2008 68% CL NNLO, CT10 NNLO [108,109] and NNPDF2.3 5f FFN PDF sets.

7. Results

The compatibility of the data with the background-only hypothesis or with the signal-plus-background hypothesis is tested with a binned likelihood fit of the discriminating variables in the categories of each individual channel. The uncertainties are included as nuisance parameters (NP) with Gaussian constraints in the likelihood fit. Additional NPs are included to take into account the

statistical uncertainties in each bin for each event category due to the limited size of the simulated samples. The likelihood function $L(\mu, \vec{\theta})$ is constructed as a product of Poisson probabilities for each bin in the discriminating variable in each category and depends on the signal-strength factor μ , which multiplies the expected signal cross-section σ , and the set of all NPs. Test statistics are based on the profile-likelihood ratio $\lambda_\mu = L(\mu, \hat{\theta}_\mu) / L(\hat{\mu}, \hat{\theta}_{\hat{\mu}})$ where $\hat{\mu}$ and $\hat{\theta}_{\hat{\mu}}$ are the values of μ and $\vec{\theta}$ that maximize the likelihood function, and $\hat{\theta}_\mu$ are the values of $\vec{\theta}$ that maximize the likelihood for a given μ [110]. Hypothesis tests are performed with RooStats [111] with statistical models implemented using RooFit [112] and HistFactory [113]. The fit procedure was first validated in pseudo-data obtained by the sum of the expected background contributions. Subsequently, the procedure and the modelling of the background were tested by including in the fit those categories in which the benchmark signal contribution is expected to be smaller than 3% of the total background. Before the final full unblinding of the data, an additional check was performed by including in the fit all bins in all analysis categories with expected signal contributions smaller than 5% of the total background in those bins.

A background-only fit to the data, in which μ is set to zero, is performed using q_0 [110] as the test statistic and no significant excess over the background expectation is observed. To obtain the final result, a simultaneous fit of all the regions and categories of both channels is performed. The results are found to be insensitive to variations of the correlation model and the following approach was adopted: all experimental and cross-section uncertainties are treated as fully correlated between the two analysis channels, while the remaining, modelling-related, uncertainties are treated as uncorrelated. Fig. 4 shows the background and observed data yields in all the analysis categories after the combined background-only fit (post-fit). Post-fit distributions of the fitted variables in the background control regions and in selected signal region categories are shown in Fig. 5 for the 2ℓ channel and in Fig. 6 for the 3ℓ channel. The figures include the expected distributions for $T\bar{T}$ signal with $m_T = 1.2$ TeV generated in the singlet configuration. The event yields for the dominant backgrounds in each event category after the background-only fit are also summarized in Table 3, which includes the number of events observed in data. The table also includes the expected yields in number of events for $T\bar{T}$ and $B\bar{B}$ production in the singlet configuration with $m_{\text{VLQ}} = 1.2$ TeV. These yields and their uncertainties are provided before any fit is performed (pre-fit).

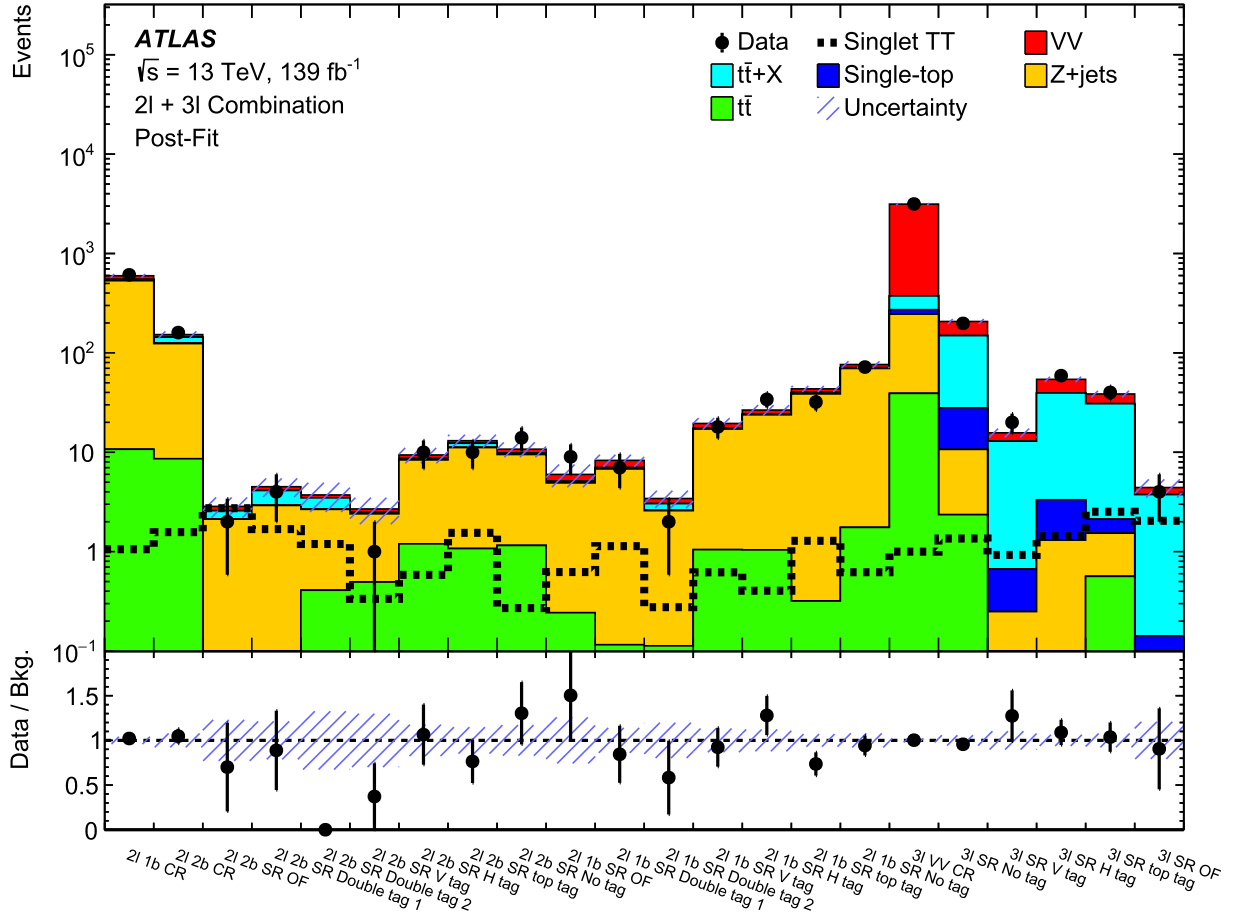


Fig. 4. Summary of data and background yields in all analysis categories after the background-only fit. The expected yields for singlet $T\bar{T}$ signal with $m_T = 1.2$ TeV are also shown for comparison. The bottom panel shows the ratio of the data over the total background prediction. The shaded band includes statistical and post-fit systematic uncertainties.

Table 3

Summary of observed and predicted yields in the control regions and signal region categories. The background prediction is shown after the combined likelihood fit to data under the background-only hypothesis across all control region and signal region categories. The uncertainties include statistical and systematic uncertainties. Due to correlations, the total background uncertainty is not necessarily equal to the sum in quadrature of the uncertainties of the individual background processes. The expected yields for benchmark signals with $m_{V\bar{V}} = 1.2$ TeV obtained by using their theoretical cross-sections are also shown with their pre-fit uncertainties. Dashes indicate negligible yields.

Event category	Data	Total background	VV	$t\bar{t} + X$	Single-top	Z+jets	$t\bar{t}$	Singlet $T\bar{T}$ $m_T = 1.2$ TeV	Singlet $B\bar{B}$ $m_B = 1.2$ TeV
2l 1b CR	610	598 ± 24	50 ± 18	13 ± 4	1.3 ± 0.6	522 ± 30	11 ± 4	1.06 ± 0.08	1.27 ± 0.09
2l 1b SR No tag	72	76 ± 6	5.5 ± 2.0	0.37 ± 0.13	0.8 ± 0.9	68 ± 6	1.8 ± 1.9	0.62 ± 0.13	1.52 ± 0.23
2l 1b SR V tag	18	19.6 ± 2.6	2.2 ± 0.8	0.22 ± 0.08	–	16.1 ± 2.1	1.1 ± 1.3	0.63 ± 0.07	1.31 ± 0.13
2l 1b SR H tag	34	26.6 ± 3.3	2.4 ± 0.9	0.38 ± 0.09	–	22.8 ± 3.0	1.1 ± 1.5	0.41 ± 0.05	0.66 ± 0.09
2l 1b SR top tag	32	43.5 ± 3.1	3.6 ± 1.3	1.25 ± 0.22	–	38.3 ± 3.3	0.3 ± 0.6	1.29 ± 0.14	1.40 ± 0.14
2l 1b SR Double tag 1	7	8.3 ± 1.2	1.3 ± 0.5	0.20 ± 0.09	–	6.7 ± 1.0	0.1 ± 0.4	1.14 ± 0.15	1.05 ± 0.17
2l 1b SR Double tag 2	2	3.4 ± 0.7	0.39 ± 0.19	0.42 ± 0.10	–	2.5 ± 0.5	0.11 ± 0.31	0.27 ± 0.06	0.19 ± 0.06
2l 1b SR OF	9	6.0 ± 1.6	0.9 ± 0.4	0.18 ± 0.05	–	4.7 ± 1.3	0.2 ± 0.7	0.62 ± 0.08	0.60 ± 0.11
2l 2b CR	160	152 ± 12	9 ± 4	18 ± 6	1.2 ± 0.6	115 ± 13	9.0 ± 3.5	1.58 ± 0.10	1.90 ± 0.13
2l 2b SR No tag	14	10.7 ± 1.9	0.9 ± 0.4	0.07 ± 0.08	0.3 ± 0.5	8.3 ± 1.1	1.2 ± 1.4	0.27 ± 0.07	1.11 ± 0.17
2l 2b SR V tag	1	2.7 ± 0.8	0.22 ± 0.13	0.06 ± 0.05	–	1.9 ± 0.5	0.5 ± 0.7	0.34 ± 0.04	0.81 ± 0.08
2l 2b SR H tag	10	9.4 ± 1.6	0.76 ± 0.34	0.26 ± 0.09	–	7.1 ± 1.0	1.2 ± 1.4	0.59 ± 0.09	1.90 ± 0.16
2l 2b SR top tag	10	13.0 ± 1.9	0.8 ± 0.4	1.10 ± 0.30	–	10.0 ± 1.6	1.1 ± 1.2	1.56 ± 0.18	1.97 ± 0.15
2l 2b SR Double tag 1	4	4.5 ± 1.0	0.40 ± 0.25	1.2 ± 0.6	–	2.9 ± 0.8	0.01 ± 0.19	1.71 ± 0.11	1.71 ± 0.18
2l 2b SR Double tag 2	0	3.7 ± 1.2	0.25 ± 0.14	0.78 ± 0.18	–	2.3 ± 0.6	0.4 ± 1.1	1.22 ± 0.10	1.12 ± 0.10
2l 2b SR OF	2	2.8 ± 0.7	0.28 ± 0.15	0.44 ± 0.20	–	2.1 ± 0.6	–	2.76 ± 0.25	2.02 ± 0.26
3l VV CR	3149	3140 ± 70	2770 ± 90	98 ± 9	26.7 ± 1.6	210 ± 60	40 ± 18	1.00 ± 0.14	0.90 ± 0.14
3l SR No tag	198	203 ± 11	59 ± 5	117 ± 10	17.3 ± 0.6	8.5 ± 3.0	2.4 ± 2.0	1.37 ± 0.17	1.31 ± 0.17
3l SR V tag	20	15.3 ± 1.5	2.82 ± 0.34	11.8 ± 1.5	0.42 ± 0.06	0.25 ± 0.11	–	0.94 ± 0.07	0.71 ± 0.09
3l SR H tag	59	52.9 ± 2.8	14.9 ± 1.2	34.7 ± 2.7	2.03 ± 0.14	1.3 ± 0.4	–	1.44 ± 0.10	0.96 ± 0.08
3l SR top tag	40	37.7 ± 2.6	7.9 ± 0.6	27.6 ± 2.4	0.59 ± 0.07	1.0 ± 0.4	0.6 ± 1.2	2.54 ± 0.16	1.73 ± 0.12
3l SR OF	4	4.3 ± 0.9	0.68 ± 0.11	3.4 ± 0.8	0.07 ± 0.03	0.07 ± 0.05	–	2.07 ± 0.16	0.69 ± 0.13

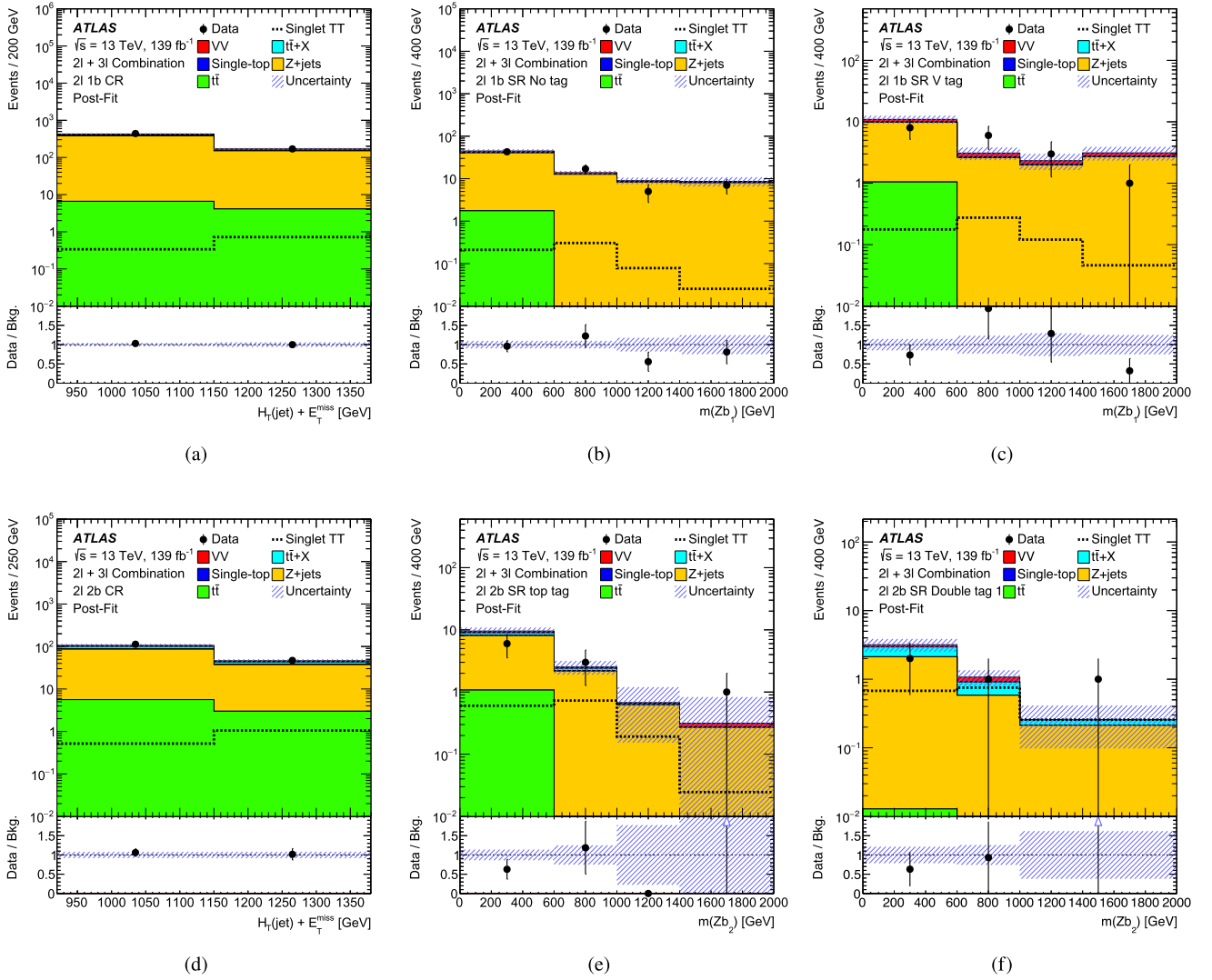


Fig. 5. Distributions of the final discriminants for the 2ℓ channel in the control regions and in selected event categories of the signal regions: (a) control region and (b,c) categories requiring exactly one b -jet or (d) control region and (e,f) categories requiring at least two b -jets. The distributions are shown after the combined background-only fit. The distributions expected for singlet $T\bar{T}$ signal with $m_T = 1.2$ TeV are also shown in overlay. The bottom panels show the ratio of the data over the total background prediction. The two blue triangles indicate points beyond the vertical range. The last bin contains the overflow.

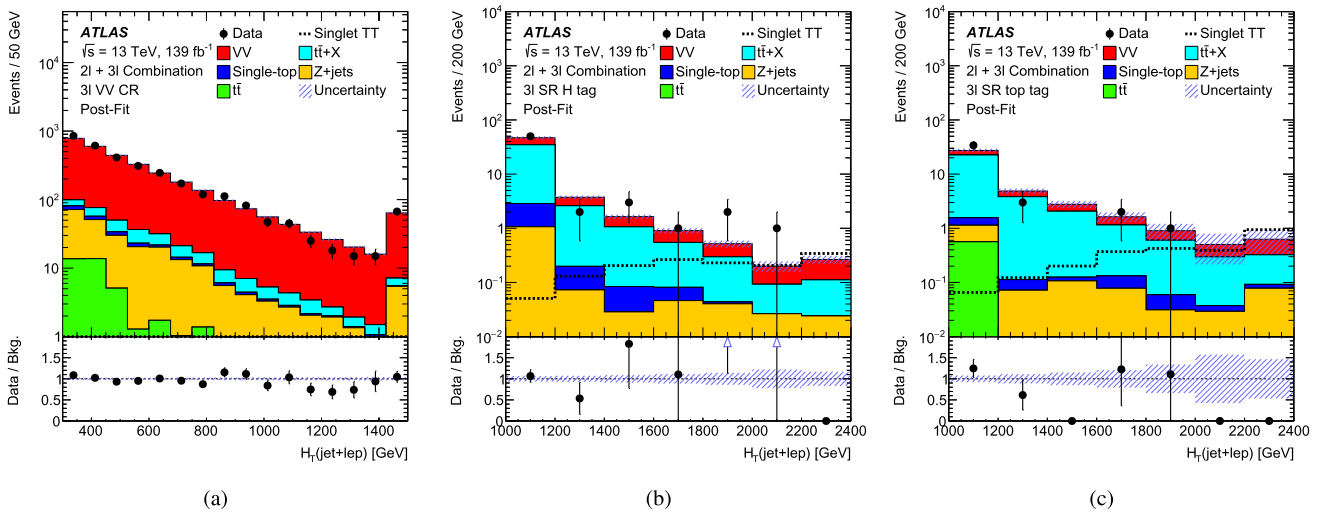


Fig. 6. Distributions of the final discriminants for the 3ℓ channel in the (a) VV control region and in (b,c) selected event categories of the signal region. The distributions are shown after the combined background-only fit. The distributions expected for singlet $T\bar{T}$ signal with $m_T = 1.2$ TeV are also shown in overlay. The bottom panels show the ratio of the data over the total background prediction. The two blue triangles indicate points beyond the vertical range. The last bin contains the overflow.

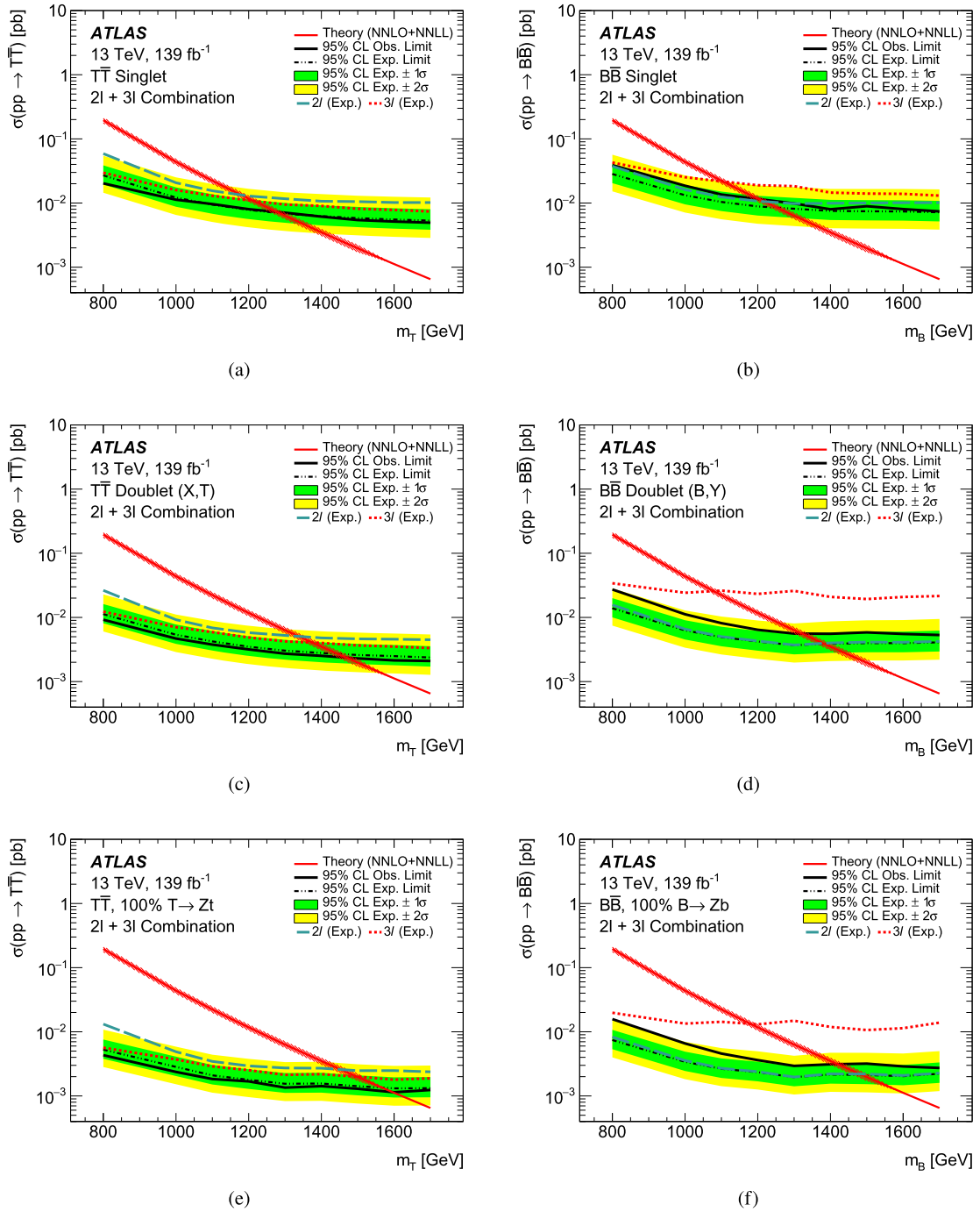


Fig. 7. Expected and observed combined limits at 95% CL on the production cross-section for (a,c, and e) $T\bar{T}$ and (b,d, and f) $B\bar{B}$ for three representative BR compositions. The expected limits for the two individual channels are also shown.

Upper limits on the pair-production cross-section as a function of the VLQ mass are derived at 95% CL for the T and B quarks. These limits are derived by using \tilde{q}_μ [110] as the test statistic with the CL_s technique [114,115] in the asymptotic approximation [110]. The limits are found to agree within a few percent with the limits obtained with pseudo-experiments. For the 1σ uncertainty contours, the limits agree within 10%, with the -1σ band being slightly too narrow in the asymptotic approximation and the $+1\sigma$ band being slightly too wide. The expected and observed upper limits on the cross-section obtained from the combination of the two channels are shown in Fig. 7. To demonstrate the complementarity of the two channels, their individually obtained expected limits are also shown. Three benchmark scenar-

ios for each of B and T are shown, namely the singlet, doublet, and 100% BR configurations, with increasingly high BR to Zb or Zt . Comparisons with the respective theoretical predictions of the cross-sections give the lowest-allowed VLQ masses as summarized in Table 4. The higher signal purity in the 3ℓ channel results in an overall higher sensitivity for T than in the 2ℓ channel, while the larger data sample and finer categorization of the latter manifests in a performance that is dominant in the results for B . For models with 100% BR to the Z boson and a third-generation quark, T (B) masses up to 1.60 TeV (1.42 TeV) are excluded at 95% CL, while for the singlet and doublet configurations, masses are excluded up to 1.27 TeV (1.20 TeV) and up to 1.27 TeV (1.32 TeV), respectively. The combination of the two channels with their fine categorization re-

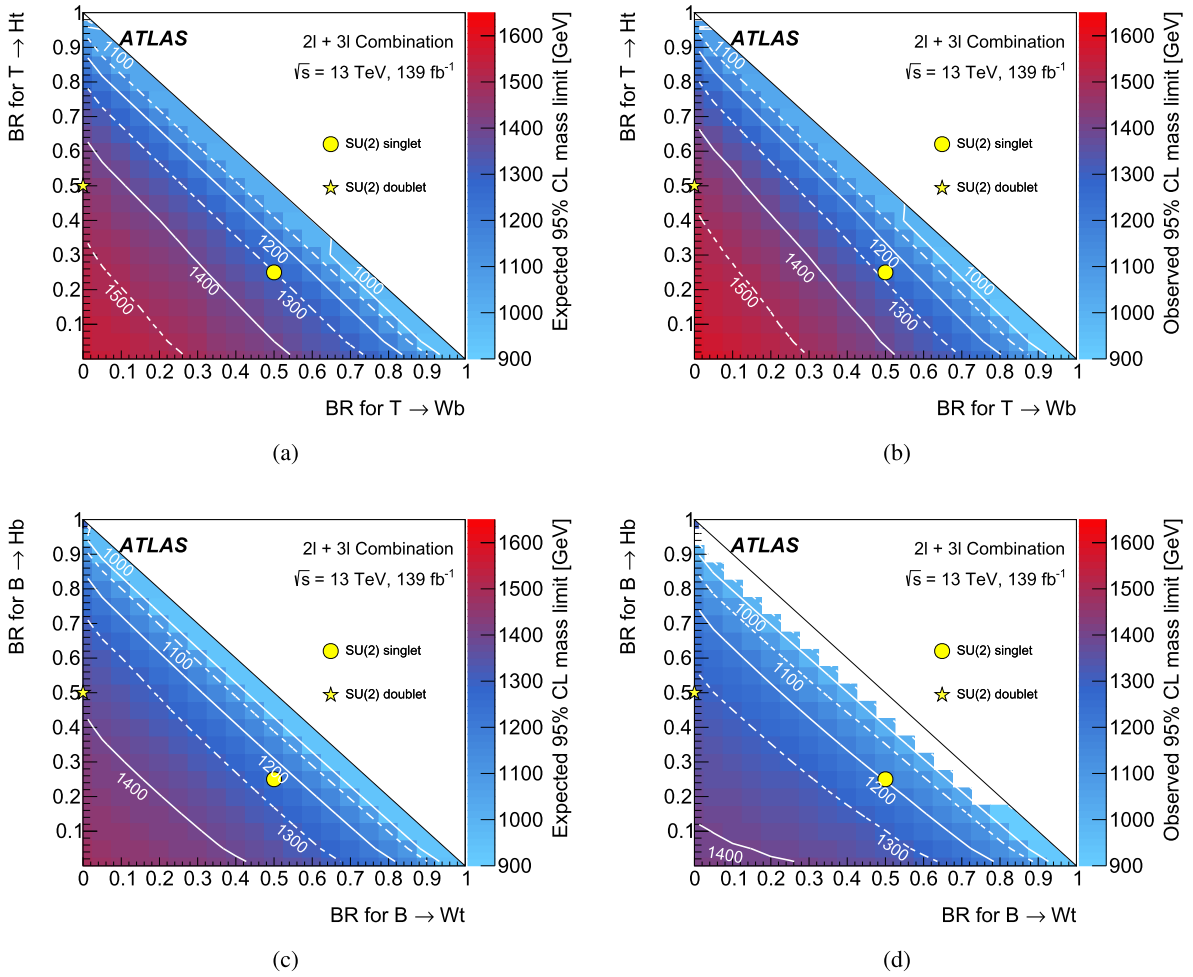


Fig. 8. The (a,c) expected and (b,d) observed lower limits on the T and B masses at 95% CL in the BR plane from the combination of the two analysis channels for the production of (a,b) $T\bar{T}$ and (c,d) $B\bar{B}$, for all BR configurations when assuming a total BR of 100% for $T \rightarrow Zt$, $T \rightarrow Wb$, and $T \rightarrow Ht$ decays or $B \rightarrow Zb$, $B \rightarrow Wt$, and $B \rightarrow Hb$ decays, respectively. The white lines represent the contours of fixed m_{VLQ} .

Table 4

Observed (expected) mass limits in TeV for the T and B singlet, doublet, and models with 100% BR to Z for the two channels and their combination.

Model	Observed (Expected) Mass Limits [TeV]		
	2ℓ	3ℓ	Combination
$T\bar{T}$ Singlet	1.14 (1.16)	1.22 (1.21)	1.27 (1.28)
$T\bar{T}$ Doublet	1.34 (1.32)	1.38 (1.37)	1.46 (1.44)
100% $T \rightarrow Zt$	1.43 (1.43)	1.54 (1.50)	1.60 (1.56)
$B\bar{B}$ Singlet	1.14 (1.21)	1.11 (1.10)	1.20 (1.25)
$B\bar{B}$ Doublet	1.31 (1.37)	1.07 (1.04)	1.32 (1.38)
100% $B \rightarrow Zb$	1.40 (1.47)	1.16 (1.18)	1.42 (1.48)

sults in the observed sensitivity, however, the limits are evidently driven by the categories with high expected signal-to-background fractions, namely, ‘2l 2b SR OF’ (100%) and ‘3l SR OF’ (45%).

Intermediate BR configurations are obtained by reweighting the simulated signal events to any target BR composition using generator-level information and assuming a total BR of 100% for the $T \rightarrow Zt$, $T \rightarrow Wb$, and $T \rightarrow Ht$ decay modes or the $B \rightarrow Zb$, $B \rightarrow Wt$, and $B \rightarrow Hb$ decay modes. The reweighting procedure allows 95% CL upper limits on the production cross-section to be set across the BR plane for each considered VLQ mass. By comparison with the theoretical prediction, lower limits on the T and B masses as a function of the BR composition can be obtained, as shown in Fig. 8. As can be seen, the analysis is sensitive to a large

subset of the possible BR compositions but the limits are more stringent closer to the lower-left corner of the BR plane, and thus for a higher BR for VLQ decays to a Z boson.

8. Conclusions

A search for the pair production of vector-like quarks T or B , with electric charges $(2/3)e$ and $-(1/3)e$, respectively, is presented in which at least one of the VLQs decays into a leptonically decaying Z boson and a third-generation quark. Two orthogonal channels based on the number of selected leptons are separately optimized and their results are statistically combined to obtain the final result. In both channels a multi-class boosted object tagger for large-radius jets reclustered from smaller-radius jets is used to categorize events according to the numbers of V -tags, H -tags, and top-tags. The expected SM background is modelled with MC simulation and a maximum-likelihood fit to the data is performed. No significant excess over the background expectation is observed, and therefore 95% CL upper limits on the T and B pair-production cross-sections are derived.

The combined results exclude T (B) masses up to 1.27 TeV and 1.46 TeV (up to 1.20 TeV and 1.32 TeV) for the singlet and doublet configurations, respectively. For the doublet configuration, the lower limits on the T mass are extended by 90 GeV compared to the most stringent previous ATLAS results, while the limits on the excluded T and B masses are extended by more than 200 GeV compared to the earlier ATLAS analysis using a subset of the Run 2

data. Finally, for exclusive VLQ decays to the Z boson and a third-generation quark, this search marginally extends the limits on the T and B masses to obtain the most stringent limits to date.

Declaration of competing interest

The authors declare that they have no known competing financial interests or personal relationships that could have appeared to influence the work reported in this paper.

Data availability

The data for this manuscript are not available. The values in the plots and tables associated to this article are stored in HEPDATA (<https://www.hepdata.net/>)

Acknowledgements

We thank CERN for the very successful operation of the LHC, as well as the support staff from our institutions without whom ATLAS could not be operated efficiently.

We acknowledge the support of ANPCyT, Argentina; YerPhI, Armenia; ARC, Australia; BMWFW and FWF, Austria; ANAS, Azerbaijan; CNPq and FAPESP, Brazil; NSERC, NRC and CFI, Canada; CERN; ANID, Chile; CAS, MOST and NSFC, China; Minciencias, Colombia; MEYS CR, Czech Republic; DNRF and DNSRC, Denmark; IN2P3-CNRS and CEA-DRF/IRFU, France; SRNSFG, Georgia; BMBF, HGF and MPG, Germany; GSRI, Greece; RGC and Hong Kong SAR, China; ISF and Benozio Center, Israel; INFN, Italy; MEXT and JSPS, Japan; CNRST, Morocco; NWO, Netherlands; RCN, Norway; MEIN, Poland; FCT, Portugal; MNE/IFA, Romania; MESTD, Serbia; MSSR, Slovakia; ARRS and MIZŠ, Slovenia; DSI/NRF, South Africa; MICINN, Spain; SRC and Wallenberg Foundation, Sweden; SERI, SNSF and Cantons of Bern and Geneva, Switzerland; MOST, Taiwan; TENMAK, Türkiye; STFC, United Kingdom; DOE and NSF, United States of America. In addition, individual groups and members have received support from BCKDF, CANARIE, Compute Canada and CRC, Canada; PRIMUS 21/SCI/017 and UNCE SCI/013, Czech Republic; COST, ERC, ERDF, Horizon 2020 and Marie Skłodowska-Curie Actions, European Union; Investissements d'Avenir Labex, Investissements d'Avenir Idex and ANR, France; DFG and AvH Foundation, Germany; Herakleitos, Thales and Aristeia programmes co-financed by EU-ESF and the Greek NSRF, Greece; BSF-NSF and MINERVA, Israel; Norwegian Financial Mechanism 2014-2021, Norway; NCN and NAWA, Poland; La Caixa Banking Foundation, CERCA Programme Generalitat de Catalunya and PROMETEO and GenT Programmes Generalitat Valenciana, Spain; Göran Gustafssons Stiftelse, Sweden; The Royal Society and Leverhulme Trust, United Kingdom.

The crucial computing support from all WLCG partners is acknowledged gratefully, in particular from CERN, the ATLAS Tier-1 facilities at TRIUMF (Canada), NDGF (Denmark, Norway, Sweden), CC-IN2P3 (France), KIT/GridKA (Germany), INFN-CNAF (Italy), NL-T1 (Netherlands), PIC (Spain), ASGC (Taiwan), RAL (UK) and BNL (USA), the Tier-2 facilities worldwide and large non-WLCG resource providers. Major contributors of computing resources are listed in Ref. [116].

References

- [1] ATLAS Collaboration, Observation of a new particle in the search for the standard model Higgs boson with the ATLAS detector at the LHC, *Phys. Lett. B* 716 (2012) 1, arXiv:1207.7214 [hep-ex].
- [2] CMS Collaboration, Observation of a new boson at a mass of 125 GeV with the CMS experiment at the LHC, *Phys. Lett. B* 716 (2012) 30, arXiv:1207.7235 [hep-ex].
- [3] L. Susskind, Dynamics of spontaneous symmetry breaking in the Weinberg-Salam theory, *Phys. Rev. D* 20 (1979) 2619.

- [4] D.B. Kaplan, H. Georgi, S. Dimopoulos, Composite Higgs scalars, *Phys. Lett. B* 136 (1984) 187.
- [5] K. Agashe, R. Contino, A. Pomarol, The minimal composite Higgs model, *Nucl. Phys. B* 719 (2005) 165, arXiv:hep-ph/0412089 [hep-ph].
- [6] N. Arkani-Hamed, A.G. Cohen, E. Katz, A.E. Nelson, The littlest Higgs, *J. High Energy Phys.* 07 (2002) 034, arXiv:hep-ph/0206021 [hep-ph].
- [7] M. Schmaltz, D. Tucker-Smith, Little Higgs theories, *Annu. Rev. Nucl. Part. Sci.* 55 (2005) 229, arXiv:hep-ph/0502182 [hep-ph].
- [8] F. del Aguila, M.J. Bowick, The possibility of new fermions with $\Delta I = 0$ mass, *Nucl. Phys. B* 224 (1983) 107.
- [9] F. del Aguila, M. Perez-Victoria, J. Santiago, Effective description of quark mixing, *Phys. Lett. B* 492 (2000) 98, arXiv:hep-ph/0007160 [hep-ph].
- [10] F. del Aguila, J. Santiago, M. Perez-Victoria, Observable contributions of new exotic quarks to quark mixing, *J. High Energy Phys.* 09 (2000) 011, arXiv:hep-ph/0007316 [hep-ph].
- [11] J.A. Aguilar-Saavedra, Identifying top partners at LHC, *J. High Energy Phys.* 11 (2009) 030, arXiv:0907.3155 [hep-ph].
- [12] ATLAS Collaboration, Combination of the searches for pair-produced vector-like partners of the third-generation quarks at $\sqrt{s} = 13 \text{ TeV}$ with the ATLAS detector, *Phys. Rev. Lett.* 121 (2018) 211801, arXiv:1808.02343 [hep-ex].
- [13] ATLAS Collaboration, Search for pair- and single-production of vector-like quarks in final states with at least one Z boson decaying into a pair of electrons or muons in pp collision data collected with the ATLAS detector, *Phys. Rev. D* 98 (2018) 112010, arXiv:1806.10555 [hep-ex].
- [14] ATLAS Collaboration, Search for pair production of heavy vector-like quarks decaying into hadronic final states in pp collisions at $\sqrt{s} = 13 \text{ TeV}$ with the ATLAS detector, *Phys. Rev. D* 98 (2018) 092005, arXiv:1808.01771 [hep-ex].
- [15] ATLAS Collaboration, Search for new phenomena in events with same-charge leptons and b -jets in pp collisions at $\sqrt{s} = 13 \text{ TeV}$ with the ATLAS detector, *J. High Energy Phys.* 12 (2018) 039, arXiv:1807.11883 [hep-ex].
- [16] ATLAS Collaboration, Search for pair production of heavy vector-like quarks decaying into high- p_T W bosons and top quarks in the lepton-plus-jets final state in pp collisions at $\sqrt{s} = 13 \text{ TeV}$ with the ATLAS detector, *J. High Energy Phys.* 08 (2018) 048, arXiv:1806.01762 [hep-ex].
- [17] ATLAS Collaboration, Search for pair production of up-type vector-like quarks and for four-top-quark events in final states with multiple b -jets with the ATLAS detector, *J. High Energy Phys.* 07 (2018) 089, arXiv:1803.09678 [hep-ex].
- [18] ATLAS Collaboration, Search for pair production of heavy vector-like quarks decaying to high- p_T W bosons and b quarks in the lepton-plus-jets final state in pp collisions at $\sqrt{s} = 13 \text{ TeV}$ with the ATLAS detector, *J. High Energy Phys.* 10 (2017) 141, arXiv:1707.03347 [hep-ex].
- [19] ATLAS Collaboration, Search for pair production of vector-like top quarks in events with one lepton, jets, and missing transverse momentum in $\sqrt{s} = 13 \text{ TeV}$ pp collisions with the ATLAS detector, *J. High Energy Phys.* 08 (2017) 052, arXiv:1705.10751 [hep-ex].
- [20] CMS Collaboration, Search for pair production of vector-like quarks in the fully hadronic final state, *Phys. Rev. D* 100 (2019) 072001, arXiv:1906.11903 [hep-ex].
- [21] CMS Collaboration, Search for vector-like quarks in events with two oppositely charged leptons and jets in proton-proton collisions at $\sqrt{s} = 13 \text{ TeV}$, *Eur. Phys. J. C* 79 (2019) 364, arXiv:1812.09768 [hep-ex].
- [22] CMS Collaboration, Search for vector-like T and B quark pairs in final states with leptons at $\sqrt{s} = 13 \text{ TeV}$, *J. High Energy Phys.* 08 (2018) 177, arXiv:1805.04758 [hep-ex].
- [23] CMS Collaboration, Search for pair production of vector-like quarks in the $bW\bar{b}W$ channel from proton-proton collisions at $\sqrt{s} = 13 \text{ TeV}$, *Phys. Lett. B* 779 (2018) 82, arXiv:1710.01539 [hep-ex].
- [24] CMS Collaboration, A search for bottom-type, vector-like quark pair production in a fully hadronic final state in proton-proton collisions at $\sqrt{s} = 13 \text{ TeV}$, *Phys. Rev. D* 102 (2020) 112004, arXiv:2008.09835 [hep-ex].
- [25] CMS Collaboration, Search for pair production of vector-like quarks in leptonic final states in proton-proton collisions at $\sqrt{s} = 13 \text{ TeV}$, arXiv:2209.07327 [hep-ex], 2022.
- [26] A. Buckley, J.M. Butterworth, L. Corpe, D. Huang, P. Sun, New sensitivity of current LHC measurements to vector-like quarks, *SciPost Phys.* 9 (2020) 069, arXiv:2006.07172 [hep-ph].
- [27] ATLAS Collaboration, Search for large missing transverse momentum in association with one top-quark in proton-proton collisions at $\sqrt{s} = 13 \text{ TeV}$ with the ATLAS detector, *J. High Energy Phys.* 05 (2019) 041, arXiv:1812.09743 [hep-ex].
- [28] ATLAS Collaboration, Search for single production of vector-like quarks decaying into Wb in pp collisions at $\sqrt{s} = 13 \text{ TeV}$ with the ATLAS detector, *J. High Energy Phys.* 05 (2019) 164, arXiv:1812.07343 [hep-ex].
- [29] CMS Collaboration, Search for electroweak production of a vector-like T quark using fully hadronic final states, *J. High Energy Phys.* 01 (2020) 036, arXiv:1909.04721 [hep-ex].
- [30] CMS Collaboration, Search for single production of vector-like quarks decaying to a top quark and a W boson in proton-proton collisions at $\sqrt{s} = 13 \text{ TeV}$, *Eur. Phys. J. C* 79 (2019) 90, arXiv:1809.08597 [hep-ex].

- [31] CMS Collaboration, Search for single production of vector-like quarks decaying to a b quark and a Higgs boson, *J. High Energy Phys.* 06 (2018) 031, arXiv:1802.01486 [hep-ex].
- [32] CMS Collaboration, Search for single production of a vector-like T quark decaying to a top quark and a Z boson in the final state with jets and missing transverse momentum at $\sqrt{s} = 13 \text{ TeV}$, *J. High Energy Phys.* 05 (2022) 093, arXiv:2201.02227 [hep-ex].
- [33] CMS Collaboration, Search for a W' boson decaying to a vector-like quark and a top or bottom quark in the all-jets final state at $\sqrt{s} = 13 \text{ TeV}$, *J. High Energy Phys.* 09 (2022) 088, arXiv:2202.12988 [hep-ex].
- [34] A. Roy, N. Nikiforou, N. Castro, T. Andeen, Novel interpretation strategy for searches of singly produced vectorlike quarks at the LHC, *Phys. Rev. D* 101 (2020) 115027, arXiv:2003.00640 [hep-ph].
- [35] ATLAS Collaboration, The ATLAS experiment at the CERN large hadron collider, *J. Instrum.* 3 (2008) S08003.
- [36] ATLAS Collaboration, ATLAS insertable B-layer technical design report, ATLAS-TDR-19; CERN-LHCC-2010-013, <https://cds.cern.ch/record/1291633>, 2010, Addendum: ATLAS-TDR-19-ADD-1; CERN-LHCC-2012-009, <https://cds.cern.ch/record/1451888>, 2012.
- [37] B. Abbott, et al., Production and integration of the ATLAS insertable B-layer, *J. Instrum.* 13 (2018) T05008, arXiv:1803.00844 [physics.ins-det].
- [38] ATLAS Collaboration, Performance of the ATLAS trigger system in 2015, *Eur. Phys. J. C* 77 (2017) 317, arXiv:1611.09661 [hep-ex].
- [39] ATLAS Collaboration, The ATLAS collaboration software and firmware, ATLSOFT-PUB-2021-001, <https://cds.cern.ch/record/2767187>, 2021.
- [40] ATLAS Collaboration, The ATLAS simulation infrastructure, *Eur. Phys. J. C* 70 (2010) 823, arXiv:1005.4568 [physics.ins-det].
- [41] GEANT4 Collaboration, S. Agostinelli, et al., GEANT4 – a simulation toolkit, *Nucl. Instrum. Methods A* 506 (2003) 250.
- [42] T. Gleisberg, et al., Event generation with SHERPA 1.1, *J. High Energy Phys.* 02 (2009) 007, arXiv:0811.4622 [hep-ph].
- [43] S. Höche, F. Krauss, S. Schumann, F. Siegert, QCD matrix elements and truncated showers, *J. High Energy Phys.* 05 (2009) 053, arXiv:0903.1219 [hep-ph].
- [44] T. Gleisberg, S. Höche, Comix, a new matrix element generator, *J. High Energy Phys.* 12 (2008) 039, arXiv:0808.3674 [hep-ph].
- [45] S. Schumann, F. Krauss, A parton shower algorithm based on Catani–Seymour dipole factorisation, *J. High Energy Phys.* 03 (2008) 038, arXiv:0709.1027 [hep-ph].
- [46] R.D. Ball, et al., Parton distributions for the LHC run II, *J. High Energy Phys.* 04 (2015) 040, arXiv:1410.8849 [hep-ph].
- [47] C. Anastasiou, L. Dixon, K. Melnikov, F. Petriello, High-precision QCD at hadron colliders: electroweak gauge boson rapidity distributions at next-to-next-to leading order, *Phys. Rev. D* 69 (2004) 094008, arXiv:hep-ph/0312266.
- [48] F. Cascioli, P. Maierhöfer, S. Pozzorini, Scattering amplitudes with open loops, *Phys. Rev. Lett.* 108 (2012) 111601, arXiv:1111.5206 [hep-ph].
- [49] S. Höche, F. Krauss, M. Schönherr, F. Siegert, QCD matrix elements + parton showers. The NLO case, *J. High Energy Phys.* 04 (2013) 027, arXiv:1207.5030 [hep-ph].
- [50] J. Alwall, et al., The automated computation of tree-level and next-to-leading order differential cross sections, and their matching to parton shower simulations, *J. High Energy Phys.* 07 (2014) 079, arXiv:1405.0301 [hep-ph].
- [51] T. Sjöstrand, et al., An introduction to PYTHIA 8.2, *Comput. Phys. Commun.* 191 (2015) 159, arXiv:1410.3012 [hep-ph].
- [52] ATLAS Collaboration, ATLAS Pythia 8 tunes to 7 TeV data, ATL-PHYS-PUB-2014-021, <https://cds.cern.ch/record/1966419>, 2014.
- [53] ATLAS Collaboration, Monte Carlo generators for the production of a W or Z/γ^* boson in association with jets at ATLAS in Run 2, ATL-PHYS-PUB-2016-003, <https://cds.cern.ch/record/2120133>, 2016.
- [54] P. Nason, A new method for combining NLO QCD with shower Monte Carlo algorithms, *J. High Energy Phys.* 11 (2004) 040, arXiv:hep-ph/0409146.
- [55] S. Frixione, P. Nason, C. Oleari, Matching NLO QCD computations with parton shower simulations: the POWHEG method, *J. High Energy Phys.* 11 (2007) 070, arXiv:0709.2092 [hep-ph].
- [56] S. Alioli, P. Nason, C. Oleari, E. Re, A general framework for implementing NLO calculations in shower Monte Carlo programs: the POWHEG BOX, *J. High Energy Phys.* 06 (2010) 043, arXiv:1002.2581 [hep-ph].
- [57] J.M. Campbell, R.K. Ellis, P. Nason, E. Re, Top-pair production and decay at NLO matched with parton showers, *J. High Energy Phys.* 04 (2015) 114, arXiv:1412.1828 [hep-ph].
- [58] M. Czakon, A. Mitov, Top++: a program for the calculation of the top-pair cross-section at hadron colliders, *Comput. Phys. Commun.* 185 (2014) 2930, arXiv:1112.5675 [hep-ph].
- [59] M. Czakon, P. Fiedler, A. Mitov, Total top-quark pair-production cross section at hadron colliders through $O(\alpha_s^4)$, *Phys. Rev. Lett.* 110 (2013) 252004, arXiv:1303.6254 [hep-ph].
- [60] M. Beneke, P. Falgari, S. Klein, C. Schwinn, Hadronic top-quark pair production with NNLL threshold resummation, *Nucl. Phys. B* 855 (2012) 695, arXiv:1109.1536 [hep-ph].
- [61] M. Cacciari, M. Czakon, M. Mangano, A. Mitov, P. Nason, Top-pair production at hadron colliders with next-to-next-to-leading logarithmic soft-gluon resummation, *Phys. Lett. B* 710 (2012) 612, arXiv:1111.5869 [hep-ph].
- [62] M. Czakon, A. Mitov, NNLO corrections to top pair production at hadron colliders: the quark-gluon reaction, *J. High Energy Phys.* 01 (2013) 080, arXiv:1210.6832 [hep-ph].
- [63] M. Czakon, A. Mitov, NNLO corrections to top-pair production at hadron colliders: the all-fermionic scattering channels, *J. High Energy Phys.* 12 (2012) 054, arXiv:1207.0236 [hep-ph].
- [64] P. Bärnreuther, M. Czakon, A. Mitov, Percent-level-precision physics at the LHC: next-to-next-to-leading order QCD corrections to $q\bar{q} \rightarrow t\bar{t} + X$, *Phys. Rev. Lett.* 109 (2012) 132001, arXiv:1204.5201 [hep-ph].
- [65] J. Bellm, et al., Herwig 7.0/Herwig++ 3.0 release note, *Eur. Phys. J. C* 76 (2016) 196, arXiv:1512.01178 [hep-ph].
- [66] ATLAS Collaboration, Improvements in $t\bar{t}$ modelling using NLO+PS Monte Carlo generators for Run 2, ATL-PHYS-PUB-2018-009, <https://cds.cern.ch/record/2630327>, 2018.
- [67] R. Frederix, D. Pagani, M. Zaro, Large NLO corrections in $t\bar{t}W^\pm$ and $t\bar{t}t\bar{t}$ hadroproduction from supposedly subleading EW contributions, *J. High Energy Phys.* 02 (2018) 031, arXiv:1711.02116 [hep-ph].
- [68] R. Frederix, E. Re, P. Torrielli, Single-top t -channel hadroproduction in the four-flavour scheme with POWHEG and aMC@NLO, *J. High Energy Phys.* 09 (2012) 130, arXiv:1207.5391 [hep-ph].
- [69] E. Re, Single-top Wt -channel production matched with parton showers using the POWHEG method, *Eur. Phys. J. C* 71 (2011) 1547, arXiv:1009.2450 [hep-ph].
- [70] M. Aliev, et al., HATHOR – HAdronic top and heavy quarks cross section calculator, *Comput. Phys. Commun.* 182 (2011) 1034, arXiv:1007.1327 [hep-ph].
- [71] P. Kant, et al., HatHor for single top-quark production: updated predictions and uncertainty estimates for single top-quark production in hadronic collisions, *Comput. Phys. Commun.* 191 (2015) 74, arXiv:1406.4403 [hep-ph].
- [72] N. Kidonakis, Next-to-next-to-leading-order collinear and soft gluon corrections for t -channel single top quark production, *Phys. Rev. D* 83 (2011) 091503, arXiv:1103.2792 [hep-ph].
- [73] N. Kidonakis, Two-loop soft anomalous dimensions for single top quark associated production with a W^- or H^- , *Phys. Rev. D* 82 (2010) 054018, arXiv:1005.4451 [hep-ph].
- [74] N. Kidonakis, Next-to-next-to-leading logarithm resummation for s -channel single top quark production, *Phys. Rev. D* 81 (2010) 054028, arXiv:1001.5034 [hep-ph].
- [75] S. Frixione, E. Laenen, P. Motylinski, C. White, B.R. Webber, Single-top hadroproduction in association with a W boson, *J. High Energy Phys.* 07 (2008) 029, arXiv:0805.3067 [hep-ph].
- [76] J.A. Aguilar-Saavedra, Protos - PROGRAM for TOP simulations, <http://jaguilar.web.cern.ch/jaguilar/protos>.
- [77] A.D. Martin, W.J. Stirling, R.S. Thorne, G. Watt, Parton distributions for the LHC, *Eur. Phys. J. C* 63 (2009) 189, arXiv:0901.0002 [hep-ph].
- [78] A.D. Martin, W.J. Stirling, R.S. Thorne, G. Watt, Uncertainties on α_s in global PDF analyses and implications for predicted hadronic cross sections, *Eur. Phys. J. C* 64 (2009) 653, arXiv:0905.3531 [hep-ph].
- [79] A.D. Martin, W.J. Stirling, R.S. Thorne, G. Watt, Heavy-quark mass dependence in global PDF analyses and 3- and 4-flavour parton distributions, *Eur. Phys. J. C* 70 (2010) 51, arXiv:1007.2624 [hep-ph].
- [80] ATLAS Collaboration, Electron and photon performance measurements with the ATLAS detector using the 2015–2017 LHC proton–proton collision data, *J. Instrum.* 14 (2019) P12006, arXiv:1908.00005 [hep-ex].
- [81] ATLAS Collaboration, Muon reconstruction and identification efficiency in ATLAS using the full Run 2 pp collision data set at $\sqrt{s} = 13 \text{ TeV}$, *Eur. Phys. J. C* 81 (2021) 578, arXiv:2012.00578 [hep-ex].
- [82] ATLAS Collaboration, Studies of the muon momentum calibration and performance of the ATLAS detector with pp collisions at $\sqrt{s} = 13 \text{ TeV}$, arXiv:2212.07338 [hep-ex], 2022.
- [83] M. Cacciari, G.P. Salam, G. Soyez, The anti- k_r jet clustering algorithm, *J. High Energy Phys.* 04 (2008) 063, arXiv:0802.1189 [hep-ph].
- [84] M. Cacciari, G.P. Salam, G. Soyez, FastJet user manual, *Eur. Phys. J. C* 72 (2012) 1896, arXiv:1111.6097 [hep-ph].
- [85] ATLAS Collaboration, Topological cell clustering in the ATLAS calorimeters and its performance in LHC Run 1, *Eur. Phys. J. C* 77 (2017) 490, arXiv:1603.02934 [hep-ex].
- [86] ATLAS Collaboration, Properties of jets and inputs to jet reconstruction and calibration with the ATLAS detector using proton–proton collisions at $\sqrt{s} = 13 \text{ TeV}$, ATL-PHYS-PUB-2015-036, <https://cds.cern.ch/record/2044564>, 2015.
- [87] ATLAS Collaboration, Jet energy scale measurements and their systematic uncertainties in proton–proton collisions at $\sqrt{s} = 13 \text{ TeV}$ with the ATLAS detector, *Phys. Rev. D* 96 (2017) 072002, arXiv:1703.09665 [hep-ex].
- [88] ATLAS Collaboration, Performance of pile-up mitigation techniques for jets in pp collisions at $\sqrt{s} = 8 \text{ TeV}$ using the ATLAS detector, *Eur. Phys. J. C* 76 (2016) 581, arXiv:1510.03823 [hep-ex].
- [89] ATLAS Collaboration, ATLAS b -jet identification performance and efficiency measurement with $t\bar{t}$ events in pp collisions at $\sqrt{s} = 13 \text{ TeV}$, *Eur. Phys. J. C* 79 (2019) 970, arXiv:1907.05120 [hep-ex].
- [90] ATLAS Collaboration, Performance of missing transverse momentum reconstruction with the ATLAS detector using proton–proton collisions at $\sqrt{s} = 13 \text{ TeV}$, *Eur. Phys. J. C* 78 (2018) 903, arXiv:1802.08168 [hep-ex].

- [91] B. Nachman, P. Nef, A. Schwartzman, M. Swiatlowski, C. Wanotayaroj, Jets from jets: re-clustering as a tool for large radius jet reconstruction and grooming at the LHC, *J. High Energy Phys.* 02 (2015) 075, arXiv:1407.2922 [hep-ph].
- [92] D. Krohn, J. Thaler, L.-T. Wang, Jet trimming, *J. High Energy Phys.* 02 (2010) 084, arXiv:0912.1342 [hep-ph].
- [93] ATLAS Collaboration, Performance of the ATLAS muon triggers in Run 2, *J. Instrum.* 15 (2020) P09015, arXiv:2004.13447 [hep-ex].
- [94] ATLAS Collaboration, Performance of electron and photon triggers in ATLAS during LHC Run 2, *Eur. Phys. J. C* 80 (2020) 47, arXiv:1909.00761 [hep-ex].
- [95] F. Chollet, et al., Keras, <https://keras.io>, 2015.
- [96] Martín Abadi, et al., TensorFlow: large-scale machine learning on heterogeneous systems, <https://www.tensorflow.org/>, 2015.
- [97] K. Agashe, H. Davoudiasl, G. Perez, A. Soni, Warped gravitons at the CERN LHC and beyond, *Phys. Rev. D* 76 (2007) 036006, arXiv:hep-ph/0701186.
- [98] J. Schmidhuber, Deep learning in neural networks: an overview, *Neural Netw.* 61 (2015) 85.
- [99] I. Goodfellow, Y. Bengio, A. Courville, Deep Learning, MIT Press, 2016, <http://www.deeplearningbook.org>.
- [100] D.P. Kingma, J. Ba, Adam: a method for stochastic optimization, arXiv:1412.6980 [cs.LG], 2014.
- [101] ATLAS Collaboration, Optimisation of large-radius jet reconstruction for the ATLAS detector in 13 TeV proton–proton collisions, *Eur. Phys. J. C* 81 (2020) 334, arXiv:2009.04986 [hep-ex].
- [102] ATLAS Collaboration, Measurement of the c -jet mistagging efficiency in $t\bar{t}$ events using pp collision data at $\sqrt{s} = 13$ TeV collected with the ATLAS detector, *Eur. Phys. J. C* 82 (2021) 95, arXiv:2109.10627 [hep-ex].
- [103] ATLAS Collaboration, Calibration of light-flavour b -jet mistagging rates using ATLAS proton–proton collision data at $\sqrt{s} = 13$ TeV, ATLAS-CONF-2018-006, <https://cds.cern.ch/record/2314418>, 2018.
- [104] ATLAS Collaboration, Luminosity determination in pp collisions at $\sqrt{s} = 13$ TeV using the ATLAS detector at the LHC, ATLAS-CONF-2019-021, <https://cds.cern.ch/record/2677054>, 2019.
- [105] ATLAS Collaboration, Measurements of the inclusive and differential production cross sections of a top-quark-antiquark pair in association with a Z boson at $\sqrt{s} = 13$ TeV with the ATLAS detector, *Eur. Phys. J. C* 81 (2021) 737, arXiv:2103.12603 [hep-ex].
- [106] ATLAS Collaboration, Higgs boson production cross-section measurements and their EFT interpretation in the 4ℓ decay channel at $\sqrt{s} = 13$ TeV with the ATLAS detector, *Eur. Phys. J. C* 80 (2020) 957, arXiv:2004.03447 [hep-ex], Erratum: *Eur. Phys. J. C* 81 (2021) 29.
- [107] J. Butterworth, et al., PDF4LHC recommendations for LHC Run II, *J. Phys. G* 43 (2016) 023001, arXiv:1510.03865 [hep-ph].
- [108] H.-L. Lai, et al., New parton distributions for collider physics, *Phys. Rev. D* 82 (2010) 074024, arXiv:1007.2241 [hep-ph].
- [109] J. Gao, et al., CT10 next-to-next-to-leading order global analysis of QCD, *Phys. Rev. D* 89 (2014) 033009, arXiv:1302.6246 [hep-ph].
- [110] G. Cowan, K. Cranmer, E. Gross, O. Vitells, Asymptotic formulae for likelihood-based tests of new physics, *Eur. Phys. J. C* 71 (2011) 1554, arXiv:1007.1727 [physics.data-an], Erratum: *Eur. Phys. J. C* 73 (2013) 2501.
- [111] L. Moneta, et al., The RooStats project, in: T. Speer, et al. (Eds.), PoS ACAT2010 (2010) 057, arXiv:1009.1003 [physics.data-an].
- [112] W. Verkerke, D. Kirkby, The RooFit toolkit for data modeling, arXiv:physics/0306116 [physics.data-an], 2003.
- [113] K. Cranmer, G. Lewis, L. Moneta, A. Shibata, W. Verkerke, HistFactory: a tool for creating statistical models for use with RooFit and RooStats, tech. Rep., New York U., 2012, <https://cds.cern.ch/record/1456844>.
- [114] T. Junk, Confidence level computation for combining searches with small statistics, *Nucl. Instrum. Methods A* 434 (1999) 435, arXiv:hep-ex/9902006 [hep-ex].
- [115] A.L. Read, Presentation of search results: the CL_s technique, *J. Phys. G* 28 (2002) 2693.
- [116] ATLAS Collaboration, ATLAS computing acknowledgements, ATL-SOFT-PUB-2021-003, <https://cds.cern.ch/record/2776662>, 2021.

The ATLAS Collaboration

G. Aad¹⁰⁰, B. Abbott¹¹⁷, D.C. Abbott¹⁰¹, A. Abed Abud³⁴, K. Abeling⁵³, D.K. Abhayasinghe⁹², S.H. Abidi²⁷, H. Abramowicz¹⁴⁹, H. Abreu¹⁴⁸, Y. Abulaiti⁵, A.C. Abusleme Hoffman^{134a}, B.S. Acharya^{66a,66b,q}, B. Achkar⁵³, L. Adam⁹⁸, C. Adam Bourdarios⁴, L. Adamczyk^{82a}, L. Adamek¹⁵³, S.V. Addepalli²⁴, J. Adelman¹¹³, A. Adiguzel^{11c,ac}, S. Adorni⁵⁴, T. Adye¹³¹, A.A. Affolder¹³³, Y. Afik¹⁴⁸, C. Agapopoulou⁶⁴, M.N. Agaras¹², J. Agarwala^{70a,70b}, A. Aggarwal¹¹¹, C. Agheorghiesei^{25c}, J.A. Aguilar-Saavedra^{127f,127a,ab}, A. Ahmad³⁴, F. Ahmadov^{36,z}, W.S. Ahmed¹⁰², X. Ai⁴⁶, G. Aielli^{73a,73b}, I. Aizenberg¹⁶⁶, S. Akatsuka⁸⁴, M. Akbiyik⁹⁸, T.P.A. Åkesson⁹⁵, A.V. Akimov³⁵, K. Al Khoury³⁹, G.L. Alberghi^{21b}, J. Albert¹⁶², P. Albicocco⁵¹, M.J. Alconada Verzini⁸⁷, S. Alderweireldt⁵⁰, M. Aleksa³⁴, I.N. Aleksandrov³⁶, C. Alexa^{25b}, T. Alexopoulos⁹, A. Alfonsi¹¹², F. Alfonsi^{21b}, M. Alhroob¹¹⁷, B. Ali¹²⁹, S. Ali¹⁴⁶, M. Aliev³⁵, G. Alimonti^{68a}, C. Allaire³⁴, B.M.M. Allbrooke¹⁴⁴, P.P. Allport¹⁹, A. Aloisio^{69a,69b}, F. Alonso⁸⁷, C. Alpigiani¹³⁶, E. Alunno Camelia^{73a,73b}, M. Alvarez Estevez⁹⁷, M.G. Alviggi^{69a,69b}, Y. Amaral Coutinho^{79b}, A. Ambler¹⁰², L. Ambroz¹²³, C. Amelung³⁴, D. Amidei¹⁰⁴, S.P. Amor Dos Santos^{127a}, S. Amoroso⁴⁶, C.S. Amrouche⁵⁴, C. Anastopoulos¹³⁷, N. Andari¹³², T. Andeen¹⁰, J.K. Anders¹⁸, S.Y. Andrean^{45a,45b}, A. Andreazza^{68a,68b}, S. Angelidakis⁸, A. Angerami³⁹, A.V. Anisenkov³⁵, A. Annovi^{71a}, C. Antel⁵⁴, M.T. Anthony¹³⁷, E. Antipov¹¹⁸, M. Antonelli⁵¹, D.J.A. Antrim^{16a}, F. Anulli^{72a}, M. Aoki⁸⁰, J.A. Aparisi Pozo¹⁶⁰, M.A. Aparo¹⁴⁴, L. Aperio Bella⁴⁶, N. Aranzabal³⁴, V. Araujo Ferraz^{79a}, C. Arcangeletti⁵¹, A.T.H. Arce⁴⁹, E. Arena⁸⁹, J.-F. Arguin¹⁰⁶, S. Argyropoulos⁵², J.-H. Arling⁴⁶, A.J. Armbruster³⁴, A. Armstrong¹⁵⁷, O. Arnaez¹⁵³, H. Arnold³⁴, Z.P. Arrubarrena Tame¹⁰⁷, G. Artoni¹²³, H. Asada¹⁰⁹, K. Asai¹¹⁵, S. Asai¹⁵¹, N.A. Asbah⁵⁹, E.M. Asimakopoulou¹⁵⁸, L. Asquith¹⁴⁴, J. Assahsah^{33d}, K. Assamagan²⁷, R. Astalos^{26a}, R.J. Atkin^{31a}, M. Atkinson¹⁵⁹, N.B. Atlay¹⁷, H. Atmani^{60b}, P.A. Atlasidha¹⁰⁴, K. Augsten¹²⁹, S. Auricchio^{69a,69b}, V.A. Austrup¹⁶⁸, G. Avner¹⁴⁸, G. Avolio³⁴, M.K. Ayoub^{13c}, G. Azuelos^{106,ah}, D. Babal^{26a}, H. Bachacou¹³², K. Bachas¹⁵⁰, A. Bachiu³², F. Backman^{45a,45b}, A. Badea⁵⁹, P. Bagnaia^{72a,72b}, H. Bahrasemani¹⁴⁰, A.J. Bailey¹⁶⁰, V.R. Bailey¹⁵⁹, J.T. Baines¹³¹, C. Bakalis⁹, O.K. Baker¹⁶⁹, P.J. Bakker¹¹², E. Bakos¹⁴, D. Bakshi Gupta⁷, S. Balaji¹⁴⁵, R. Balasubramanian¹¹², E.M. Baldin³⁵, P. Balek¹³⁰, E. Ballabene^{68a,68b}, F. Balli¹³², W.K. Balunas¹²³, J. Balz⁹⁸, E. Banas⁸³, M. Bandieramonte¹²⁶, A. Bandyopadhyay¹⁷, S. Bansal²², L. Barak¹⁴⁹, E.L. Barberio¹⁰³, D. Barberis^{55b,55a}, M. Barbero¹⁰⁰, G. Barbour⁹³, K.N. Barends^{31a}, T. Barillari¹⁰⁸, M.-S. Barisits³⁴, J. Barkeloo¹²⁰, T. Barklow¹⁴¹, B.M. Barnett¹³¹, R.M. Barnett^{16a}, A. Baroncelli^{60a}, G. Barone²⁷, A.J. Barr¹²³, L. Barranco Navarro^{45a,45b}, F. Barreiro⁹⁷, J. Barreiro Guimarães da Costa^{13a}, U. Barron¹⁴⁹, S. Barsov³⁵, F. Bartels^{61a}, R. Bartoldus¹⁴¹,

G. Bartolini¹⁰⁰, A.E. Barton⁸⁸, P. Bartos^{26a}, A. Basalaev⁴⁶, A. Basan⁹⁸, I. Bashta^{74a,74b}, A. Bassalat^{64.ad}, M.J. Basso¹⁵³, C.R. Basson⁹⁹, R.L. Bates⁵⁷, S. Batlamous^{33e}, J.R. Batley³⁰, B. Batool¹³⁹, M. Battaglia¹³³, M. Bauce^{72a,72b}, F. Bauer^{132.*}, P. Bauer²², H.S. Bawa²⁹, A. Bayirli^{11c}, J.B. Beacham⁴⁹, T. Beau¹²⁴, P.H. Beauchemin¹⁵⁶, F. Becherer⁵², P. Bechtler²², H.P. Beck^{18.r}, K. Becker¹⁶⁴, C. Becot⁴⁶, A.J. Beddall^{11a}, V.A. Bednyakov³⁶, C.P. Bee¹⁴³, T.A. Beermann¹⁶⁸, M. Begalli^{79b}, M. Begel²⁷, A. Behera¹⁴³, J.K. Behr⁴⁶, C. Beirao Da Cruz E Silva³⁴, J.F. Beirer^{53,34}, F. Beisiegel²², M. Belfkir⁴, G. Bella¹⁴⁹, L. Bellagamba^{21b}, A. Bellerive³², P. Bellos¹⁹, K. Beloborodov³⁵, K. Belotskiy³⁵, N.L. Belyaev³⁵, D. Benchekroun^{33a}, Y. Benhammou¹⁴⁹, D.P. Benjamin²⁷, M. Benoit²⁷, J.R. Bensinger²⁴, S. Bentvelsen¹¹², L. Beresford³⁴, M. Beretta⁵¹, D. Berge¹⁷, E. Bergeaas Kuutmann¹⁵⁸, N. Berger⁴, B. Bergmann¹²⁹, L.J. Bergsten²⁴, J. Beringer^{16a}, S. Berlendis⁶, G. Bernardi¹²⁴, C. Bernius¹⁴¹, F.U. Bernlochner²², T. Berry⁹², P. Berta¹³⁰, A. Berthold⁴⁸, I.A. Bertram⁸⁸, O. Bessidskaia Bylund¹⁶⁸, S. Bethke¹⁰⁸, A. Betti⁴², A.J. Bevan⁹¹, S. Bhatta¹⁴³, D.S. Bhattacharya¹⁶³, P. Bhattarai²⁴, V.S. Bhopatkar⁵, R. Bi¹²⁶, R.M. Bianchi¹²⁶, O. Biebel¹⁰⁷, R. Bielski¹²⁰, N.V. Biesuz^{71a,71b}, M. Biglietti^{74a}, T.R.V. Billoud¹²⁹, M. Bindi⁵³, A. Bingul^{11d}, C. Bini^{72a,72b}, S. Biondi^{21b,21a}, A. Biondini⁸⁹, C.J. Birch-sykes⁹⁹, G.A. Bird^{19,131}, M. Birman¹⁶⁶, T. Bisanz³⁴, D. Biswas^{167.l}, A. Bitadze⁹⁹, C. Bittrich⁴⁸, K. Bjørke¹²², I. Bloch⁴⁶, C. Blocker²⁴, A. Blue⁵⁷, U. Blumenschein⁹¹, J. Blumenthal⁹⁸, G.J. Bobbink¹¹², V.S. Bobrovnikov³⁵, M. Boehler⁵², D. Bogavac¹², A.G. Bogdanchikov³⁵, C. Bohm^{45a}, V. Boisvert⁹², P. Bokan⁴⁶, T. Bold^{82a}, M. Bomben¹²⁴, M. Bona⁹¹, M. Boonekamp¹³², C.D. Booth⁹², A.G. Borbély⁵⁷, H.M. Borecka-Bielska¹⁰⁶, L.S. Borgna⁹³, G. Borissov⁸⁸, D. Bortoletto¹²³, D. Boscherini^{21b}, M. Bosman¹², J.D. Bossio Sola³⁴, K. Bouaouda^{33a}, J. Boudreau¹²⁶, E.V. Bouhova-Thacker⁸⁸, D. Boumediene³⁸, R. Bouquet¹²⁴, A. Boveia¹¹⁶, J. Boyd³⁴, D. Boye²⁷, I.R. Boyko³⁶, A.J. Bozson⁹², J. Bracinik¹⁹, N. Brahimi^{60d,60c}, G. Brandt¹⁶⁸, O. Brandt³⁰, F. Braren⁴⁶, B. Brau¹⁰¹, J.E. Brau¹²⁰, W.D. Breaden Madden⁵⁷, K. Brendlinger⁴⁶, R. Brenner¹⁶⁶, L. Brenner³⁴, R. Brenner¹⁵⁸, S. Bressler¹⁶⁶, B. Brickwedde⁹⁸, D.L. Briglin¹⁹, D. Britton⁵⁷, D. Britzger¹⁰⁸, I. Brock²², R. Brock¹⁰⁵, G. Brooijmans³⁹, W.K. Brooks^{134e}, E. Brost²⁷, P.A. Bruckman de Renstrom⁸³, B. Brüers⁴⁶, D. Bruncko^{26b.*}, A. Bruni^{21b}, G. Bruni^{21b}, M. Bruschi^{21b}, N. Bruscinò^{72a,72b}, L. Bryngemark¹⁴¹, T. Buanes¹⁵, Q. Buat¹⁴³, P. Buchholz¹³⁹, A.G. Buckley⁵⁷, I.A. Budagov^{36.*}, M.K. Bugge¹²², O. Bulekov³⁵, B.A. Bullard⁵⁹, T.J. Burch¹¹³, S. Burdin⁸⁹, C.D. Burgard⁴⁶, A.M. Burger¹¹⁸, B. Burghgrave⁷, J.T.P. Burr⁴⁶, C.D. Burton¹⁰, J.C. Burzynski¹⁰¹, V. Büscher⁹⁸, P.J. Bussey⁵⁷, J.M. Butler²³, C.M. Buttar⁵⁷, J.M. Butterworth⁹³, W. Buttinger¹³¹, C.J. Buxo Vazquez¹⁰⁵, A.R. Buzykaev³⁵, G. Cabras^{21b}, S. Cabrera Urbán¹⁶⁰, D. Caforio⁵⁶, H. Cai¹²⁶, V.M.M. Cairo¹⁴¹, O. Cakir^{3a}, N. Calace³⁴, P. Calafiura^{16a}, G. Calderini¹²⁴, P. Calfayan⁶⁵, G. Callea⁵⁷, L.P. Caloba^{79b}, S. Calvente Lopez⁹⁷, D. Calvet³⁸, S. Calvet³⁸, T.P. Calvet¹⁰⁰, M. Calvetti^{71a,71b}, R. Camacho Toro¹²⁴, S. Camarda³⁴, D. Camarero Munoz⁹⁷, P. Camarri^{73a,73b}, M.T. Camerlingo^{74a,74b}, D. Cameron¹²², C. Camincher¹⁶², M. Campanelli⁹³, A. Camplani⁴⁰, V. Canale^{69a,69b}, A. Canesse¹⁰², M. Cano Bret⁷⁷, J. Cantero¹¹⁸, Y. Cao¹⁵⁹, F. Capocasa²⁴, M. Capua^{41b,41a}, A. Carbone^{68a,68b}, R. Cardarelli^{73a}, J.C.J. Cardenas⁷, F. Cardillo¹⁶⁰, T. Carli³⁴, G. Carlino^{69a}, B.T. Carlson¹²⁶, E.M. Carlson^{162,154a}, L. Carminati^{68a,68b}, M. Carnesale^{72a,72b}, R.M.D. Carney¹⁴¹, S. Caron¹¹¹, E. Carquin^{134e}, S. Carrá⁴⁶, G. Carratta^{21b,21a}, J.W.S. Carter¹⁵³, T.M. Carter⁵⁰, D. Casadei^{31c}, M.P. Casado^{12.i}, A.F. Casha¹⁵³, E.G. Castiglia¹⁶⁹, F.L. Castillo^{61a}, L. Castillo Garcia¹², V. Castillo Gimenez¹⁶⁰, N.F. Castro^{127a,127e}, A. Catinaccio³⁴, J.R. Catmore¹²², A. Cattai³⁴, V. Cavaliere²⁷, N. Cavalli^{21b,21a}, V. Cavasinni^{71a,71b}, E. Celebi^{11b}, F. Celli¹²³, M.S. Centonze^{67a,67b}, K. Cerny¹¹⁹, A.S. Cerqueira^{79a}, A. Cerri¹⁴⁴, L. Cerrito^{73a,73b}, F. Cerutti^{16a}, A. Cervelli^{21b}, S.A. Cetin^{11b}, Z. Chadi^{33a}, D. Chakraborty¹¹³, M. Chala^{127f}, J. Chan¹⁶⁷, W.S. Chan¹¹², W.Y. Chan⁸⁹, J.D. Chapman³⁰, B. Chargeishvili^{147b}, D.G. Charlton¹⁹, T.P. Charman⁹¹, M. Chatterjee¹⁸, S. Chekanov⁵, S.V. Chekulaev^{154a}, G.A. Chelkov^{36.a}, A. Chen¹⁰⁴, B. Chen¹⁴⁹, C. Chen^{60a}, C.H. Chen⁷⁸, H. Chen^{13c}, H. Chen²⁷, J. Chen^{60c}, J. Chen²⁴, S. Chen¹²⁵, S.J. Chen^{13c}, X. Chen^{60c}, X. Chen^{13b.ag}, Y. Chen^{60a}, Y-H. Chen⁴⁶, C.L. Cheng¹⁶⁷, H.C. Cheng^{62a}, A. Cheplakov³⁶, E. Cheremushkina⁴⁶, E. Cherepanova³⁶, R. Cherkaoui El Moursli^{33e}, E. Cheu⁶, K. Cheung⁶³, L. Chevalier¹³², V. Chiarella⁵¹, G. Chiarelli^{71a}, G. Chiodini^{67a}, A.S. Chisholm¹⁹, A. Chitan^{25b}, Y.H. Chiu¹⁶², M.V. Chizhov^{36.s}, K. Choi¹⁰, A.R. Chomont^{72a,72b}, Y. Chou¹⁰¹, E.Y.S. Chow¹¹², L.D. Christopher^{31f}, M.C. Chu^{62a}, X. Chu^{13a,13d}, J. Chudoba¹²⁸, J.J. Chwastowski⁸³, D. Cieri¹⁰⁸, K.M. Ciesla⁸³, V. Cindro⁹⁰, I.A. Cioară^{25b}, A. Ciocio^{16a}, F. Ciroto^{69a,69b}, Z.H. Citron^{166.m}, M. Citterio^{68a}, D.A. Ciubotaru^{25b}, B.M. Ciungu¹⁵³, A. Clark⁵⁴, P.J. Clark⁵⁰, J.M. Clavijo Columbie⁴⁶, S.E. Clawson⁹⁹, C. Clement^{45a,45b}, L. Clissa^{21b,21a}, Y. Coadou¹⁰⁰, M. Cobal^{66a,66c}, A. Coccaro^{55b}, J. Cochran⁷⁸, R.F. Coelho Barrue^{127a}, R. Coelho Lopes De Sa¹⁰¹,

S. Coelli ^{68a}, H. Cohen ¹⁴⁹, A.E.C. Coimbra ³⁴, B. Cole ³⁹, J. Collot ⁵⁸, P. Conde Muiño ^{127a,127h}, S.H. Connell ^{31c}, I.A. Connelly ⁵⁷, E.I. Conroy ¹²³, F. Conventi ^{69a,ai}, H.G. Cooke ¹⁹, A.M. Cooper-Sarkar ¹²³, F. Cormier ¹⁶¹, L.D. Corpe ³⁴, M. Corradi ^{72a,72b}, E.E. Corrigan ⁹⁵, F. Corriveau ^{102,y}, M.J. Costa ¹⁶⁰, F. Costanza ⁴, D. Costanzo ¹³⁷, B.M. Cote ¹¹⁶, G. Cowan ⁹², J.W. Cowley ³⁰, K. Cranmer ¹¹⁴, S. Crépe-Renaudin ⁵⁸, F. Crescioli ¹²⁴, M. Cristinziani ¹³⁹, M. Cristoforetti ^{75a,75b,c}, V. Croft ¹⁵⁶, G. Crosetti ^{41b,41a}, A. Cueto ³⁴, T. Cuhadar Donszelmann ¹⁵⁷, H. Cui ^{13a,13d}, A.R. Cukierman ¹⁴¹, W.R. Cunningham ⁵⁷, P. Czodrowski ³⁴, M.M. Czurylo ^{61b}, M.J. Da Cunha Sargedas De Sousa ^{60a}, J.V. Da Fonseca Pinto ^{79b}, C. Da Via ⁹⁹, W. Dabrowski ^{82a}, T. Dado ⁴⁷, S. Dahbi ^{31f}, T. Dai ¹⁰⁴, C. Dallapiccola ¹⁰¹, M. Dam ⁴⁰, G. D'amen ²⁷, V. D'Amico ^{74a,74b}, J. Damp ⁹⁸, J.R. Dandoy ¹²⁵, M.F. Daneri ²⁸, M. Danninger ¹⁴⁰, V. Dao ³⁴, G. Darbo ^{55b}, S. Darmora ⁵, A. Dattagupta ¹²⁰, S. D'Auria ^{68a,68b}, C. David ^{154b}, T. Davidek ¹³⁰, D.R. Davis ⁴⁹, B. Davis-Purcell ³², I. Dawson ⁹¹, K. De ⁷, R. De Asmundis ^{69a}, M. De Beurs ¹¹², S. De Castro ^{21b,21a}, N. De Groot ¹¹¹, P. de Jong ¹¹², H. De la Torre ¹⁰⁵, A. De Maria ^{13c}, D. De Pedis ^{72a}, A. De Salvo ^{72a}, U. De Sanctis ^{73a,73b}, M. De Santis ^{73a,73b}, A. De Santo ¹⁴⁴, J.B. De Vivie De Regie ⁵⁸, D.V. Dedovich ³⁶, J. Degens ¹¹², A.M. Deiana ⁴², J. Del Peso ⁹⁷, Y. Delabat Diaz ⁴⁶, F. Deliot ¹³², C.M. Delitzsch ⁶, M. Della Pietra ^{69a,69b}, D. Della Volpe ⁵⁴, A. Dell'Acqua ³⁴, L. Dell'Asta ^{68a,68b}, M. Delmastro ⁴, P.A. Delsart ⁵⁸, S. Demers ¹⁶⁹, M. Demichev ³⁶, S.P. Denisov ³⁵, L. D'Eramo ¹¹³, D. Derendarz ⁸³, J.E. Derkaoui ^{33d}, F. Derue ¹²⁴, P. Dervan ⁸⁹, K. Desch ²², K. Dette ¹⁵³, C. Deutsch ²², P.O. Deviveiros ³⁴, F.A. Di Bello ^{72a,72b}, A. Di Ciaccio ^{73a,73b}, L. Di Ciaccio ⁴, C. Di Donato ^{69a,69b}, A. Di Girolamo ³⁴, G. Di Gregorio ^{71a,71b}, A. Di Luca ^{75a,75b}, B. Di Micco ^{74a,74b}, R. Di Nardo ^{74a,74b}, C. Diaconu ¹⁰⁰, F.A. Dias ¹¹², T. Dias Do Vale ^{127a}, M.A. Diaz ^{134a,134b}, F.G. Diaz Capriles ²², J. Dickinson ^{16a}, M. Didenko ¹⁶⁰, E.B. Diehl ¹⁰⁴, J. Dietrich ¹⁷, S. Díez Cornell ⁴⁶, C. Diez Pardos ¹³⁹, A. Dimitrievska ^{16a}, W. Ding ^{13b}, J. Dingfelder ²², I.-M. Dinu ^{25b}, S.J. Dittmeier ^{61b}, F. Dittus ³⁴, F. Djama ¹⁰⁰, T. Djobava ^{147b}, J.I. Djuvsland ¹⁵, M.A.B. Do Vale ¹³⁵, D. Dodsworth ²⁴, C. Doglioni ⁹⁵, J. Dolejsi ¹³⁰, Z. Dolezal ¹³⁰, M. Donadelli ^{79c}, B. Dong ^{60c}, J. Donini ³⁸, A. D'Onofrio ^{13c}, M. D'Onofrio ⁸⁹, J. Dopke ¹³¹, A. Doria ^{69a}, M.T. Dova ⁸⁷, A.T. Doyle ⁵⁷, E. Drechsler ¹⁴⁰, E. Dreyer ¹⁴⁰, T. Dreyer ⁵³, A.S. Drobac ¹⁵⁶, D. Du ^{60b}, T.A. du Pree ¹¹², F. Dubinin ³⁵, M. Dubovsky ^{26a}, A. Dubreuil ⁵⁴, E. Duchovni ¹⁶⁶, G. Duckeck ¹⁰⁷, O.A. Ducu ^{34,25b}, D. Duda ¹⁰⁸, A. Dudarev ³⁴, M. D'uffizi ⁹⁹, L. Duflot ⁶⁴, M. Dührssen ³⁴, C. Dülsen ¹⁶⁸, A.E. Dumitriu ^{25b}, M. Dunford ^{61a}, S. Dungs ⁴⁷, K. Dunne ^{45a,45b}, A. Duperrin ¹⁰⁰, H. Duran Yildiz ^{3a}, M. Düren ⁵⁶, A. Durglishvili ^{147b}, B. Dutta ⁴⁶, B.L. Dwyer ¹¹³, G.I. Dyckes ¹²⁵, M. Dyndal ^{82a}, S. Dysch ⁹⁹, B.S. Dziedzic ⁸³, B. Eckerova ^{26a}, M.G. Eggleston ⁴⁹, E. Egidio Purcino De Souza ^{79b}, L.F. Ehrke ⁵⁴, T. Eifert ⁷, G. Eigen ¹⁵, K. Einsweiler ^{16a}, T. Ekelof ¹⁵⁸, Y. El Ghazali ^{33b}, H. El Jarrari ^{33e}, A. El Moussaouy ^{33a}, V. Ellajosyula ¹⁵⁸, M. Ellert ¹⁵⁸, F. Ellinghaus ¹⁶⁸, A.A. Elliot ⁹¹, N. Ellis ³⁴, J. Elmsheuser ²⁷, M. Elsing ³⁴, D. Emelianov ¹³¹, A. Emerman ³⁹, Y. Enari ¹⁵¹, J. Erdmann ^{47,al}, A. Ereditato ¹⁸, P.A. Erland ⁸³, M. Errenst ¹⁶⁸, M. Escalier ⁶⁴, C. Escobar ¹⁶⁰, O. Estrada Pastor ¹⁶⁰, E. Etzion ¹⁴⁹, G. Evans ^{127a}, H. Evans ⁶⁵, M.O. Evans ¹⁴⁴, A. Ezhilov ³⁵, F. Fabbri ⁵⁷, L. Fabbri ^{21b,21a}, V. Fabiani ¹¹¹, G. Facini ¹⁶⁴, V. Fadeyev ¹³³, R.M. Fakhrutdinov ³⁵, S. Falciano ^{72a}, P.J. Falke ²², S. Falke ³⁴, J. Faltova ¹³⁰, Y. Fan ^{13a}, Y. Fang ^{13a}, Y. Fang ^{13a,13d}, G. Fanourakis ⁴⁴, M. Fanti ^{68a,68b}, M. Faraj ^{60c}, A. Farbin ⁷, A. Farilla ^{74a}, E.M. Farina ^{70a,70b}, T. Farooque ¹⁰⁵, S.M. Farrington ⁵⁰, P. Farthouat ³⁴, F. Fassi ^{33e}, D. Fassouliotis ⁸, M. Fauci Giannelli ^{73a,73b}, W.J. Fawcett ³⁰, L. Fayard ⁶⁴, O.L. Fedin ^{35,a}, M. Feickert ¹⁵⁹, L. Felgioni ¹⁰⁰, A. Fell ¹³⁷, C. Feng ^{60b}, M. Feng ^{13b}, M.J. Fenton ¹⁵⁷, A.B. Fenyuk ³⁵, S.W. Ferguson ⁴³, J. Ferrando ⁴⁶, A. Ferrari ¹⁵⁸, P. Ferrari ¹¹², R. Ferrari ^{70a}, D. Ferrere ⁵⁴, C. Ferretti ¹⁰⁴, F. Fiedler ⁹⁸, A. Filipčič ⁹⁰, F. Filthaut ¹¹¹, M.C.N. Fiolhais ^{127a,127c,b}, L. Fiorini ¹⁶⁰, F. Fischer ¹³⁹, W.C. Fisher ¹⁰⁵, T. Fitschen ¹⁹, I. Fleck ¹³⁹, P. Fleischmann ¹⁰⁴, T. Flick ¹⁶⁸, B.M. Flierl ¹⁰⁷, L. Flores ¹²⁵, L.R. Flores Castillo ^{62a}, F.M. Follega ^{75a,75b}, N. Fomin ¹⁵, J.H. Foo ¹⁵³, B.C. Forland ⁶⁵, A. Formica ¹³², F.A. Förster ¹², A.C. Forti ⁹⁹, E. Fortin ¹⁰⁰, M.G. Foti ¹²³, D. Fournier ⁶⁴, H. Fox ⁸⁸, P. Francavilla ^{71a,71b}, S. Francescato ⁵⁹, M. Franchini ^{21b,21a}, S. Franchino ^{61a}, D. Francis ³⁴, L. Franco ⁴, L. Franconi ¹⁸, M. Franklin ⁵⁹, G. Frattari ^{72a,72b}, A.C. Freegard ⁹¹, P.M. Freeman ¹⁹, W.S. Freund ^{79b}, E.M. Freundlich ⁴⁷, D. Froidevaux ³⁴, J.A. Frost ¹²³, Y. Fu ^{60a}, M. Fujimoto ¹¹⁵, E. Fullana Torregrosa ^{160,*}, J. Fuster ¹⁶⁰, A. Gabrielli ^{21b,21a}, A. Gabrielli ³⁴, P. Gadov ⁴⁶, G. Gagliardi ^{55b,55a}, L.G. Gagnon ^{16a}, G.E. Gallardo ¹²³, E.J. Gallas ¹²³, B.J. Gallop ¹³¹, R. Gamboa Goni ⁹¹, K.K. Gan ¹¹⁶, S. Ganguly ¹⁶⁶, J. Gao ^{60a}, Y. Gao ⁵⁰, Y.S. Gao ^{29,o}, F.M. Garay Walls ^{134a}, C. García ¹⁶⁰, J.E. García Navarro ¹⁶⁰, J.A. García Pascual ^{13a}, M. Garcia-Sciveres ^{16a}, R.W. Gardner ³⁷, D. Garg ⁷⁷, S. Gargiulo ⁵², C.A. Garner ¹⁵³, V. Garonne ¹²², S.J. Gasiorowski ¹³⁶, P. Gaspar ^{79b}, G. Gaudio ^{70a}, P. Gauzzi ^{72a,72b}, I.L. Gavrilenko ³⁵, A. Gavrilyuk ³⁵, C. Gay ¹⁶¹, G. Gaycken ⁴⁶, E.N. Gazis ⁹, A.A. Geanta ^{25b},

C.M. Gee¹³³, C.N.P. Gee¹³¹, J. Geisen⁹⁵, M. Geisen⁹⁸, C. Gemme^{55b}, M.H. Genest⁵⁸, S. Gentile^{72a,72b}, S. George⁹², W.F. George¹⁹, T. Gerialis⁴⁴, L.O. Gerlach⁵³, P. Gessinger-Befurt³⁴, M. Ghasemi Bostanabad¹⁶², M. Ghneimat¹³⁹, A. Ghosh¹⁵⁷, A. Ghosh⁷⁷, B. Giacobbe^{21b}, S. Giagu^{72a,72b}, N. Giangiacomi¹⁵³, P. Giannetti^{71a}, A. Giannini^{69a,69b}, S.M. Gibson⁹², M. Gignac¹³³, D.T. Gil^{82b}, B.J. Gilbert³⁹, D. Gillberg³², G. Gilles¹¹², N.E.K. Gillwald⁴⁶, D.M. Gingrich^{2,ah}, M.P. Giordani^{66a,66c}, P.F. Giraud¹³², G. Giugliarelli^{66a,66c}, D. Giugni^{68a}, F. Giuli^{73a,73b}, I. Gkialas^{8,j}, P. Kountoumis⁹, L.K. Gladilin³⁵, C. Glasman⁹⁷, G.R. Gledhill¹²⁰, M. Glisic¹²⁰, I. Gnesi^{41b,e}, M. Goblirsch-Kolb²⁴, D. Godin¹⁰⁶, S. Goldfarb¹⁰³, T. Golling⁵⁴, D. Golubkov³⁵, J.P. Gombas¹⁰⁵, A. Gomes^{127a,127b}, R. Goncalves Gama⁵³, R. Gonçalo^{127a,127c}, G. Gonella¹²⁰, L. Gonella¹⁹, A. Gongadze³⁶, F. Gonnella¹⁹, J.L. Gonski³⁹, S. González de la Hoz¹⁶⁰, S. Gonzalez Fernandez¹², R. Gonzalez Lopez⁸⁹, C. Gonzalez Renteria^{16a}, R. Gonzalez Suarez¹⁵⁸, S. Gonzalez-Sevilla⁵⁴, G.R. Gonzalvo Rodriguez¹⁶⁰, R.Y. González Andana^{134a}, L. Goossens³⁴, N.A. Gorasia¹⁹, P.A. Gorbounov³⁵, B. Gorini³⁴, E. Gorini^{67a,67b}, A. Gorišek⁹⁰, A.T. Goshaw⁴⁹, M.I. Gostkin³⁶, C.A. Gottardo¹¹¹, M. Goughri^{33b}, V. Goumarre⁴⁶, A.G. Goussiou¹³⁶, N. Govender^{31c}, C. Goy⁴, I. Grabowska-Bold^{82a}, K. Graham³², E. Gramstad¹²², S. Grancagnolo¹⁷, M. Grandi¹⁴⁴, V. Gratchev^{35,*}, P.M. Gravila^{25f}, F.G. Gravili^{67a,67b}, H.M. Gray^{16a}, C. Grefe²², I.M. Gregor⁴⁶, P. Grenier¹⁴¹, K. Grevtsov⁴⁶, C. Grieco¹², N.A. Grieser¹¹⁷, A.A. Grillo¹³³, K. Grimm^{29,n}, S. Grinstein^{12,v}, J.-F. Grivaz⁶⁴, S. Groh⁹⁸, E. Gross¹⁶⁶, J. Grosse-Knetter⁵³, C. Grud¹⁰⁴, A. Grummer¹¹⁰, J.C. Grundy¹²³, L. Guan¹⁰⁴, W. Guan¹⁶⁷, C. Gubbels¹⁶¹, J. Guenther³⁴, J.G.R. Guerrero Rojas¹⁶⁰, F. Guescini¹⁰⁸, R. Gugel⁹⁸, A. Guida⁴⁶, T. Guillemin⁴, S. Guindon³⁴, J. Guo^{60c}, L. Guo⁶⁴, Y. Guo¹⁰⁴, R. Gupta⁴⁶, S. Gurbuz²², G. Gustavino¹¹⁷, M. Guth⁵⁴, P. Gutierrez¹¹⁷, L.F. Gutierrez Zagazeta¹²⁵, C. Gutsche⁹³, C. Guyot¹³², C. Gwenlan¹²³, C.B. Gwilliam⁸⁹, E.S. Haaland¹²², A. Haas¹¹⁴, M. Habedank¹⁷, C. Haber^{16a}, H.K. Hadavand⁷, A. Hadeef⁹⁸, S. Hadzic¹⁰⁸, M. Haleem¹⁶³, J. Haley¹¹⁸, J.J. Hall¹³⁷, G. Halladjian¹⁰⁵, G.D. Hallowell¹⁰⁰, L. Halser¹⁸, K. Hamano¹⁶², H. Hamdaoui^{33e}, M. Hamer²², G.N. Hamity⁵⁰, K. Han^{60a}, L. Han^{13c}, L. Han^{60a}, S. Han^{16a}, Y.F. Han¹⁵³, K. Hanagaki⁸⁰, M. Hance¹³³, M.D. Hank³⁷, R. Hankache⁹⁹, E. Hansen⁹⁵, J.B. Hansen⁴⁰, J.D. Hansen⁴⁰, M.C. Hansen²², P.H. Hansen⁴⁰, K. Hara¹⁵⁵, T. Harenberg¹⁶⁸, S. Harkusha³⁵, Y.T. Harris¹²³, P.F. Harrison¹⁶⁴, N.M. Hartman¹⁴¹, N.M. Hartmann¹⁰⁷, Y. Hasegawa¹³⁸, A. Hasib⁵⁰, S. Hassani¹³², S. Haug¹⁸, R. Hauser¹⁰⁵, M. Havranek¹²⁹, C.M. Hawkes¹⁹, R.J. Hawkins³⁴, S. Hayashida¹⁰⁹, D. Hayden¹⁰⁵, C. Hayes¹⁰⁴, R.L. Hayes¹⁶¹, C.P. Hays¹²³, J.M. Hays⁹¹, H.S. Hayward⁸⁹, S.J. Haywood¹³¹, F. He^{60a}, Y. He¹⁵², Y. He¹²⁴, M.P. Heath⁵⁰, V. Hedberg⁹⁵, A.L. Heggelund¹²², N.D. Hehir⁹¹, C. Heidegger⁵², K.K. Heidegger⁵², W.D. Heidorn⁷⁸, J. Heilman³², S. Heim⁴⁶, T. Heim^{16a}, B. Heinemann^{46,ae}, J.G. Heinlein¹²⁵, J.J. Heinrich¹²⁰, L. Heinrich³⁴, J. Hejbal¹²⁸, L. Helary⁴⁶, A. Held¹¹⁴, S. Hellesund¹²², C.M. Helling¹³³, S. Hellman^{45a,45b}, C. Helsen³⁴, R.C.W. Henderson⁸⁸, L. Henkelmann³⁰, A.M. Henriques Correia³⁴, H. Herde¹⁴¹, Y. Hernández Jiménez¹⁴³, H. Herr⁹⁸, M.G. Herrmann¹⁰⁷, T. Herrmann⁴⁸, G. Herten⁵², R. Hertenberger¹⁰⁷, L. Hervas³⁴, N.P. Hessey^{154a}, H. Hibi⁸¹, S. Higashino⁸⁰, E. Higón-Rodríguez¹⁶⁰, K.K. Hill²⁷, K.H. Hiller⁴⁶, S.J. Hillier¹⁹, M. Hils⁴⁸, I. Hinchliffe^{16a}, F. Hinterkeuser²², M. Hirose¹²¹, S. Hirose¹⁵⁵, D. Hirschbuehl¹⁶⁸, B. Hiti⁹⁰, O. Hladik¹²⁸, J. Hobbs¹⁴³, R. Hobincu^{25e}, N. Hod¹⁶⁶, M.C. Hodgkinson¹³⁷, B.H. Hodgkinson³⁰, A. Hoecker³⁴, J. Hofer⁴⁶, D. Hohn⁵², T. Holm²², T.R. Holmes³⁷, M. Holzbock¹⁰⁸, L.B.A.H. Hommels³⁰, B.P. Honan⁹⁹, J. Hong^{60c}, T.M. Hong¹²⁶, J.C. Honig⁵², A. Hönle¹⁰⁸, B.H. Hooberman¹⁵⁹, W.H. Hopkins⁵, Y. Horii¹⁰⁹, L.A. Horyn³⁷, S. Hou¹⁴⁶, J. Howarth⁵⁷, J. Hoya⁸⁷, M. Hrabovsky¹¹⁹, A. Hrynevich³⁵, T. Hryn'ova⁴, P.J. Hsu⁶³, S.-C. Hsu¹³⁶, Q. Hu³⁹, S. Hu^{60c}, Y.F. Hu^{13a,13d,aj}, D.P. Huang⁹³, X. Huang^{13c}, Y. Huang^{60a}, Y. Huang^{13a}, Z. Hubacek¹²⁹, F. Hubaut¹⁰⁰, M. Huebner²², F. Huegging²², T.B. Huffman¹²³, M. Huhtinen³⁴, R. Hulsken⁵⁸, N. Huseynov^{36,z}, J. Huston¹⁰⁵, J. Huth⁵⁹, R. Hyneman¹⁴¹, S. Hyrych^{26a}, G. Iacobucci⁵⁴, G. Iakovidis²⁷, I. Ibragimov¹³⁹, L. Iconomidou-Fayard⁶⁴, P. Iengo³⁴, R. Iguchi¹⁵¹, T. Iizawa⁵⁴, Y. Ikegami⁸⁰, A. Ilg¹⁸, N. Ilic¹⁵³, H. Imam^{33a}, T. Ingebretsen Carlson^{45a,45b}, G. Introzzi^{70a,70b}, M. Iodice^{74a}, V. Ippolito^{72a,72b}, M. Ishino¹⁵¹, W. Islam¹¹⁸, C. Issever^{17,46}, S. Istin^{11c,ak}, J.M. Iturbe Ponce^{62a}, R. Iuppa^{75a,75b}, A. Ivina¹⁶⁶, J.M. Izen⁴³, V. Izzo^{69a}, P. Jacka¹²⁸, P. Jackson¹, R.M. Jacobs⁴⁶, B.P. Jaeger¹⁴⁰, C.S. Jagfeld¹⁰⁷, G. Jäkel¹⁶⁸, K. Jakobs⁵², T. Jakoubek¹⁶⁶, J. Jamieson⁵⁷, K.W. Janas^{82a}, G. Jarlskog⁹⁵, A.E. Jaspán⁸⁹, N. Javadov^{36,z}, T. Javůrek³⁴, M. Javurkova¹⁰¹, F. Jeanneau¹³², L. Jeanty¹²⁰, J. Jejelava^{147a,aa}, P. Jenni^{52,f}, S. Jézéquel⁴, J. Jia¹⁴³, Z. Jia^{13c}, Y. Jiang^{60a}, S. Jiggins⁵², J. Jimenez Pena¹⁰⁸, S. Jin^{13c}, A. Jinaru^{25b}, O. Jinnouchi¹⁵², H. Jivan^{31f}, P. Johansson¹³⁷, K.A. Johns⁶, C.A. Johnson⁶⁵, D.M. Jones³⁰, E. Jones¹⁶⁴, R.W.L. Jones⁸⁸, T.J. Jones⁸⁹, J. Jovicevic⁵³, X. Ju^{16a}, J.J. Jungeburth³⁴, A. Juste Rozas^{12,v}, S. Kabana^{134d},

A. Kaczmarska⁸³, M. Kado^{72a,72b}, H. Kagan¹¹⁶, M. Kagan¹⁴¹, A. Kahn³⁹, C. Kahra⁹⁸, T. Kaji¹⁶⁵,
 E. Kajomovitz¹⁴⁸, C.W. Kalderon²⁷, A. Kamenshchikov³⁵, M. Kaneda¹⁵¹, N.J. Kang¹³³, S. Kang⁷⁸,
 Y. Kano¹⁰⁹, J. Kanzaki⁸⁰, D. Kar^{31f}, K. Karava¹²³, M.J. Kareem^{154b}, I. Karkanias¹⁵⁰, S.N. Karpov³⁶,
 Z.M. Karpova³⁶, V. Kartvelishvili⁸⁸, A.N. Karyukhin³⁵, E. Kasimi¹⁵⁰, C. Kato^{60d}, J. Katzy⁴⁶,
 K. Kawade¹³⁸, K. Kawagoe⁸⁶, T. Kawaguchi¹⁰⁹, T. Kawamoto¹³², G. Kawamura⁵³, E.F. Kay¹⁶²,
 F.I. Kaya¹⁵⁶, S. Kazakos¹², V.F. Kazanin³⁵, Y. Ke¹⁴³, J.M. Keaveney^{31a}, R. Keeler¹⁶², J.S. Keller³²,
 D. Kelsey¹⁴⁴, J.J. Kempster¹⁹, J. Kendrick¹⁹, K.E. Kennedy³⁹, O. Kepka¹²⁸, S. Kersten¹⁶⁸, B.P. Kerševan⁹⁰,
 S. Ketabchi Haghighat¹⁵³, M. Khandoga¹²⁴, A. Khanov¹¹⁸, A.G. Kharlamov³⁵, T. Kharlamova³⁵,
 E.E. Khoda¹³⁶, T.J. Khoo¹⁷, G. Khoriauli¹⁶³, J. Khubua^{147b}, S. Kido⁸¹, M. Kiehn³⁴, A. Kilgallon¹²⁰,
 E. Kim¹⁵², Y.K. Kim³⁷, N. Kimura⁹³, A. Kirchhoff⁵³, D. Kirchmeier⁴⁸, C. Kirfel²², J. Kirk¹³¹,
 A.E. Kiryunin¹⁰⁸, T. Kishimoto¹⁵¹, D.P. Kisliuk¹⁵³, V. Kitali⁴⁶, C. Kitsaki⁹, O. Kivernyk²²,
 T. Klapdor-Kleingrothaus⁵², M. Klassen^{61a}, C. Klein³², L. Klein¹⁶³, M.H. Klein¹⁰⁴, M. Klein⁸⁹, U. Klein⁸⁹,
 P. Klimek³⁴, A. Klimentov²⁷, F. Klimpel³⁴, T. Klingl²², T. Klioutchnikova³⁴, F.F. Klitzner¹⁰⁷, P. Kluit¹¹²,
 S. Kluth¹⁰⁸, E. Kneringer⁷⁶, T.M. Knight¹⁵³, A. Knue⁵², D. Kobayashi⁸⁶, M. Kobel⁴⁸, M. Kocian¹⁴¹,
 T. Kodama¹⁵¹, P. Kodyš¹³⁰, D.M. Koeck¹⁴⁴, P.T. Koenig²², T. Koffas³², N.M. Köhler³⁴, M. Kolb¹³²,
 I. Koletsou⁴, T. Komarek¹¹⁹, K. Köneke⁵², A.X.Y. Kong¹, T. Kono¹¹⁵, V. Konstantinides⁹³,
 N. Konstantinidis⁹³, B. Konya⁹⁵, R. Kopeliansky⁶⁵, S. Koperny^{82a}, K. Korcyl⁸³, K. Kordas¹⁵⁰, G. Koren¹⁴⁹,
 A. Korn⁹³, S. Korn⁵³, I. Korolkov¹², E.V. Korolkova¹³⁷, N. Korotkova³⁵, B. Kortman¹¹², O. Kortner¹⁰⁸,
 S. Kortner¹⁰⁸, W.H. KostECKa¹¹³, V.V. Kostyukhin^{137,35}, A. Kotskechagia⁶⁴, A. Kotwal⁴⁹, A. Koulouris³⁴,
 A. Kourkoumeli-Charalampidi^{70a,70b}, C. Kourkoumelis⁸, E. Kourlitis⁵, O. Kovanda¹⁴⁴, R. Kowalewski¹⁶²,
 W. Kozanecki¹³², A.S. Kozhin³⁵, V.A. Kramarenko³⁵, G. Kramberger⁹⁰, D. Krasnoperstev^{60a},
 M.W. Krasny¹²⁴, A. Krasznahorkay³⁴, J.A. Kremer⁹⁸, J. Kretzschmar⁸⁹, K. Kreul¹⁷, P. Krieger¹⁵³,
 F. Krieter¹⁰⁷, S. Krishnamurthy¹⁰¹, A. Krishnan^{61b}, M. Krivos¹³⁰, K. Krizka^{16a}, K. Kroeninger⁴⁷,
 H. Kroha¹⁰⁸, J. Kroll¹²⁸, J. Kroll¹²⁵, K.S. Krowpman¹⁰⁵, U. Kruchonak³⁶, H. Krüger²², N. Krumnack⁷⁸,
 M.C. Kruse⁴⁹, J.A. Krzysiak⁸³, A. Kubota¹⁵², O. Kuchinskaia³⁵, S. Kудay^{3b}, D. Kuechler⁴⁶, J.T. Kuechler⁴⁶,
 S. Kuehn³⁴, T. Kuhl⁴⁶, V. Kukhtin³⁶, Y. Kulchitsky^{35,a}, S. Kuleshov^{134c}, M. Kumar^{31f}, N. Kumari¹⁰⁰,
 M. Kuna⁵⁸, A. Kupco¹²⁸, T. Kupfer⁴⁷, O. Kuprash⁵², H. Kurashige⁸¹, L.L. Kurchaninov^{154a},
 Y.A. Kurochkin³⁵, A. Kurova³⁵, M.G. Kurth^{13a,13d}, E.S. Kuwertz³⁴, M. Kuze¹⁵², A.K. Kvam¹³⁶, J. Kvita¹¹⁹,
 T. Kwan¹⁰², K.W. Kwok^{62a}, C. Lacasta¹⁶⁰, F. Lacava^{72a,72b}, H. Lacker¹⁷, D. Lacour¹²⁴, N.N. Lad⁹³,
 E. Ladygin³⁶, R. Lafaye⁴, B. Laforge¹²⁴, T. Lagouri^{134d}, S. Lai⁵³, I.K. Lakomic^{82a}, N. Lalloue⁵⁸,
 J.E. Lambert¹¹⁷, S. Lammers⁶⁵, W. Lampl⁶, C. Lampoudis¹⁵⁰, E. Lançon²⁷, U. Landgraf⁵²,
 M.P.J. Landon⁹¹, V.S. Lang⁵², J.C. Lange⁵³, R.J. Langenberg¹⁰¹, A.J. Lankford¹⁵⁷, F. Lanni²⁷, K. Lantzsch²²,
 A. Lanza^{70a}, A. Lapertosa^{55b,55a}, J.F. Laporte¹³², T. Lari^{68a}, F. Lasagni Manghi^{21b}, M. Lassnig³⁴,
 V. Latonova¹²⁸, T.S. Lau^{62a}, A. Laudrain⁹⁸, A. Laurier³², M. Lavorgna^{69a,69b}, S.D. Lawlor⁹²,
 Z. Lawrence⁹⁹, M. Lazzaroni^{68a,68b}, B. Le⁹⁹, B. Leban⁹⁰, A. Lebedev⁷⁸, M. LeBlanc³⁴, T. LeCompte⁵,
 F. Ledroit-Guillon⁵⁸, A.C.A. Lee⁹³, G.R. Lee¹⁵, L. Lee⁵⁹, S.C. Lee¹⁴⁶, S. Lee⁷⁸, L.L. Leeuw^{31c},
 B. Lefebvre^{154a}, H.P. Lefebvre⁹², M. Lefebvre¹⁶², C. Leggett^{16a}, K. Lehmann¹⁴⁰, N. Lehmann¹⁸,
 G. Lehmann Miotto³⁴, W.A. Leight⁴⁶, A. Leisos^{150,u}, M.A.L. Leite^{79c}, C.E. Leitgeb⁴⁶, R. Leitner¹³⁰,
 K.J.C. Leney⁴², T. Lenz²², S. Leone^{71a}, C. Leonidopoulos⁵⁰, A. Leopold¹²⁴, C. Leroy¹⁰⁶, R. Les¹⁰⁵,
 C.G. Lester³⁰, M. Levchenko³⁵, J. Levêque⁴, D. Levin¹⁰⁴, L.J. Levinson¹⁶⁶, D.J. Lewis¹⁹, B. Li^{13b}, B. Li^{60b},
 C. Li^{60a}, C-Q. Li^{60c,60d}, H. Li^{60a}, H. Li^{60b}, H. Li^{60b}, J. Li^{60c}, K. Li¹³⁶, L. Li^{60c}, M. Li^{13a,13d}, Q.Y. Li^{60a},
 S. Li^{60d,60c,d}, T. Li^{60b}, X. Li⁴⁶, Y. Li⁴⁶, Z. Li^{60b}, Z. Li¹²³, Z. Li¹⁰², Z. Li⁸⁹, Z. Liang^{13a}, M. Liberatore⁴⁶,
 B. Liberti^{73a}, K. Lie^{62c}, K. Lin¹⁰⁵, R.A. Linck⁶⁵, R.E. Lindley⁶, J.H. Lindon², A. Linss⁴⁶, E. Lipeles¹²⁵,
 A. Lipniacka¹⁵, T.M. Liss^{159,af}, A. Lister¹⁶¹, J.D. Little⁷, B. Liu^{13a}, B.X. Liu¹⁴⁰, J.B. Liu^{60a}, J.K.K. Liu³⁷,
 K. Liu^{60d,60c}, M. Liu^{60a}, M.Y. Liu^{60a}, P. Liu^{13a}, X. Liu^{60a}, Y. Liu⁴⁶, Y. Liu^{13c,13d}, Y.L. Liu¹⁰⁴, Y.W. Liu^{60a},
 M. Livan^{70a,70b}, A. Lleres⁵⁸, J. Llorente Merino¹⁴⁰, S.L. Lloyd⁹¹, E.M. Lobodzinska⁴⁶, P. Loch⁶,
 S. Loffredo^{73a,73b}, T. Lohse¹⁷, K. Lohwasser¹³⁷, M. Lokajicek¹²⁸, J.D. Long¹⁵⁹, I. Longarini^{72a,72b},
 L. Longo³⁴, R. Longo¹⁵⁹, I. Lopez Paz¹², A. Lopez Solis⁴⁶, J. Lorenz¹⁰⁷, N. Lorenzo Martinez⁴,
 A.M. Lory¹⁰⁷, A. Lösle⁵², X. Lou^{45a,45b}, X. Lou^{13a,13d}, A. Lounis⁶⁴, J. Love⁵, P.A. Love⁸⁸,
 J.J. Lozano Bahilo¹⁶⁰, G. Lu^{13a,13d}, M. Lu^{60a}, S. Lu¹²⁵, Y.J. Lu⁶³, H.J. Lubatti¹³⁶, C. Luci^{72a,72b},
 F.L. Lucio Alves^{13c}, A. Lucotte⁵⁸, F. Luehring⁶⁵, I. Luise¹⁴³, L. Luminari^{72a}, O. Lundberg¹⁴²,
 B. Lund-Jensen¹⁴², N.A. Luongo¹²⁰, M.S. Lutz¹⁴⁹, D. Lynn²⁷, H. Lyons⁸⁹, R. Lysak¹²⁸, E. Lytken⁹⁵,
 F. Lyu^{13a}, V. Lyubushkin³⁶, T. Lyubushkina³⁶, H. Ma²⁷, L.L. Ma^{60b}, Y. Ma⁹³, D.M. Mac Donell¹⁶²,

G. Maccarrone⁵¹, C.M. Macdonald¹³⁷, J.C. MacDonald¹³⁷, R. Madar³⁸, W.F. Mader⁴⁸, M. Madugoda Ralalage Don¹¹⁸, N. Madysa⁴⁸, J. Maeda⁸¹, T. Maeno²⁷, M. Maerker⁴⁸, V. Magerl⁵², J. Magro^{66a,66c}, D.J. Mahon³⁹, C. Maidantchik^{79b}, A. Maio^{127a,127b,127d}, K. Maj^{82a}, O. Majersky^{26a}, S. Majewski¹²⁰, N. Makovec⁶⁴, B. Malaescu¹²⁴, Pa. Malecki⁸³, V.P. Maleev³⁵, F. Malek⁵⁸, D. Malito^{41b,41a}, U. Mallik⁷⁷, C. Malone³⁰, S. Maltezos⁹, S. Malyukov³⁶, J. Mamuzic¹⁶⁰, G. Mancini⁵¹, J.P. Mandalia⁹¹, I. Mandić⁹⁰, L. Manhaes de Andrade Filho^{79a}, I.M. Maniatis¹⁵⁰, M. Manisha¹³², J. Manjarres Ramos⁴⁸, K.H. Mankinen⁹⁵, A. Mann¹⁰⁷, A. Manousos⁷⁶, B. Mansoulie¹³², I. Mantos¹⁵⁰, S. Manzoni¹¹², A. Marantis^{150,u}, G. Marchiori¹²⁴, M. Marcisovsky¹²⁸, L. Marcocchia^{73a,73b}, C. Marcon⁹⁵, M. Marjanovic¹¹⁷, Z. Marshall^{16a}, S. Marti-Garcia¹⁶⁰, T.A. Martin¹⁶⁴, V.J. Martin⁵⁰, B. Martin dit Latour¹⁵, L. Martinelli^{72a,72b}, M. Martinez^{12,v}, P. Martinez Agullo¹⁶⁰, V.I. Martinez Outschoorn¹⁰¹, S. Martin-Haugh¹³¹, V.S. Martoiu^{25b}, A.C. Martyniuk⁹³, A. Marzin³⁴, S.R. Maschek¹⁰⁸, L. Masetti⁹⁸, T. Mashimo¹⁵¹, J. Masik⁹⁹, A.L. Maslennikov³⁵, L. Massa^{21b}, P. Massarotti^{69a,69b}, P. Mastrandrea^{71a,71b}, A. Mastroberardino^{41b,41a}, T. Masubuchi¹⁵¹, D. Matakias²⁷, T. Mathisen¹⁵⁸, A. Matic¹⁰⁷, N. Matsuzawa¹⁵¹, J. Maurer^{25b}, B. Maček⁹⁰, D.A. Maximov³⁵, R. Mazini¹⁴⁶, I. Maznas¹⁵⁰, S.M. Mazza¹³³, C. Mc Ginn²⁷, J.P. Mc Gowan¹⁰², S.P. Mc Kee¹⁰⁴, T.G. McCarthy¹⁰⁸, W.P. McCormack^{16a}, E.F. McDonald¹⁰³, A.E. McDougall¹¹², J.A. Mcfayden¹⁴⁴, G. Mchedlidze^{147b}, M.A. McKay⁴², K.D. McLean¹⁶², S.J. McMahon¹³¹, P.C. McNamara¹⁰³, R.A. McPherson^{162,y}, J.E. Mdhului^{31f}, Z.A. Meadows¹⁰¹, S. Meehan³⁴, T. Megy³⁸, S. Mehlhase¹⁰⁷, A. Mehta⁸⁹, B. Meirose⁴³, D. Melini¹⁴⁸, B.R. Mellado Garcia^{31f}, A.H. Melo⁵³, F. Meloni⁴⁶, A. Melzer²², E.D. Mendes Gouveia^{127a}, A.M. Mendes Jacques Da Costa¹⁹, H.Y. Meng¹⁵³, L. Meng³⁴, S. Menke¹⁰⁸, M. Mentink³⁴, E. Meoni^{41b,41a}, C. Merlassino¹²³, P. Mermod^{54,*}, L. Merola^{69a,69b}, C. Meroni^{68a}, G. Merz¹⁰⁴, O. Meshkov³⁵, J.K.R. Meshreki¹³⁹, J. Metcalfe⁵, A.S. Mete⁵, C. Meyer⁶⁵, J-P. Meyer¹³², M. Michetti¹⁷, R.P. Middleton¹³¹, L. Mijović⁵⁰, G. Mikenberg¹⁶⁶, M. Mikestikova¹²⁸, M. Mikuž⁹⁰, H. Mildner¹³⁷, A. Milic¹⁵³, C.D. Milke⁴², D.W. Miller³⁷, L.S. Miller³², A. Milov¹⁶⁶, D.A. Milstead^{45a,45b}, T. Min^{13c}, A.A. Minaenko³⁵, I.A. Minashvili^{147b}, L. Mince⁵⁷, A.I. Mincer¹¹⁴, B. Mindur^{82a}, M. Mineev³⁶, Y. Minegishi¹⁵¹, Y. Mino⁸⁴, L.M. Mir¹², M. Miralles Lopez¹⁶⁰, M. Mironova¹²³, T. Mitani¹⁶⁵, V.A. Mitsou¹⁶⁰, M. Mittal^{60c}, O. Miu¹⁵³, P.S. Miyagawa⁹¹, Y. Miyazaki⁸⁶, A. Mizukami⁸⁰, J.U. Mjörnmark⁹⁵, T. Mkrtychyan^{61a}, M. Mlynarikova¹¹³, T. Moa^{45a,45b}, S. Mobius⁵³, K. Mochizuki¹⁰⁶, P. Moder⁴⁶, P. Mogg¹⁰⁷, A.F. Mohammed^{13a,13d}, S. Mohapatra³⁹, G. Mokgatitswane^{31f}, B. Mondal¹³⁹, S. Mondal¹²⁹, K. Mönig⁴⁶, E. Monnier¹⁰⁰, A. Montalbano¹⁴⁰, J. Montejo Berlingen³⁴, M. Montella¹¹⁶, F. Monticelli⁸⁷, N. Morange⁶⁴, A.L. Moreira De Carvalho^{127a}, M. Moreno Llácer¹⁶⁰, C. Moreno Martinez¹², P. Morettini^{55b}, M. Morgenstern¹⁴⁸, S. Morgenstern¹⁶⁴, D. Mori¹⁴⁰, M. Morii⁵⁹, M. Morinaga¹⁵¹, V. Morisbak¹²², A.K. Morley³⁴, A.P. Morris⁹³, L. Morvaj³⁴, P. Moschovakos³⁴, B. Moser¹¹², M. Mosidze^{147b}, T. Moskalets⁵², P. Moskvitina¹¹¹, J. Moss^{29,p}, E.J.W. Moyse¹⁰¹, S. Muanza¹⁰⁰, J. Mueller¹²⁶, D. Muenstermann⁸⁸, R. Müller¹⁸, G.A. Mullier⁹⁵, J.J. Mullin¹²⁵, D.P. Mungo^{68a,68b}, J.L. Munoz Martinez¹², F.J. Munoz Sanchez⁹⁹, M. Murin⁹⁹, P. Murin^{26b}, W.J. Murray^{164,131}, A. Murrone^{68a,68b}, J.M. Muse¹¹⁷, M. Muškinja^{16a}, C. Mwewa²⁷, A.G. Myagkov^{35,a}, A.J. Myers⁷, A.A. Myers¹²⁶, G. Myers⁶⁵, M. Myska¹²⁹, B.P. Nachman^{16a}, O. Nackenhorst⁴⁷, A. Nag⁴⁸, K. Nagai¹²³, K. Nagano⁸⁰, J.L. Nagle²⁷, E. Nagy¹⁰⁰, A.M. Nairz³⁴, Y. Nakahama¹⁰⁹, K. Nakamura⁸⁰, H. Nanjo¹²¹, F. Napolitano^{61a}, R. Narayan⁴², I. Naryshkin³⁵, M. Naseri³², C. Nass²², T. Naumann⁴⁶, G. Navarro^{20a}, J. Navarro-Gonzalez¹⁶⁰, R. Nayak¹⁴⁹, P.Y. Nechaeva³⁵, F. Nechansky⁴⁶, T.J. Neep¹⁹, A. Negri^{70a,70b}, M. Negrini^{21b}, C. Nellist¹¹¹, C. Nelson¹⁰², K. Nelson¹⁰⁴, S. Nemecek¹²⁸, M. Nessi^{34,h}, M.S. Neubauer¹⁵⁹, F. Neuhaus⁹⁸, J. Neundorff⁴⁶, R. Newhouse¹⁶¹, P.R. Newman¹⁹, C.W. Ng¹²⁶, Y.S. Ng¹⁷, Y.W.Y. Ng¹⁵⁷, B. Ngair^{33e}, H.D.N. Nguyen¹⁰⁰, R.B. Nickerson¹²³, R. Nicolaidou¹³², D.S. Nielsen⁴⁰, J. Nielsen¹³³, M. Niemeyer⁵³, N. Nikiforou¹⁰, V. Nikolaenko^{35,a}, I. Nikolic-Audit¹²⁴, K. Nikolopoulos¹⁹, P. Nilsson²⁷, H.R. Nindhito⁵⁴, A. Nisati^{72a}, N. Nishu², R. Nisius¹⁰⁸, T. Nitta¹⁶⁵, T. Nobe¹⁵¹, D.L. Noel³⁰, Y. Noguchi⁸⁴, I. Nomidis¹²⁴, M.A. Nomura²⁷, M.B. Norfolk¹³⁷, R.R.B. Norisam⁹³, J. Novak⁹⁰, T. Novak⁴⁶, O. Novgorodova⁴⁸, L. Novotny¹²⁹, R. Novotny¹¹⁰, L. Nozka¹¹⁹, K. Ntekas¹⁵⁷, E. Nurse⁹³, F.G. Oakham^{32,ah}, J. Ocariz¹²⁴, A. Ochi⁸¹, I. Ochoa^{127a}, J.P. Ochoa-Ricoux^{134a}, S. Oda⁸⁶, S. Odaka⁸⁰, S. Oerdek¹⁵⁸, A. Ogrodnik^{82a}, A. Oh⁹⁹, C.C. Ohm¹⁴², H. Oide¹⁵², R. Oishi¹⁵¹, M.L. Ojeda¹⁵³, Y. Okazaki⁸⁴, M.W. O'Keefe⁸⁹, Y. Okumura¹⁵¹, A. Olariu^{25b}, L.F. Oleiro Seabra^{127a}, S.A. Olivares Pino^{134d}, D. Oliveira Damazio²⁷, D. Oliveira Goncalves^{79a}, J.L. Oliver¹⁵⁷, M.J.R. Olsson¹⁵⁷, A. Olszewski⁸³, J. Olszowska^{83,*}, Ö.O. Öncel²², D.C. O'Neil¹⁴⁰, A.P. O'Neill¹²³, A. Onofre^{127a,127e}, P.U.E. Onyisi¹⁰,

R.G. Oreamuno Madriz¹¹³, M.J. Oreglia³⁷, G.E. Orellana⁸⁷, D. Orestano^{74a,74b}, N. Orlando¹², R.S. Orr¹⁵³, V. O'Shea⁵⁷, R. Ospanov^{60a}, G. Otero y Garzon²⁸, H. Otono⁸⁶, P.S. Ott^{61a}, G.J. Ottino^{16a}, M. Ouchrif^{33d}, J. Ouellette²⁷, F. Ould-Saada¹²², A. Ouraou^{132,*}, Q. Ouyang^{13a}, M. Owen⁵⁷, R.E. Owen¹³¹, K.Y. Oyulmaz^{11c}, V.E. Ozcan^{11c}, N. Ozturk⁷, S. Ozturk^{11c}, J. Pacalt¹¹⁹, H.A. Pacey³⁰, K. Pachal⁴⁹, A. Pacheco Pages¹², C. Padilla Aranda¹², S. Pagan Griso^{16a}, G. Palacino⁶⁵, S. Palazzo⁵⁰, S. Palestini³⁴, M. Palka^{82b}, P. Palni^{82a}, D.K. Panchal¹⁰, C.E. Pandini⁵⁴, J.G. Panduro Vazquez⁹², P. Pani⁴⁶, G. Panizzo^{66a,66c}, L. Paolozzi⁵⁴, C. Papadatos¹⁰⁶, S. Parajuli⁴², A. Paramonov⁵, C. Paraskevopoulos⁹, D. Paredes Hernandez^{62b}, S.R. Paredes Saenz¹²³, B. Parida¹⁶⁶, T.H. Park¹⁵³, A.J. Parker²⁹, M.A. Parker³⁰, F. Parodi^{55b,55a}, E.W. Parrish¹¹³, J.A. Parsons³⁹, U. Parzefall⁵², L. Pascual Dominguez¹⁴⁹, V.R. Pascuzzi^{16a}, F. Pasquali¹¹², E. Pasqualucci^{72a}, S. Passaggio^{55b}, F. Pastore⁹², P. Pasuwan^{45a,45b}, J.R. Pater⁹⁹, A. Pathak¹⁶⁷, J. Patton⁸⁹, T. Pauly³⁴, J. Pearkes¹⁴¹, M. Pedersen¹²², L. Pedraza Diaz¹¹¹, R. Pedro^{127a}, T. Peiffer⁵³, S.V. Peleganchuk³⁵, O. Penc¹²⁸, C. Peng^{62b}, H. Peng^{60a}, M. Penzin³⁵, B.S. Peralva^{79a}, M.M. Perego⁶⁴, A.P. Pereira Peixoto^{127a}, L. Pereira Sanchez^{45a,45b}, D.V. Perepelitsa²⁷, E. Perez Codina^{154a}, M. Perganti⁹, L. Perini^{68a,68b,*}, H. Pernegger³⁴, S. Perrella³⁴, A. Perrevoort¹¹², K. Peters⁴⁶, R.F.Y. Peters⁹⁹, B.A. Petersen³⁴, T.C. Petersen⁴⁰, E. Petit¹⁰⁰, V. Petousis¹²⁹, C. Petridou¹⁵⁰, P. Petroff⁶⁴, F. Petrucci^{74a,74b}, M. Pettee¹⁶⁹, N.E. Pettersson³⁴, K. Petukhova¹³⁰, A. Peyaud¹³², R. Pezoa^{134e}, L. Pezzotti³⁴, G. Pezzullo¹⁶⁹, T. Pham¹⁰³, P.W. Phillips¹³¹, M.W. Phipps¹⁵⁹, G. Piacquadio¹⁴³, E. Pianori^{16a}, F. Piazza^{68a,68b}, A. Picazio¹⁰¹, R. Piegaia²⁸, D. Pietreanu^{25b}, J.E. Pilcher³⁷, A.D. Pilkington⁹⁹, M. Pinamonti^{66a,66c}, J.L. Pinfold², C. Pitman Donaldson⁹³, D.A. Pizzi³², L. Pizzimento^{73a,73b}, A. Pizzini¹¹², M.-A. Pleier²⁷, V. Plesanovs⁵², V. Pleskot¹³⁰, E. Plotnikova³⁶, P. Podberezko³⁵, R. Poettgen⁹⁵, R. Poggi⁵⁴, L. Poggioli¹²⁴, I. Pogrebnyak¹⁰⁵, D. Pohl²², I. Pokharel⁵³, G. Polesello^{70a}, A. Poley^{140,154a}, A. Policicchio^{72a,72b}, R. Polifka¹³⁰, A. Polini^{21b}, C.S. Pollard¹²³, Z.B. Pollock¹¹⁶, V. Polychronakos²⁷, D. Ponomarenko³⁵, L. Pontecorvo³⁴, S. Popa^{25a}, G.A. Popeneciu^{25d}, L. Portales⁴, D.M. Portillo Quintero^{154a}, S. Pospisil¹²⁹, P. Postolache^{25c}, K. Potamianos¹²³, I.N. Potrap³⁶, C.J. Potter³⁰, H. Potti¹, T. Poulsen⁴⁶, J. Poveda¹⁶⁰, T.D. Powell¹³⁷, G. Pownall⁴⁶, M.E. Pozo Astigarraga³⁴, A. Prades Ibanez¹⁶⁰, P. Pralavorio¹⁰⁰, M.M. Prapa⁴⁴, S. Prell⁷⁸, D. Price⁹⁹, M. Primavera^{67a}, M.A. Principe Martin⁹⁷, M.L. Proffitt¹³⁶, N. Proklova³⁵, K. Prokofiev^{62c}, S. Protopopescu²⁷, J. Proudfoot⁵, M. Przybycien^{82a}, D. Pudzha³⁵, P. Puzo⁶⁴, D. Pyatiizbyantseva³⁵, J. Qian¹⁰⁴, Y. Qin⁹⁹, T. Qiu⁹¹, A. Quadt⁵³, M. Queitsch-Maitland³⁴, G. Rabanal Bolanos⁵⁹, F. Ragusa^{68a,68b}, G. Rahal⁹⁶, J.A. Raine⁵⁴, S. Rajagopalan²⁷, K. Ran^{13a,13d}, D.F. Rassloff^{61a}, D.M. Rauch⁴⁶, S. Rave⁹⁸, B. Ravina⁵⁷, I. Ravinovich¹⁶⁶, M. Raymond³⁴, A.L. Read¹²², N.P. Readioff¹³⁷, D.M. Rebuzzi^{70a,70b}, G. Redlinger²⁷, K. Reeves⁴³, D. Reikher¹⁴⁹, A. Reiss⁹⁸, A. Rej¹³⁹, C. Rembser³⁴, A. Renardi⁴⁶, M. Renda^{25b}, M.B. Rendel¹⁰⁸, A.G. Rennie⁵⁷, S. Resconi^{68a}, E.D. Resseguie^{16a}, S. Rettie⁹³, B. Reynolds¹¹⁶, E. Reynolds¹⁹, M. Rezaei Estabragh¹⁶⁸, O.L. Rezanova³⁵, P. Reznicek¹³⁰, E. Ricci^{75a,75b}, R. Richter¹⁰⁸, S. Richter⁴⁶, E. Richter-Was^{82b}, M. Ridel¹²⁴, P. Rieck¹⁰⁸, P. Riedler³⁴, O. Rifki⁴⁶, M. Rijssenbeek¹⁴³, A. Rimoldi^{70a,70b}, M. Rimoldi⁴⁶, L. Rinaldi^{21b,21a}, T.T. Rinn¹⁵⁹, M.P. Rinnagel¹⁰⁷, G. Ripellino¹⁴², I. Riu¹², P. Rivadeneira⁴⁶, J.C. Rivera Vergara¹⁶², F. Rizatdinova¹¹⁸, E. Rizvi⁹¹, C. Rizzi⁵⁴, B.A. Roberts¹⁶⁴, S.H. Robertson^{102,y}, M. Robin⁴⁶, D. Robinson³⁰, C.M. Robles Gajardo^{134e}, M. Robles Manzano⁹⁸, A. Robson⁵⁷, A. Rocchi^{73a,73b}, C. Roda^{71a,71b}, S. Rodriguez Bosca^{61a}, A. Rodriguez Rodriguez⁵², A.M. Rodriguez Vera^{154b}, S. Roe³⁴, A.R. Roepe-Gier¹¹⁷, J. Roggel¹⁶⁸, O. Røhne¹²², R.A. Rojas^{134e}, B. Roland⁵², C.P.A. Roland⁶⁵, J. Roloff²⁷, A. Romaniouk³⁵, M. Romano^{21b}, A.C. Romero Hernandez¹⁵⁹, N. Rompotis⁸⁹, M. Ronzani¹¹⁴, L. Roos¹²⁴, S. Rosati^{72a}, B.J. Rosser¹²⁵, E. Rossi¹⁵³, E. Rossi⁴, E. Rossi^{69a,69b}, L.P. Rossi^{55b}, L. Rossini⁴⁶, R. Rosten¹¹⁶, M. Rotaru^{25b}, B. Rottler⁵², D. Rousseau⁶⁴, D. Rousso³⁰, G. Rovelli^{70a,70b}, A. Roy¹⁰, A. Rozanov¹⁰⁰, Y. Rozen¹⁴⁸, X. Ruan^{31f}, A.J. Ruby⁸⁹, T.A. Ruggeri¹, F. Rühr⁵², A. Ruiz-Martinez¹⁶⁰, A. Rummler³⁴, Z. Rurikova⁵², N.A. Rusakovich³⁶, H.L. Russell³⁴, L. Rustige³⁸, J.P. Rutherford⁶, E.M. Rüttinger¹³⁷, M. Rybar¹³⁰, E.B. Rye¹²², A. Ryzhov³⁵, J.A. Sabater Iglesias⁴⁶, P. Sabatini¹⁶⁰, L. Sabetta^{72a,72b}, H.F-W. Sadrozinski¹³³, F. Safai Tehrani^{72a}, B. Safarzadeh Samani¹⁴⁴, M. Safdari¹⁴¹, P. Saha¹¹³, S. Saha¹⁰², M. Sahinsoy¹⁰⁸, A. Sahu¹⁶⁸, M. Saimpert¹³², M. Saito¹⁵¹, T. Saito¹⁵¹, D. Salamani³⁴, G. Salamanna^{74a,74b}, A. Salnikov¹⁴¹, J. Salt¹⁶⁰, A. Salvador Salas¹², D. Salvatore^{41b,41a}, F. Salvatore¹⁴⁴, A. Salzburger³⁴, D. Sammel⁵², D. Sampsonidis¹⁵⁰, D. Sampsonidou^{60d,60c}, J. Sánchez¹⁶⁰, A. Sanchez Pineda⁴, V. Sanchez Sebastian¹⁶⁰, H. Sandaker¹²², C.O. Sander⁴⁶, I.G. Sanderswood⁸⁸, J.A. Sandesara¹⁰¹, M. Sandhoff¹⁶⁸, C. Sandoval^{20b}, D.P.C. Sankey¹³¹, M. Sannino^{55b,55a}, Y. Sano¹⁰⁹, A. Sansoni⁵¹, C. Santoni³⁸, H. Santos^{127a,127b},

S.N. Santpur^{16a}, A. Santra¹⁶⁶, K.A. Saoucha¹³⁷, J.G. Saraiva^{127a,127d}, J. Sardain¹⁰⁰, O. Sasaki⁸⁰, K. Sato¹⁵⁵, C. Sauer^{61b}, F. Sauerburger⁵², E. Sauvan⁴, P. Savard^{153,ah}, R. Sawada¹⁵¹, C. Sawyer¹³¹, L. Sawyer⁹⁴, I. Sayago Galvan¹⁶⁰, C. Sbarra^{21b}, A. Sbrizzi^{66a,66c}, T. Scanlon⁹³, J. Schaarschmidt¹³⁶, P. Schacht¹⁰⁸, D. Schaefer³⁷, U. Schäfer⁹⁸, A.C. Schaffer⁶⁴, D. Schaile¹⁰⁷, R.D. Schamberger¹⁴³, E. Schanet¹⁰⁷, C. Scharf¹⁷, N. Scharmberg⁹⁹, V.A. Schegelsky³⁵, D. Scheirich¹³⁰, F. Schenck¹⁷, M. Schernau¹⁵⁷, C. Schiavi^{55b,55a}, L.K. Schildgen²², Z.M. Schillaci²⁴, E.J. Schioppa^{67a,67b}, M. Schioppa^{41b,41a}, B. Schlag⁹⁸, K.E. Schleicher⁵², S. Schlenker³⁴, K. Schmieden⁹⁸, C. Schmitt⁹⁸, S. Schmitt⁴⁶, L. Schoeffel¹³², A. Schoening^{61b}, P.G. Scholer⁵², E. Schopf¹²³, M. Schott⁹⁸, J. Schovancova³⁴, S. Schramm⁵⁴, F. Schroeder¹⁶⁸, H.-C. Schultz-Coulon^{61a}, M. Schumacher⁵², B.A. Schumm¹³³, Ph. Schune¹³², A. Schwartzman¹⁴¹, T.A. Schwarz¹⁰⁴, Ph. Schwemling¹³², R. Schwienhorst¹⁰⁵, A. Sciandra¹³³, G. Sciolla²⁴, F. Scuri^{71a}, F. Scutti¹⁰³, C.D. Sebastiani⁸⁹, K. Sedlaczek⁴⁷, P. Seema¹⁷, S.C. Seidel¹¹⁰, A. Seiden¹³³, B.D. Seidlitz²⁷, T. Seiss³⁷, C. Seitz⁴⁶, J.M. Seixas^{79b}, G. Sekhniaidze^{69a}, S.J. Sekula⁴², L. Selam⁴, N. Semprini-Cesari^{21b,21a}, S. Sen⁴⁹, C. Serfon²⁷, L. Serin⁶⁴, L. Serkin^{66a,66b}, M. Sessa^{74a,74b}, H. Severini¹¹⁷, S. Sevova¹⁴¹, F. Sforza^{55b,55a}, A. Sfyrla⁵⁴, E. Shabalina⁵³, R. Shaheen¹⁴², J.D. Shahinian¹²⁵, N.W. Shaikh^{45a,45b}, D. Shaked Renous¹⁶⁶, L.Y. Shan^{13a}, M. Shapiro^{16a}, A. Sharma³⁴, A.S. Sharma¹, S. Sharma⁴⁶, P.B. Shatalov³⁵, K. Shaw¹⁴⁴, S.M. Shaw⁹⁹, P. Sherwood⁹³, L. Shi⁹³, C.O. Shimmin¹⁶⁹, Y. Shimogama¹⁶⁵, J.D. Shinner⁹², I.P.J. Shipsey¹²³, S. Shirabe⁵⁴, M. Shiyakova³⁶, J. Shlomi¹⁶⁶, M.J. Shochet³⁷, J. Shojaii¹⁰³, D.R. Shope¹⁴², S. Shrestha¹¹⁶, E.M. Shrif^{31f}, M.J. Shroff¹⁶², E. Shulga¹⁶⁶, P. Sicho¹²⁸, A.M. Sickles¹⁵⁹, E. Sideras Haddad^{31f}, O. Sidiropoulou³⁴, A. Sidoti^{21b}, F. Siegert⁴⁸, Dj. Sijacki¹⁴, J.M. Silva¹⁹, M.V. Silva Oliveira³⁴, S.B. Silverstein^{45a}, S. Simion⁶⁴, R. Simoniello³⁴, S. Simsek^{11b}, P. Sinervo¹⁵³, V. Sinetckii³⁵, S. Singh¹⁴⁰, S. Singh¹⁵³, S. Sinha⁴⁶, S. Sinha^{31f}, M. Sioli^{21b,21a}, I. Siral¹²⁰, S.Yu. Sivoklov^{35,*}, J. Sjölin^{45a,45b}, A. Skaf⁵³, E. Skorda⁹⁵, P. Skubic¹¹⁷, M. Slawinska⁸³, K. Sliwa¹⁵⁶, V. Smakhtin¹⁶⁶, B.H. Smart¹³¹, J. Smiesko¹³⁰, S.Yu. Smirnov³⁵, Y. Smirnov³⁵, L.N. Smirnova^{35,a}, O. Smirnova⁹⁵, E.A. Smith³⁷, H.A. Smith¹²³, M. Smizanska⁸⁸, K. Smolek¹²⁹, A. Smykiewicz⁸³, A.A. Snesarev³⁵, H.L. Snoek¹¹², S. Snyder²⁷, R. Sobie^{162,y}, A. Soffer¹⁴⁹, F. Sohns⁵³, C.A. Solans Sanchez³⁴, E.Yu. Soldatov³⁵, U. Soldevila¹⁶⁰, A.A. Solodkov³⁵, S. Solomon⁵², A. Soloshenko³⁶, O.V. Solovyanov³⁵, V. Solovyev³⁵, P. Sommer¹³⁷, H. Son¹⁵⁶, A. Sonay¹², W.Y. Song^{154b}, A. Sopczak¹²⁹, A.L. Sapiro⁹³, F. Sopkova^{26b}, S. Sottocornola^{70a,70b}, R. Soualah^{66a,66c}, Z. Soumami^{33e}, D. South⁴⁶, S. Spagnolo^{67a,67b}, M. Spalla¹⁰⁸, M. Spangenberg¹⁶⁴, F. Spanò⁹², D. Sperlich⁵², T.M. Spieker^{61a}, G. Spigo³⁴, M. Spina¹⁴⁴, D.P. Spiteri⁵⁷, M. Spousta¹³⁰, A. Stabile^{68a,68b}, R. Stamen^{61a}, M. Stamenkovic¹¹², A. Stampekis¹⁹, M. Standke²², E. Stanecka⁸³, B. Stanislaus³⁴, M.M. Stanitzki⁴⁶, M. Stankaityte¹²³, B. Stapf⁴⁶, E.A. Starchenko³⁵, G.H. Stark¹³³, J. Stark¹⁰⁰, D.M. Starke^{154b}, P. Staroba¹²⁸, P. Starovoitov^{61a}, S. Stärz¹⁰², R. Staszewski⁸³, G. Stavropoulos⁴⁴, P. Steinberg²⁷, A.L. Steinhebel¹²⁰, B. Stelzer^{140,154a}, H.J. Stelzer¹²⁶, O. Stelzer-Chilton^{154a}, H. Stenzel⁵⁶, T.J. Stevenson¹⁴⁴, G.A. Stewart³⁴, M.C. Stockton³⁴, G. Stoica^{25b}, M. Stolarski^{127a}, S. Stonjek¹⁰⁸, A. Straessner⁴⁸, J. Strandberg¹⁴², S. Strandberg^{45a,45b}, M. Strauss¹¹⁷, T. Strebler¹⁰⁰, P. Strizenec^{26b}, R. Ströhmer¹⁶³, D.M. Strom¹²⁰, L.R. Strom⁴⁶, R. Stroynowski⁴², A. Strubig^{45a,45b}, S.A. Stucci²⁷, B. Stugu¹⁵, J. Stupak¹¹⁷, N.A. Styles⁴⁶, D. Su¹⁴¹, S. Su^{60a}, W. Su^{60d,136,60c}, X. Su^{60a}, N.B. Suarez¹²⁶, K. Sugizaki¹⁵¹, V.V. Sulin³⁵, M.J. Sullivan⁸⁹, D.M.S. Sultan⁵⁴, S. Sultansoy^{3c}, T. Sumida⁸⁴, S. Sun¹⁰⁴, S. Sun¹⁶⁷, X. Sun⁹⁹, O. Sunneborn Gudnadottir¹⁵⁸, C.J.E. Suster¹⁴⁵, M.R. Sutton¹⁴⁴, M. Svatos¹²⁸, M. Swiatlowski^{154a}, T. Swirski¹⁶³, I. Sykora^{26a}, M. Sykora¹³⁰, T. Sykora¹³⁰, D. Ta⁹⁸, K. Tackmann^{46,w}, A. Taffard¹⁵⁷, R. Tafirout^{154a}, E. Tagiev³⁵, R.H.M. Taibah¹²⁴, R. Takashima⁸⁵, K. Takeda⁸¹, T. Takeshita¹³⁸, E.P. Takeva⁵⁰, Y. Takubo⁸⁰, M. Talby¹⁰⁰, A.A. Talyshev³⁵, K.C. Tam^{62b}, N.M. Tamir¹⁴⁹, A. Tanaka¹⁵¹, J. Tanaka¹⁵¹, R. Tanaka⁶⁴, Z. Tao¹⁶¹, S. Tapia Araya⁷⁸, S. Tapprogge⁹⁸, A. Tarek Abouelfadl Mohamed¹⁰⁵, S. Tarem¹⁴⁸, K. Tariq^{60b}, G. Tarna^{25b,g}, G.F. Tartarelli^{68a}, P. Tas¹³⁰, M. Tasevsky¹²⁸, E. Tassi^{41b,41a}, G. Tateno¹⁵¹, Y. Tayalati^{33e}, G.N. Taylor¹⁰³, W. Taylor^{154b}, H. Teagle⁸⁹, A.S. Tee¹⁶⁷, R. Teixeira De Lima¹⁴¹, P. Teixeira-Dias⁹², H. Ten Kate³⁴, J.J. Teoh¹¹², K. Terashi¹⁵¹, J. Terron⁹⁷, S. Terzo¹², M. Testa⁵¹, R.J. Teuscher^{153,y}, N. Themistokleous⁵⁰, T. Theveneaux-Pelzer¹⁷, O. Thielmann¹⁶⁸, D.W. Thomas⁹², J.P. Thomas¹⁹, E.A. Thompson⁴⁶, P.D. Thompson¹⁹, E. Thomson¹²⁵, E.J. Thorpe⁹¹, Y. Tian⁵³, V. Tikhomirov^{35,a}, Yu.A. Tikhonov³⁵, S. Timoshenko³⁵, P. Tipton¹⁶⁹, S. Tisserant¹⁰⁰, S.H. Tlou^{31f}, A. Tnourji³⁸, K. Todome^{21b,21a}, S. Todorova-Nova¹³⁰, S. Todt⁴⁸, M. Togawa⁸⁰, J. Tojo⁸⁶, S. Tokár^{26a}, K. Tokushuku⁸⁰, E. Tolley¹¹⁶, R. Tombs³⁰, M. Tomoto^{80,109}, L. Tompkins¹⁴¹, P. Tornambe¹⁰¹, E. Torrence¹²⁰, H. Torres⁴⁸,

E. Torró Pastor¹⁶⁰, M. Toscani²⁸, C. Tosciri³⁷, J. Toth^{100,x}, D.R. Tovey¹³⁷, A. Traeet¹⁵, C.J. Treado¹¹⁴, T. Trefzger¹⁶³, A. Tricoli²⁷, I.M. Trigger^{154a}, S. Trincas-Duvoid¹²⁴, D.A. Trischuk¹⁶¹, B. Trocmé⁵⁸, A. Trofymov⁶⁴, C. Troncon^{68a}, F. Trovato¹⁴⁴, L. Truong^{31c}, M. Trzebinski⁸³, A. Trzupek⁸³, F. Tsai¹⁴³, A. Tsiamis¹⁵⁰, P.V. Tsiareshka^{35,a}, A. Tsirigotis^{150,u}, V. Tsiskaridze¹⁴³, E.G. Tskhadadze^{147a}, M. Tsopoulou¹⁵⁰, I.I. Tsukerman³⁵, V. Tsulaia^{16a}, S. Tsuno⁸⁰, O. Tsur¹⁴⁸, D. Tsybychev¹⁴³, Y. Tu^{62b}, A. Tudorache^{25b}, V. Tudorache^{25b}, A.N. Tuna³⁴, S. Turchikhin³⁶, I. Turk Cakir^{3b,t}, R.J. Turner¹⁹, R. Turra^{68a}, P.M. Tuts³⁹, S. Tzamarias¹⁵⁰, P. Tzanis⁹, E. Tzovara⁹⁸, K. Uchida¹⁵¹, F. Ukegawa¹⁵⁵, G. Unal³⁴, M. Unal¹⁰, A. Undrus²⁷, G. Unel¹⁵⁷, F.C. Ungaro¹⁰³, K. Uno¹⁵¹, J. Urban^{26b}, P. Urquijo¹⁰³, G. Usai⁷, R. Ushioda¹⁵², M. Usman¹⁰⁶, Z. Uysal^{11d}, V. Vacek¹²⁹, B. Vachon¹⁰², K.O.H. Vadla¹²², T. Vafeiadis³⁴, C. Valderanis¹⁰⁷, E. Valdes Santurio^{45a,45b}, M. Valente^{154a}, S. Valentini^{21b,21a}, A. Valero¹⁶⁰, L. Valéry⁴⁶, R.A. Vallance¹⁹, A. Vallier¹⁰⁰, J.A. Valls Ferrer¹⁶⁰, T.R. Van Daalen¹³⁶, P. Van Gemmeren⁵, S. Van Stroud⁹³, I. Van Vulpen¹¹², M. Vanadia^{73a,73b}, W. Vandelli³⁴, M. Vandenbroucke¹³², E.R. Vandewall¹¹⁸, D. Vannicola¹⁴⁹, L. Vannoli^{55b,55a}, R. Vari^{72a}, E.W. Varnes⁶, C. Varni^{16a}, T. Varol¹⁴⁶, D. Varouchas⁶⁴, K.E. Varvell¹⁴⁵, M.E. Vasile^{25b}, L. Vaslin³⁸, G.A. Vasquez¹⁶², F. Vazeille³⁸, D. Vazquez Furelos¹², T. Vazquez Schroeder³⁴, J. Veatch⁵³, V. Vecchio⁹⁹, M.J. Veen¹¹², I. Veliscek¹²³, L.M. Veloce¹⁵³, F. Veloso^{127a,127c}, S. Veneziano^{72a}, A. Ventura^{67a,67b}, A. Verbitskiy¹⁰⁸, M. Verducci^{71a,71b}, C. Vergis²², M. Verissimo De Araujo^{79b}, W. Verkerke¹¹², A.T. Vermeulen¹¹², J.C. Vermeulen¹¹², C. Vernieri¹⁴¹, P.J. Verschuur⁹², M.L. Vesterbacka¹¹⁴, M.C. Vetterli^{140,ah}, A. Vgenopoulos¹⁵⁰, N. Viaux Maira^{134e}, T. Vickey¹³⁷, O.E. Vickey Boeriu¹³⁷, G.H.A. Viehhauser¹²³, L. Vigani^{61b}, M. Villa^{21b,21a}, M. Villaplana Perez¹⁶⁰, E.M. Villhauer⁵⁰, E. Vilucchi⁵¹, M.G. Vincker³², G.S. Virdee¹⁹, A. Vishwakarma⁵⁰, C. Vittori^{21b,21a}, I. Vivarelli¹⁴⁴, V. Vladimirov¹⁶⁴, E. Voevodina¹⁰⁸, M. Vogel¹⁶⁸, P. Vokac¹²⁹, J. Von Ahnen⁴⁶, S.E. von Buddenbrock^{31f}, E. Von Toerne²², V. Vorobel¹³⁰, K. Vorobev³⁵, M. Vos¹⁶⁰, J.H. Vosseveld⁸⁹, M. Vozak⁹⁹, L. Vozdecky⁹¹, N. Vranjes¹⁴, M. Vranjes Milosavljevic¹⁴, V. Vrba^{129,*}, M. Vreeswijk¹¹², R. Vuillermet³⁴, O. Vujanovic⁹⁸, I. Vukotic³⁷, S. Wada¹⁵⁵, C. Wagner¹⁰¹, W. Wagner¹⁶⁸, S. Wahdan¹⁶⁸, H. Wahlberg⁸⁷, R. Wakasa¹⁵⁵, M. Wakida¹⁰⁹, V.M. Walbrecht¹⁰⁸, J. Walder¹³¹, R. Walker¹⁰⁷, S.D. Walker⁹², W. Walkowiak¹³⁹, A.M. Wang⁵⁹, A.Z. Wang¹⁶⁷, C. Wang^{60a}, C. Wang^{60c}, H. Wang^{16a}, J. Wang^{62a}, P. Wang⁴², R.-J. Wang⁹⁸, R. Wang⁵⁹, R. Wang¹¹³, S.M. Wang¹⁴⁶, S. Wang^{60b}, T. Wang^{60a}, W.T. Wang^{60a}, W.X. Wang^{60a}, X. Wang^{13c}, X. Wang¹⁵⁹, Y. Wang^{60a}, Z. Wang¹⁰⁴, C. Wanotayaroj³⁴, A. Warburton¹⁰², C.P. Ward³⁰, R.J. Ward¹⁹, N. Warrack⁵⁷, A.T. Watson¹⁹, M.F. Watson¹⁹, G. Watts¹³⁶, B.M. Waugh⁹³, A.F. Webb¹⁰, C. Weber²⁷, M.S. Weber¹⁸, S.A. Weber³², S.M. Weber^{61a}, C. Wei^{60a}, Y. Wei¹²³, A.R. Weidberg¹²³, J. Weingarten⁴⁷, M. Weirich⁹⁸, C. Weiser⁵², T. Wenaus²⁷, B. Wendland⁴⁷, T. Wengler³⁴, S. Wenig³⁴, N. Wermes²², M. Wessels^{61a}, K. Whalen¹²⁰, A.M. Wharton⁸⁸, A.S. White⁵⁹, A. White⁷, M.J. White¹, D. Whiteson¹⁵⁷, L. Wickremasinghe¹²¹, W. Wiedenmann¹⁶⁷, C. Wiel⁴⁸, M. Wielers¹³¹, N. Wieseotte⁹⁸, C. Wiglesworth⁴⁰, L.A.M. Wiik-Fuchs⁵², D.J. Wilbern¹¹⁷, H.G. Wilkens³⁴, L.J. Wilkins⁹², D.M. Williams³⁹, H.H. Williams¹²⁵, S. Williams³⁰, S. Willocq¹⁰¹, P.J. Windischhofer¹²³, I. Wingerter-Seez⁴, F. Winklmeier¹²⁰, B.T. Winter⁵², M. Wittgen¹⁴¹, M. Wobisch⁹⁴, A. Wolf⁹⁸, R. Wölker¹²³, J. Wollrath¹⁵⁷, M.W. Wolter⁸³, H. Wolters^{127a,127c}, V.W.S. Wong¹⁶¹, A.F. Wongel⁴⁶, S.D. Worm⁴⁶, B.K. Wosiek⁸³, K.W. Woźniak⁸³, K. Wraight⁵⁷, J. Wu^{13a,13d}, S.L. Wu¹⁶⁷, X. Wu⁵⁴, Y. Wu^{60a}, Z. Wu^{132,60a}, J. Wuerzinger¹²³, T.R. Wyatt⁹⁹, B.M. Wynne⁵⁰, S. Xella⁴⁰, M. Xia^{13b}, J. Xiang^{62c}, X. Xiao¹⁰⁴, M. Xie^{60a}, X. Xie^{60a}, I. Xioidis¹⁴⁴, D. Xu^{13a}, H. Xu^{60a}, H. Xu^{60a}, L. Xu^{60a}, R. Xu¹²⁵, T. Xu^{60a}, W. Xu¹⁰⁴, Y. Xu^{13b}, Z. Xu^{60b}, Z. Xu¹⁴¹, B. Yabsley¹⁴⁵, S. Yacoob^{31a}, N. Yamaguchi⁸⁶, Y. Yamaguchi¹⁵², M. Yamatani¹⁵¹, H. Yamauchi¹⁵⁵, T. Yamazaki^{16a}, Y. Yamazaki⁸¹, J. Yan^{60c}, S. Yan¹²³, Z. Yan²³, H.J. Yang^{60c,60d}, H.T. Yang^{16a}, S. Yang^{60a}, T. Yang^{62c}, X. Yang^{60a}, X. Yang^{13a}, Y. Yang¹⁵¹, Z. Yang^{60a,104}, W.-M. Yao^{16a}, Y.C. Yap⁴⁶, H. Ye^{13c}, J. Ye⁴², S. Ye²⁷, I. Yeletsikh³⁶, M.R. Yexley⁸⁸, P. Yin³⁹, K. Yorita¹⁶⁵, K. Yoshihara⁷⁸, C.J.S. Young⁵², C. Young¹⁴¹, R. Yuan^{60b,k}, X. Yue^{61a}, M. Zaazoua^{33e}, B. Zabinski⁸³, G. Zacharis⁹, E. Zaid⁵⁰, T. Zakareishvili^{147b}, N. Zakharchuk³², S. Zambito³⁴, D. Zanzi⁵², S.V. Zeiβner⁴⁷, C. Zeitnitz¹⁶⁸, J.C. Zeng¹⁵⁹, O. Zenin³⁵, T. Ženiš^{26a}, S. Zenz⁹¹, S. Zerradi^{33a}, D. Zerwas⁶⁴, M. Zgubič¹²³, B. Zhang^{13c}, D.F. Zhang^{13b}, G. Zhang^{13b}, J. Zhang⁵, K. Zhang^{13a,13d}, L. Zhang^{13c}, M. Zhang¹⁵⁹, R. Zhang¹⁶⁷, S. Zhang¹⁰⁴, X. Zhang^{60c}, X. Zhang^{60b}, Z. Zhang⁶⁴, P. Zhao⁴⁹, Y. Zhao¹³³, Z. Zhao^{60a}, A. Zhemchugov³⁶, Z. Zheng¹⁴¹, D. Zhong¹⁵⁹, B. Zhou¹⁰⁴, C. Zhou¹⁶⁷, H. Zhou⁶, N. Zhou^{60c}, Y. Zhou⁶, C.G. Zhu^{60b}, C. Zhu^{13a,13d}, H.L. Zhu^{60a}, H. Zhu^{13a}, J. Zhu¹⁰⁴, Y. Zhu^{60a}, X. Zhuang^{13a}, K. Zhukov³⁵,

V. Zhulanov³⁵, D. Zieminska⁶⁵, N.I. Zimine³⁶, S. Zimmermann^{52,*}, J. Zinsler^{61b}, M. Ziolkowski¹³⁹,
L. Živković¹⁴, A. Zoccoli^{21b,21a}, K. Zoch⁵⁴, T.G. Zorbas¹³⁷, O. Zormpa⁴⁴, W. Zou³⁹, L. Zwalinski³⁴

¹ Department of Physics, University of Adelaide, Adelaide; Australia

² Department of Physics, University of Alberta, Edmonton AB; Canada

³ (a) Department of Physics, Ankara University, Ankara; (b) Istanbul Aydin University, Application and Research Center for Advanced Studies, Istanbul; (c) Division of Physics, TOBB University of Economics and Technology, Ankara; Türkiye

⁴ LAPP, Univ. Savoie Mont Blanc, CNRS/IN2P3, Annecy; France

⁵ High Energy Physics Division, Argonne National Laboratory, Argonne IL; United States of America

⁶ Department of Physics, University of Arizona, Tucson AZ; United States of America

⁷ Department of Physics, University of Texas at Arlington, Arlington TX; United States of America

⁸ Physics Department, National and Kapodistrian University of Athens, Athens; Greece

⁹ Physics Department, National Technical University of Athens, Zografou; Greece

¹⁰ Department of Physics, University of Texas at Austin, Austin TX; United States of America

¹¹ (a) Bahcesehir University, Faculty of Engineering and Natural Sciences, Istanbul; (b) Istanbul Bilgi University, Faculty of Engineering and Natural Sciences, Istanbul; (c) Department of Physics, Bogazici University, Istanbul; (d) Department of Physics Engineering, Gaziantep University, Gaziantep; Türkiye

¹² Institut de Física d'Altes Energies (IFAE), Barcelona Institute of Science and Technology, Barcelona; Spain

¹³ (a) Institute of High Energy Physics, Chinese Academy of Sciences, Beijing; (b) Physics Department, Tsinghua University, Beijing; (c) Department of Physics, Nanjing University, Nanjing;

(d) University of Chinese Academy of Science (UCAS), Beijing; China

¹⁴ Institute of Physics, University of Belgrade, Belgrade; Serbia

¹⁵ Department for Physics and Technology, University of Bergen, Bergen; Norway

¹⁶ (a) Physics Division, Lawrence Berkeley National Laboratory, Berkeley CA; (b) University of California, Berkeley CA; United States of America

¹⁷ Institut für Physik, Humboldt Universität zu Berlin, Berlin; Germany

¹⁸ Albert Einstein Center for Fundamental Physics and Laboratory for High Energy Physics, University of Bern, Bern; Switzerland

¹⁹ School of Physics and Astronomy, University of Birmingham, Birmingham; United Kingdom

²⁰ (a) Facultad de Ciencias y Centro de Investigaciones, Universidad Antonio Nariño, Bogotá; (b) Departamento de Física, Universidad Nacional de Colombia, Bogotá; Colombia

²¹ (a) Dipartimento di Fisica e Astronomia A. Righi, Università di Bologna, Bologna; (b) INFN Sezione di Bologna; Italy

²² Physikalisches Institut, Universität Bonn, Bonn; Germany

²³ Department of Physics, Boston University, Boston MA; United States of America

²⁴ Department of Physics, Brandeis University, Waltham MA; United States of America

²⁵ (a) Transilvania University of Brasov, Brasov; (b) Horia Hulubei National Institute of Physics and Nuclear Engineering, Bucharest; (c) Department of Physics, Alexandru Ioan Cuza University of Iasi, Iasi; (d) National Institute for Research and Development of Isotopic and Molecular Technologies, Physics Department, Cluj-Napoca; (e) University Politehnica Bucharest, Bucharest; (f) West University in Timisoara, Timisoara; Romania

²⁶ (a) Faculty of Mathematics, Physics and Informatics, Comenius University, Bratislava; (b) Department of Subnuclear Physics, Institute of Experimental Physics of the Slovak Academy of Sciences, Kosice; Slovak Republic

²⁷ Physics Department, Brookhaven National Laboratory, Upton NY; United States of America

²⁸ Universidad de Buenos Aires, Facultad de Ciencias Exactas y Naturales, Departamento de Física, y CONICET, Instituto de Física de Buenos Aires (IFIBA), Buenos Aires; Argentina

²⁹ California State University, CA; United States of America

³⁰ Cavendish Laboratory, University of Cambridge, Cambridge; United Kingdom

³¹ (a) Department of Physics, University of Cape Town, Cape Town; (b) iThemba Labs, Western Cape; (c) Department of Mechanical Engineering Science, University of Johannesburg, Johannesburg; (d) National Institute of Physics, University of the Philippines Diliman (Philippines); (e) University of South Africa, Department of Physics, Pretoria; (f) School of Physics, University of the Witwatersrand, Johannesburg; South Africa

³² Department of Physics, Carleton University, Ottawa ON; Canada

³³ (a) Faculté des Sciences Ain Chock, Réseau Universitaire de Physique des Hautes Energies - Université Hassan II, Casablanca; (b) Faculté des Sciences, Université Ibn-Tofail, Kénitra;

(c) Faculté des Sciences Semlalia, Université Cadi Ayyad, LPHEA-Marrakech; (d) LPMR, Faculté des Sciences, Université Mohamed Premier, Oujda; (e) Faculté des sciences, Université Mohammed V, Rabat; Morocco

³⁴ CERN, Geneva; Switzerland

³⁵ Affiliated with an institute covered by a cooperation agreement with CERN

³⁶ Affiliated with an international laboratory covered by a cooperation agreement with CERN

³⁷ Enrico Fermi Institute, University of Chicago, Chicago IL; United States of America

³⁸ LPC, Université Clermont Auvergne, CNRS/IN2P3, Clermont-Ferrand; France

³⁹ Nevis Laboratory, Columbia University, Irvington NY; United States of America

⁴⁰ Niels Bohr Institute, University of Copenhagen, Copenhagen; Denmark

⁴¹ (a) Dipartimento di Fisica, Università della Calabria, Rende; (b) INFN Gruppo Collegato di Cosenza, Laboratori Nazionali di Frascati; Italy

⁴² Physics Department, Southern Methodist University, Dallas TX; United States of America

⁴³ Physics Department, University of Texas at Dallas, Richardson TX; United States of America

⁴⁴ National Centre for Scientific Research "Demokritos", Agia Paraskevi; Greece

⁴⁵ (a) Department of Physics, Stockholm University; (b) Oskar Klein Centre, Stockholm; Sweden

⁴⁶ Deutsches Elektronen-Synchrotron DESY, Hamburg and Zeuthen; Germany

⁴⁷ Fakultät Physik, Technische Universität Dortmund, Dortmund; Germany

⁴⁸ Institut für Kern- und Teilchenphysik, Technische Universität Dresden, Dresden; Germany

⁴⁹ Department of Physics, Duke University, Durham NC; United States of America

⁵⁰ SUPA - School of Physics and Astronomy, University of Edinburgh, Edinburgh; United Kingdom

⁵¹ INFN e Laboratori Nazionali di Frascati, Frascati; Italy

⁵² Physikalisches Institut, Albert-Ludwigs-Universität Freiburg, Freiburg; Germany

⁵³ II. Physikalisches Institut, Georg-August-Universität Göttingen, Göttingen; Germany

⁵⁴ Département de Physique Nucléaire et Corpusculaire, Université de Genève, Genève; Switzerland

⁵⁵ (a) Dipartimento di Fisica, Università di Genova, Genova; (b) INFN Sezione di Genova; Italy

⁵⁶ II. Physikalisches Institut, Justus-Liebig-Universität Giessen, Giessen; Germany

⁵⁷ SUPA - School of Physics and Astronomy, University of Glasgow, Glasgow; United Kingdom

⁵⁸ LPSC, Université Grenoble Alpes, CNRS/IN2P3, Grenoble INP, Grenoble; France

⁵⁹ Laboratory for Particle Physics and Cosmology, Harvard University, Cambridge MA; United States of America

⁶⁰ (a) Department of Modern Physics and State Key Laboratory of Particle Detection and Electronics, University of Science and Technology of China, Hefei; (b) Institute of Frontier and Interdisciplinary Science and Key Laboratory of Particle Physics and Particle Irradiation (MOE), Shandong University, Qingdao; (c) School of Physics and Astronomy, Shanghai Jiao Tong University, Key Laboratory for Particle Astrophysics and Cosmology (MOE), SKLPPC, Shanghai; (d) Tsung-Dao Lee Institute, Shanghai; China

⁶¹ Kirchhoff-Institut für Physik, Ruprecht-Karls-Universität Heidelberg, Heidelberg; (b) Physikalisches Institut, Ruprecht-Karls-Universität Heidelberg, Heidelberg; Germany

⁶² (a) Department of Physics, Chinese University of Hong Kong, Shatin, N.T., Hong Kong; (b) Department of Physics, University of Hong Kong, Hong Kong; (c) Department of Physics and Institute for Advanced Study, Hong Kong University of Science and Technology, Clear Water Bay, Kowloon, Hong Kong; China

⁶³ Department of Physics, National Tsing Hua University, Hsinchu; Taiwan

- 64 JCLab, Université Paris-Saclay, CNRS/IN2P3, 91405, Orsay; France
- 65 Department of Physics, Indiana University, Bloomington IN; United States of America
- 66 (a) INFN Gruppo Collegato di Udine, Sezione di Trieste, Udine; (b) ICTP, Trieste; (c) Dipartimento Politecnico di Ingegneria e Architettura, Università di Udine, Udine; Italy
- 67 (a) INFN Sezione di Lecce; (b) Dipartimento di Matematica e Fisica, Università del Salento, Lecce; Italy
- 68 (a) INFN Sezione di Milano; (b) Dipartimento di Fisica, Università di Milano, Milano; Italy
- 69 (a) INFN Sezione di Napoli; (b) Dipartimento di Fisica, Università di Napoli, Napoli; Italy
- 70 (a) INFN Sezione di Pavia; (b) Dipartimento di Fisica, Università di Pavia, Pavia; Italy
- 71 (a) INFN Sezione di Pisa; (b) Dipartimento di Fisica E. Fermi, Università di Pisa, Pisa; Italy
- 72 (a) INFN Sezione di Roma; (b) Dipartimento di Fisica, Sapienza Università di Roma, Roma; Italy
- 73 (a) INFN Sezione di Roma Tor Vergata; (b) Dipartimento di Fisica, Università di Roma Tor Vergata, Roma; Italy
- 74 (a) INFN Sezione di Roma Tre; (b) Dipartimento di Matematica e Fisica, Università Roma Tre, Roma; Italy
- 75 (a) INFN-TIFPA; (b) Università degli Studi di Trento, Trento; Italy
- 76 Universität Innsbruck, Department of Astro and Particle Physics, Innsbruck; Austria
- 77 University of Iowa, Iowa City IA; United States of America
- 78 Department of Physics and Astronomy, Iowa State University, Ames IA; United States of America
- 79 (a) Departamento de Engenharia Elétrica, Universidade Federal de Juiz de Fora (UFJF), Juiz de Fora; (b) Universidade Federal do Rio De Janeiro COPPE/EE/IF, Rio de Janeiro; (c) Instituto de Física, Universidade de São Paulo, São Paulo; Brazil
- 80 KEK, High Energy Accelerator Research Organization, Tsukuba; Japan
- 81 Graduate School of Science, Kobe University, Kobe; Japan
- 82 (a) AGH University of Science and Technology, Faculty of Physics and Applied Computer Science, Krakow; (b) Marian Smoluchowski Institute of Physics, Jagiellonian University, Krakow; Poland
- 83 Institute of Nuclear Physics Polish Academy of Sciences, Krakow; Poland
- 84 Faculty of Science, Kyoto University, Kyoto; Japan
- 85 Kyoto University of Education, Kyoto; Japan
- 86 Research Center for Advanced Particle Physics and Department of Physics, Kyushu University, Fukuoka; Japan
- 87 Instituto de Física La Plata, Universidad Nacional de La Plata and CONICET, La Plata; Argentina
- 88 Physics Department, Lancaster University, Lancaster; United Kingdom
- 89 Oliver Lodge Laboratory, University of Liverpool, Liverpool; United Kingdom
- 90 Department of Experimental Particle Physics, Jožef Stefan Institute and Department of Physics, University of Ljubljana, Ljubljana; Slovenia
- 91 School of Physics and Astronomy, Queen Mary University of London, London; United Kingdom
- 92 Department of Physics, Royal Holloway University of London, Egham; United Kingdom
- 93 Department of Physics and Astronomy, University College London, London; United Kingdom
- 94 Louisiana Tech University, Ruston LA; United States of America
- 95 Fysiska institutionen, Lunds universitet, Lund; Sweden
- 96 Centre de Calcul de l'Institut National de Physique Nucléaire et de Physique des Particules (IN2P3), Villeurbanne; France
- 97 Departamento de Física Teórica C-15 and CIAFF, Universidad Autónoma de Madrid, Madrid; Spain
- 98 Institut für Physik, Universität Mainz, Mainz; Germany
- 99 School of Physics and Astronomy, University of Manchester, Manchester; United Kingdom
- 100 CPPM, Aix-Marseille Université, CNRS/IN2P3, Marseille; France
- 101 Department of Physics, University of Massachusetts, Amherst MA; United States of America
- 102 Department of Physics, McGill University, Montreal QC; Canada
- 103 School of Physics, University of Melbourne, Victoria; Australia
- 104 Department of Physics, University of Michigan, Ann Arbor MI; United States of America
- 105 Department of Physics and Astronomy, Michigan State University, East Lansing MI; United States of America
- 106 Group of Particle Physics, University of Montreal, Montreal QC; Canada
- 107 Fakultät für Physik, Ludwig-Maximilians-Universität München, München; Germany
- 108 Max-Planck-Institut für Physik (Werner-Heisenberg-Institut), München; Germany
- 109 Graduate School of Science and Kobayashi-Maskawa Institute, Nagoya University, Nagoya; Japan
- 110 Department of Physics and Astronomy, University of New Mexico, Albuquerque NM; United States of America
- 111 Institute for Mathematics, Astrophysics and Particle Physics, Radboud University/Nikhef, Nijmegen; Netherlands
- 112 Nikhef National Institute for Subatomic Physics and University of Amsterdam, Amsterdam; Netherlands
- 113 Department of Physics, Northern Illinois University, DeKalb IL; United States of America
- 114 Department of Physics, New York University, New York NY; United States of America
- 115 Ochanomizu University, Otsuka, Bunkyo-ku, Tokyo; Japan
- 116 Ohio State University, Columbus OH; United States of America
- 117 Homer L. Dodge Department of Physics and Astronomy, University of Oklahoma, Norman OK; United States of America
- 118 Department of Physics, Oklahoma State University, Stillwater OK; United States of America
- 119 Palacký University, Joint Laboratory of Optics, Olomouc; Czech Republic
- 120 Institute for Fundamental Science, University of Oregon, Eugene, OR; United States of America
- 121 Graduate School of Science, Osaka University, Osaka; Japan
- 122 Department of Physics, University of Oslo, Oslo; Norway
- 123 Department of Physics, Oxford University, Oxford; United Kingdom
- 124 LPNHE, Sorbonne Université, Université Paris Cité, CNRS/IN2P3, Paris; France
- 125 Department of Physics, University of Pennsylvania, Philadelphia PA; United States of America
- 126 Department of Physics and Astronomy, University of Pittsburgh, Pittsburgh PA; United States of America
- 127 (a) Laboratório de Instrumentação e Física Experimental de Partículas - LIP, Lisboa; (b) Departamento de Física, Faculdade de Ciências, Universidade de Lisboa, Lisboa; (c) Departamento de Física, Universidade de Coimbra, Coimbra; (d) Centro de Física Nuclear da Universidade de Lisboa, Lisboa; (e) Departamento de Física, Universidade do Minho, Braga; (f) Departamento de Física Teórica y del Cosmos, Universidad de Granada, Granada (Spain); (g) Dep Física and CEFITEC of Faculdade de Ciências e Tecnologia, Universidade Nova de Lisboa, Caparica; (h) Instituto Superior Técnico, Universidade de Lisboa, Lisboa; Portugal
- 128 Institute of Physics of the Czech Academy of Sciences, Prague; Czech Republic
- 129 Czech Technical University in Prague, Prague; Czech Republic
- 130 Charles University, Faculty of Mathematics and Physics, Prague; Czech Republic
- 131 Particle Physics Department, Rutherford Appleton Laboratory, Didcot; United Kingdom
- 132 IRFU, CEA, Université Paris-Saclay, Gif-sur-Yvette; France
- 133 Santa Cruz Institute for Particle Physics, University of California Santa Cruz, Santa Cruz CA; United States of America
- 134 (a) Departamento de Física, Pontificia Universidad Católica de Chile, Santiago; (b) Millennium Institute for Subatomic physics at high energy frontier (SAPHIR), Santiago; (c) Universidad Andres Bello, Department of Physics, Santiago; (d) Instituto de Alta Investigación, Universidad de Tarapacá, Arica; (e) Departamento de Física, Universidad Técnica Federico Santa María, Valparaíso; Chile
- 135 Universidade Federal de São João del Rei (UFSJ), São João del Rei; Brazil
- 136 Department of Physics, University of Washington, Seattle WA; United States of America

- 137 Department of Physics and Astronomy, University of Sheffield, Sheffield; United Kingdom
 138 Department of Physics, Shinshu University, Nagano; Japan
 139 Department Physik, Universität Siegen, Siegen; Germany
 140 Department of Physics, Simon Fraser University, Burnaby BC; Canada
 141 SLAC National Accelerator Laboratory, Stanford CA; United States of America
 142 Department of Physics, Royal Institute of Technology, Stockholm; Sweden
 143 Departments of Physics and Astronomy, Stony Brook University, Stony Brook NY; United States of America
 144 Department of Physics and Astronomy, University of Sussex, Brighton; United Kingdom
 145 School of Physics, University of Sydney, Sydney; Australia
 146 Institute of Physics, Academia Sinica, Taipei; Taiwan
 147 ^(a) E. Andronikashvili Institute of Physics, Iv. Javakhsishvili Tbilisi State University, Tbilisi; ^(b) High Energy Physics Institute, Tbilisi State University, Tbilisi; Georgia
 148 Department of Physics, Technion, Israel Institute of Technology, Haifa; Israel
 149 Raymond and Beverly Sackler School of Physics and Astronomy, Tel Aviv University, Tel Aviv; Israel
 150 Department of Physics, Aristotle University of Thessaloniki, Thessaloniki; Greece
 151 International Center for Elementary Particle Physics and Department of Physics, University of Tokyo, Tokyo; Japan
 152 Department of Physics, Tokyo Institute of Technology, Tokyo; Japan
 153 Department of Physics, University of Toronto, Toronto ON; Canada
 154 ^(a) TRIUMF, Vancouver BC; ^(b) Department of Physics and Astronomy, York University, Toronto ON; Canada
 155 Division of Physics and Tomonaga Center for the History of the Universe, Faculty of Pure and Applied Sciences, University of Tsukuba, Tsukuba; Japan
 156 Department of Physics and Astronomy, Tufts University, Medford MA; United States of America
 157 Department of Physics and Astronomy, University of California Irvine, Irvine CA; United States of America
 158 Department of Physics and Astronomy, University of Uppsala, Uppsala; Sweden
 159 Department of Physics, University of Illinois, Urbana IL; United States of America
 160 Instituto de Física Corpuscular (IFIC), Centro Mixto Universidad de Valencia - CSIC, Valencia; Spain
 161 Department of Physics, University of British Columbia, Vancouver BC; Canada
 162 Department of Physics and Astronomy, University of Victoria, Victoria BC; Canada
 163 Fakultät für Physik und Astronomie, Julius-Maximilians-Universität Würzburg, Würzburg; Germany
 164 Department of Physics, University of Warwick, Coventry; United Kingdom
 165 Waseda University, Tokyo; Japan
 166 Department of Particle Physics and Astrophysics, Weizmann Institute of Science, Rehovot; Israel
 167 Department of Physics, University of Wisconsin, Madison WI; United States of America
 168 Fakultät für Mathematik und Naturwissenschaften, Fachgruppe Physik, Bergische Universität Wuppertal, Wuppertal; Germany
 169 Department of Physics, Yale University, New Haven CT; United States of America

^a Also Affiliated with an institute covered by a cooperation agreement with CERN.

^b Also at Borough of Manhattan Community College, City University of New York, New York NY; United States of America.

^c Also at Bruno Kessler Foundation, Trento; Italy.

^d Also at Center for High Energy Physics, Peking University; China.

^e Also at Centro Studi e Ricerche Enrico Fermi; Italy.

^f Also at CERN, Geneva; Switzerland.

^g Also at CPPM, Aix-Marseille Université, CNRS/IN2P3, Marseille; France.

^h Also at Département de Physique Nucléaire et Corpusculaire, Université de Genève, Genève; Switzerland.

ⁱ Also at Departament de Física de la Universitat Autònoma de Barcelona, Barcelona; Spain.

^j Also at Department of Financial and Management Engineering, University of the Aegean, Chios; Greece.

^k Also at Department of Physics and Astronomy, Michigan State University, East Lansing MI; United States of America.

^l Also at Department of Physics and Astronomy, University of Louisville, Louisville, KY; United States of America.

^m Also at Department of Physics, Ben Gurion University of the Negev, Beer Sheva; Israel.

ⁿ Also at Department of Physics, California State University, East Bay; United States of America.

^o Also at Department of Physics, California State University, Fresno; United States of America.

^p Also at Department of Physics, California State University, Sacramento; United States of America.

^q Also at Department of Physics, King's College London, London; United Kingdom.

^r Also at Department of Physics, University of Fribourg, Fribourg; Switzerland.

^s Also at Faculty of Physics, Sofia University, 'St. Kliment Ohridski', Sofia; Bulgaria.

^t Also at Giresun University, Faculty of Engineering, Giresun; Türkiye.

^u Also at Hellenic Open University, Patras; Greece.

^v Also at Institutio Catalana de Recerca i Estudis Avancats, ICREA, Barcelona; Spain.

^w Also at Institut für Experimentalphysik, Universität Hamburg, Hamburg; Germany.

^x Also at Institute for Particle and Nuclear Physics, Wigner Research Centre for Physics, Budapest; Hungary.

^y Also at Institute of Particle Physics (IPP); Canada.

^z Also at Institute of Physics, Azerbaijan Academy of Sciences, Baku; Azerbaijan.

^{aa} Also at Institute of Theoretical Physics, Ilia State University, Tbilisi; Georgia.

^{ab} Also at Instituto de Física Teórica, IFT-UAM/CSIC, Madrid; Spain.

^{ac} Also at Istanbul University, Dept. of Physics, Istanbul; Türkiye.

^{ad} Also at Physics Department, An-Najah National University, Nablus; Palestine.

^{ae} Also at Physikalisches Institut, Albert-Ludwigs-Universität Freiburg, Freiburg; Germany.

^{af} Also at The City College of New York, New York NY; United States of America.

^{ag} Also at The Collaborative Innovation Center of Quantum Matter (CICQM), Beijing; China.

^{ah} Also at TRIUMF, Vancouver BC; Canada.

^{ai} Also at Università di Napoli Parthenope, Napoli; Italy.

^{aj} Also at University of Chinese Academy of Sciences (UCAS), Beijing; China.

^{ak} Also at Yeditepe University, Physics Department, Istanbul; Türkiye.

^{al} Also at RWTH Aachen University, III. Physikalisches Institut A, Aachen; Germany.

* Deceased.